NPS-EC-98-012

NAVAL POSTGRADUATE SCHOOL
Monterey, California

**IMOM Field Test Study and
Accuracy Verification**

Engineering Report

by

Fred Levien
Paul Buczynski

August 1998

Approved for public release; distribution is unlimited.

Prepared for: Naval Air Warfare Center China Lake
China Lake, CA

NAVAL POSTGRADUATE SCHOOL
Monterey, California

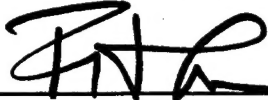RADM ROBERT C. CHAPLIN   R. Elster
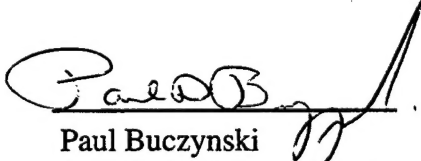Superintendent   Provost

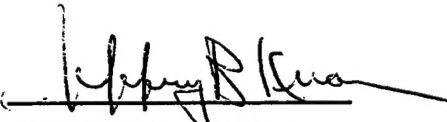This report was sponsored by the Naval Air Warfare Center China Lake, CA.

Approved for public release; distribution is unlimited.
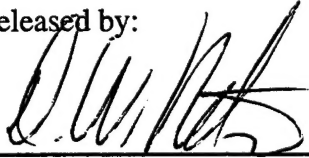
The report was prepared by:

Fred Levien   Paul Buczynski
Senior Lecturer   Radar/EW Laboratory Director
Department of Electrical and   Department of Electrical and
Computer Engineering   Computer Engineering

Reviewed by: Released by:

JEFFREY B. KNORR   DAVID W. NETZER
Chairman   Associate Provost and
Department of Electrical and   Dean of Research
Computer Engineering

ii

REPORT DOCUMENTATION PAGE			Form Approved OMB No. 0704-0188
Public reporting burden for the collection of information is estimated to average 1 hour per response, including the time for reviewing instructions, searching existing data sources, gathering and maintaining the data needed, and completing and reviewing the collection of information. Send comments regarding this burden estimate or any other aspect of this collection of information, including suggestions for reducing this burden to Washington Headquarters Services, Directorate for Information Operations and Reports, 1215 Jefferson Davis Highway, Suite 1204, Arlington VA 22202-4302, and to the Office of Management and Budget, Paperwork Reduction Project (0704-0188), Washington DC 20503.			
1. AGENCY USE ONLY (Leave blank)	2. REPORT DATE August 1998	3. REPORT TYPE AND DATES COVERED Engineering Report	
4. TITLE AND SUBTITLE IMOM Field Test Study and Accuracy Verification		5. FUNDING NUMBERS MIPR NO. N0042198 WR05074	
6. AUTHOR(S) Fred Levien and Paul Buczynski			
7. PERFORMING ORGANIZATION NAME(S) AND ADDRESS(ES) Department of Electrical and Computer Engineering Naval Postgraduate School Monterey, CA 93943-5000		8. PERFORMING ORGANIZATION REPORT NUMBER NPS-EC-98-012	
9. SPONSORING/MONITORING AGENCY NAME(S) AND ADDRESS(ES) Naval Air Warfare Center China Lake 1 Administration Circle China Lake, CA 93555		10. SPONSORING/MONITORING AGENCY REPORT NUMBER	
11. SUPPLEMENTARY NOTES The views expressed in this report are those of the author and do not reflect the official policy or position of the Department of Defense or the United States Government.			
12a. DISTRIBUTION/AVAILABILITY STATEMENT Approved for public release; distribution is unlimited.		12b. DISTRIBUTION CODE A	

13. ABSTRACT (Maximum 200 words)

This report is the second and final document presenting the results of this cooperative effort. It analyzes and discusses the results of two days of intensive testing at NAWC China Lake on the 9th and 10th of July 1997. These tests were performed to determine the ability of IMOM to be used as a predictive tool when employed in the role of mission planning. The genesis of this study was to answer a question that had arisen in comparison of field results being obtained from the TAMPS modeling and simulation system. It was desired to obtain flight test data for both TAMPS and IMOM in order to compare their ability to accurately predict the effects of Radar Terrain Masking (RTM). It was initially planned to have NPS compare predictive data from both of these systems and then do analysis of how they compared to actual field test data.

14. SUBJECT TERMS Modeling and simulation, radar electronic warfare			15. NUMBER OF PAGES 129
			16. PRICE CODE
17. SECURITY CLASSIFICATION OF REPORT UNCLASSIFIED	18. SECURITY CLASSIFICATION OF THIS PAGE UNCLASSIFIED	19. SECURITY CLASSIFICATION OF ABSTRACT UNCLASSIFIED	20. LIMITATION OF ABSTRACT SAR

IMOM Field Test Study
and
Accuracy Verification

July 30, 1998

1. BACKGROUND

In 1993 the Naval Postgraduate School with the help of the Air Force Information Warfare Facility (AFIWC) in San Antonio, installed IMOM in the Modeling and Simulation classified laboratory facility in Spanagel Hall. It was intended to support student studies on campus and thesis work in the field of Radar and Electronic Warfare. The two curriculum that primarily employed this facility were the Electrical and Computer Engineering and the Electronic Warfare Curricula. However, with the passage of time, there have been additional curriculum that have found this facility of use including the Electronic Warfare Department, the Aeronautical Engineering Department, and the newly formed Information Warfare Group. The school was excited and pleased to have been chosen as a recipient of IMOM, and has since invested well over $100,000 in added facilities to properly support the use of IMOM for both laboratory instruction and research. Use of IMOM adds greatly to students' skill set by helping them apply the knowledge learned in class, to actual operating scenarios. Furthermore, when structured as a mini-war game, IMOM allows teams to pit their knowledge in a real world tactical scenario and practice on employing combat tactics both from an offensive and defensive position.

In recent years several opportunities have arisen for research assignments using IMOM as a tool. The most visible of these tasks was the adaptation of the system to accommodate the IMOM program code for the EA-6B which was assigned as a replacement for the EF-111 when the Navy assumed responsibility for the SEAD role from the Air Force. This effort was completed in 1996 and has been working satisfactorily since then. The Naval Postgraduate School in it's role as the DoD's University, stands ready at all times to not only provide education for all of the Services (Army, Air Force, and Marines as well as Navy) but to also provide assistance in any area of research in which it feels competent, to help a DoD organization. Toward this end, when the Information Warfare Group at NPS was approached by a team from VX-9, NAWC China Lake and the AFIWC in mid-1997 with a request to assist in analyzing field test data taken to calibrate the accuracy of IMOM predictions, the response was a resounding "Let's Go!"

2. INTRODUCTION

This report is the second and final document presenting the results of this cooperative effort. It analyzes and discusses the results of two days of intensive testing at NAWC China Lake on the 9th and 10th of July, 1997. These tests were performed to determine the ability of IMOM to be used as a predictive tool when employed in the role of mission planning. The genesis of this study was to answer a question that had arisen in comparison of field results being obtained from the TAMPS modeling and simulation system. It was desired to obtain flight test data for both TAMPS and IMOM in order to compare their ability to accurately predict the effects of Radar Terrain Masking (RTM). It

was initially planned to have NPS compare predictive data from both these systems and then do an analysis of how they compared to actual field test data.

TAMPS

Shortly into the study, NPS was notified that it was clear that there would be no inputs available for analysis from the TAMPS system. This necessitated NPS having to disregard TAMPS in this study and to simply run the IMOM predictive results and concentrate on comparing that to "ground truth" determined from the field tests.

A PowerPoint presentation, prepared by VX-9 in May of 1998, is included in this report as Attachment 1.*

AFMSS

It was also initially planned to include the Air Force AFMSS radar terrain masking (RTM) program in this study as well. A more careful review of the structure of the AFMSS modeling code, however, revealed a feature called "high point." This particular algorithm was designed to move the radar site from the actually plotted position of a specific radar, to a position located at the highest altitude within a 1500 meter radius of the actual site. This particular feature of the computer program in AFMSS made the program unsuitable for the accuracy comparison required in this study. NPS did not examine the AMSS system during the conduct of this study. However, information on AFMSS testing was received from VX-9 and is quoted here:

---

* Comments in this font throughout this report represent verbatim inputs from VX-9.

AFMSS Test Results

1. AFMSS testing was performed by AFIWC personnel at San Antonio, TX using version 2.0C. The raw data was reported to VX-9 for analysis and reporting.

2. AFMSS displays RTM coverage in a detection line format with a resolution of 1 degree by 1 NM based on calculations performed using Level 1 DTED (3 arc second). The model has an automatic feature called "highpoint" which adjusts the elevation of the threat emitter to the highest DTED elevation within a 1 NM rectangle of the input coordinates. This feature could not be disabled. AFMSS can display overhead and profile views of the radar coverage. The AFMSS on which testing was conducted did not have a printing capability, so no visual outputs are provided.

3. Test runs consisted of 5 EO points and 4 FSA points. The data and results are as follows:

Time	Sensor	Actual Range	Range Error	% Error
163332	EO	26.5	-0.2 NM	0.8
165907	EO	9.4	-0.4	4.3
165957	EO	7.5	+0.5	6.7
175213	EO	5.8	+0.3	5.2
164009	FSA	14.6	-0.6	4.1
164025	FSA	15.8	+0.1	0.6
164210	FSA	20.8	+1.1	5.3
164514	FSA	14.0	0.0	0.0
171226	FSA	3.6	-0.6	16.7
		RMS Error: 0.52 NM		RMS % Error: 6.8%

4. Conclusions: AFMSS was reasonably accurate within the limitations of its display resolution (1 NM × 1 degree). In IMOM testing it was found that the highpoint feature tended to rotate the detection line envelope about

4

the site while usually not appreciable affecting range or overall shape of the envelope. This feature was deemed to be useful for sites where exact location is not known, but should be operator selectable and default to off. Data on processing speed or ability to fuse multiple envelopes was not collected.

IMOM

IMOM is a powerful predictive model that allows a mission planner the opportunity to select any of a wide variety of adversarial radars, and by using National Imagery and Mapping Agency (NIMA) terrain data, locate that radar at a particular latitude and longitude. The planner is then free to select a wide range of US aircraft platforms and plot their track assuming a hypothetical mission to attack a target within the range of the radar's emissions. The planner is free to choose speed, bearing, and altitude to minimize the likelihood of the friendly attacking aircraft being detected by both the enemy's search radar and downed by his fire control radar on the missile or gun system. One very useful outcome of this planning procedure is the ability of IMOM to ascertain when and where the attacking aircraft when flying in mountainous areas will be terrain masked thereby permitting mission planners to select a less risky environment for both approach and egress from the target area.

With the present predictive ability of the GPS system to accurately locate both an aircraft's position and that of the radar, coupled with 3 arc-sec resolution of the NIMA terrain database, it has now become possible to analyze this degree of IMOM accuracy. The field test data was planned around a carefully programmed flight test schedule. The

recorded field test data compared actual detection results to predicted IMOM horizontal direction ray plots, along with IMOM and vertical cross-sectional plots. Display examples of each of these plots is shown in Attachment 2. The accuracy of this IMOM predictive data is of critical importance to the mission planner and the pilot of the attacking aircraft. To the best of our knowledge, a chance to perform this calibration and analysis has never before presented itself. This opportunity for NPS to carry out original research in this field for the first time was one of the intriguing aspects of this assignment that moved us so quickly to sign on for the project. Additional information received form VX-9 is presented below.

1. **Model Sophistication.** None of the models tested addressed anomalous propagation. All used some form of NIMA DTED. TAMPS and IMOM allowed the operator to vary DTED sampling interval from 3 arc second (100 m) to 60 arc second (2000 m) to trade accuracy for processing speed. This was deemed to be a desirable feature for mission planning where time constraints are common. IMOM and AFMSS had a "highpoint" feature which moved the location of a threat radar to the highest terrain point within a finite radius around the input coordinates. This feature may be useful for cases where the emitter location is not precisely known, but actually reduced RTM accuracy for the test cases where the location was precisely known. The feature may be desirable if it is an option which defaults to off, and can selectively be set to on for individual sites.

6

2. **IMOM** is part of the USAF Contingency Theater Air Planning System (CTAPS) and its successor, the Theater Battle Management Command System (TBMCS), as well as the unit-level Combat Intelligence System (CIS). IMOM is endorsed by the Air Force Operational Test and Evaluation Command (AFOTEC) for operation testing of AFMSS.

3. **Accuracy.** The 3 arc second DTED version of IMOM (ver 3.9) was the most accurate of the three systems tested. The 15 arc second version of IMOM and AFMSS were roughly comparable and reasonably accurate. TAMPS has gross errors attributed to both database and algorithm shortcomings.

3. IMOM FUNDAMENTALS

The type of radars normally used for aircraft detection and to control gun and missile system fire control systems have RF emissions that are unable to penetrate solid earth. Therefore, where a radar is aimed at a low flying incoming target such that the radar antenna angle of elevation is low enough to be screened by mountains, it produces a blind area, or 'shadow' for detection behind these land masses. In this volume of air space, an aircraft in flight cannot be detected. The entire process has been given the name "terrain masking", often abbreviated with the acronym RTM (Radar Terrain Masking). The effect of this RTM is clearly displayed by IMOM when examining the ring display. This ring display is a picture of a series of fingers, or lines extending out from the location of the radar. The end of each of these fingers represents the longest range that a target can be

detected on a specific bearing while at a specifically selected altitude, using the particular combination of radar and aircraft chosen in the given scenario. It is based on a mathematical solution of the radar range equation (RRE). The RRE is a straight forward relationship which takes into account all the physical principals on which a radar system is designed. The RRE cannot by itself, however, calculate the effect of terrain masking. Therefore, there is another control built into IMOM which truncates the length of this detection ray based on the interference generated by terrain. The terrain model is that provided to IMOM by the NIMA standard program. That is one of the strengths of IMOM, the ability to predict RTM in a combat scenario. The question that we have designed this study to assess, is the accuracy of this prediction. Additional information from VX-9 is presented below:

1. **Detection Line vs. Rays.** The detection line display is more useful for mission planning purposes because of display clutter inherent with rays and need to simultaneously display other data like waypoints, targets, surface order of battle, imagery, etc. TAMPS and AFMSS display detection lines. IMOM defaults to "rings" (more appropriately labeled "rays") but has a detection line option. The IMOM detection line seems to trace a line just beyond the end of the rays rather than connecting their end points.

2. **Display of Multiple Envelopes.** The IMOM ability to fuse multiple detection line envelopes into a single collective detection line envelope for each of two classes of system (detection and threat) further

8

reduced clutter and greatly simplified mission planning. This should be the default display if multiple threat sites are selected.

4. STUDY METHODOLOGY

a. System Physical Arrangements

The initial plan was to fly three different aircraft types, two fixed wing and one helo, along predetermined flight paths at low level through the mountainous terrain located on the R-2524 EW (Echo) range southeast of the NAWC China Lake. The aircraft types selected were:

(1)   FA-18, equipped with a GPS tracking pod – fixed wing

(2)   EA-6B equipped with a GPS tracking pod – fixed wing

(3)   AH-1W – helicopter

These targets would be observed by four NIKE tracker radars located at three different sites on the range. These radars were designated:

(1)   J-1E-12 (NATO site)

(2)   A-2

(3)   I-5

(4)   J-17

The aircraft flight paths would place them alternately within radar visibility and then, although still within radar range, cause them to be hidden by terrain masking. It was intended that these runs would be tracked optically as well as using a low power I-band RF line-of-sight marker beacon aboard the EA-6B, which would provide a backup indication on a Frequency Spectrum Analyzer (FSA) at the J-1E-12 NATO site, along

9

with visual LOS sighting through a telescope (recorded on video tape from each site). The very low power I-band signal was intended to simply provide one way propagation information rather than jam the ground radars, and it was deconflicted with all ground radars before the tests were run. Thus, when the radar signal from a particular site impinged on a target, this fact would be verified by three different signal sources:

(1)   Optical/visual observation (video recorded with time tic)

(2)   Receipt of RF beacon signal on FSA (recorded with time tic)

(3)   Observation of the target on the radar CRT screen

The raw data collected included radar track acquisition and radar drop track times as well as continuous three dimensional aircraft time-space-position information (TSPI) data from GPS or NIKE at one second intervals. Also, A-scope and B-scope video was taken of the A-2, E-12, and J-17 sites as well as optics video from the I-5, J-17, J-12 of the NIKE trackers as well as audio for all ground and aircraft operators. The data set of approximately 250 points was sent in EXCEL format spreadsheet to NPS. It represents all the points that NAWC was able to positively verify that radar acquisition or drop track was related to terrain masking.

The data supplied by NAWC for this RTM analysis was collected during two 2-hour periods between 0900 and 1100 on the 9th and 10th of July, 1997. After the field tests were completed and during the initial period of data analysis, it was realized that there was an inherent built-in variable time error present if one were to use the man-in-the-loop input for determining when a target emerged from (or entered into) the shadow of a mountain due to terrain masking. Therefore, it was concluded that the only reliable indicator of LOS contact between the radar and the moving target was the receipt by the

10

radar site of the I-band signal that was being generated by the low power jamming pod on the EA-6B. Since the EA-6B was the only platform to have this pod, the decision was agreed to by both NAWC and NPS to use this combination of I-band signal and its appearance on the FSA at the radar site, as the only dependable signal for accurately measuring the time tic of when these RTM events occurred. With the time then accurately fixed on both the radar site and the aircraft, these RTM events could be accurately plotted. This procedure is more fully explained in the next section of the report. As events turned out, because of a failure of the GPS pod on the EA-6B to operate properly during the first days runs, all data from the July 9th flight test was eliminated from this study. Editorial inputs from VX-9 follow.

TSPI Anomalies. Several points in the flight database plotted well inside the detection line envelopes of IMOM and AFMSS. Upon further analysis of the raw time-space-position information (TSPI) data streams, the following explanations were found:

#	Time	Explanation
1	161315	A/C in climb
2	161405	A/C in climb
3	163043	A/C in climb
4	170333	A/C in climb
5	171606	A/C in climb
6	171624	A/C maneuvering (beginning descent)
7	171734	A/C maneuvering (leveling from descent)
8	172954	RTM for 7k, A/C at 2K
9	173048	RTM for 7k, A/C at 2K
10	173508	TSPI error wrong A/C (no TSPI available for EA-6B)
11	174214	TSPI error wrong A/C (no TSPI available for EA-6B)
12	174222	TSPI error wrong A/C (no TSPI available for EA-6B)

It was found that the aircraft flight path for each of the first five cases was a steep climb from a masked region into the unmasked region (aircraft was resetting from the end of one data run to begin the next). Thus these are valid "popup" target points, but reflect some delays in detection due to aircraft maneuvering. Aircraft maneuvering also affected points 6 and 7. The FSA collected energy from an EA-6B J band jamming pod (essentially a high power, directional beacon). The pod antenna is only stabilized in two dimensions, and may not be able to point toward a ground site while the aircraft is in steep climbs or descents, or while the aircraft is maneuvering aggressively. Points 8 and 9 were valid, but the IMOM plots were done at the wrong altitude. Agreement should be better if replotted for an aircraft at 2000' AGL vice 7000' AGL. Points 10-12 had TSPI from the wrong aircraft. Data for the EA-6B was not available for these times. VX-9 recommends we remove points 1-7 and 10-12 from the database. Points 8 and 9 are valid and should remain.

b. Raw Data Screening

As the testing progressed at NAWC, it soon became apparent that using the recorded time of the operator sighting the target by observation of that target on the radar CRT, was not going to be a workable technique. The problem that arose was tied to the fact that there was a finite time required (somewhere between 6 to 8 seconds) for the radar antenna to rotate through one complete revolution. If the target a/c flew out of a RTM position at a time immediately after the sweep passed on the particular bearing angle of the target,

then this fact would not be detected by the man-in-the-loop observing the signal on the CRT until up to 8 seconds later in time. With the nearness of the targets in range, and their high rate of speed, this lag could introduce an enormous error in the human observations with the "truth" of the situation. This would have of course provided an inaccurate picture of reality. The IMOM model assumed a non-rotating antenna. Further, it was impossible to coordinate the sweeps of the real antenna to avoid this variable man-in-the-loop delay.

Given this realization, it was determined that the only data that could be confidently used to provide the reality desired in the test, was the time at which the FSA signal appeared (or disappeared) and was confirmed by optical confirmations of the slaved video recording that optical confirmation, at the same time tic as the FSA readings. This screening process was then applied to about 85 sets of data runs, resulting initially in about 40 sets of acceptable raw data runs.

Prior to this process, of the thousands of acquisition and drop track events also initially reviewed by NAWC, it was determined that most were related to slew rate or clutter rather than terrain masking and therefore NAWC eliminated this data from earlier consideration. At that time the remaining points which NAWC determined to be valid were confirmed to be terrain impacted events by viewing tagged videos of the various optical systems co-located with emitters of interest, while at the same time observing terrain impacting of the optical line of sight. The radar track data was not directly correlated to which aircraft was being tracked. Consequently, NAWC had to perform this correlation manually by reviewing video tapes to identify the target either visually or by run number and azimuth. NAWC then faxed 37 pages of vertical profile data to NPS for

analysis. These 40 runs represented what they thought were the most revelant cases of acquisition or drop track near or beyond the optical line of sight. NAWC made the determination as explained above, that at the conclusion of data screening, the only reliable and useful data was that received from the EA-6B platform. Consequently, data from the remaining two aircraft were not analyzed by NPS. Additional inputs from VX-9 are included below:

(1) PHYSICAL TEST ELEMENTS. Three different aircraft were used for test: two fixed wing (FA-18, EA-6B), and one rotary wing (AH-1W). These targets were tracked by two actual threat SAM radar systems (J-17, I-5), two actual threat surveillance radar systems (A-2, E-12), one threat gun radar simulator (J-1), and a frequency spectrum analyzer (FSA) each with co-located optical camera systems. In addition, three Nike tracking radars provided three-dimensional time-space-position information (TSPI) data for the AH-1 helicopter, and for the EA-6B during the first day when its GPS pod failed. The test range layout and location of the various threat systems is depicted in Attachment 1.

The aircraft flight paths were designed to ensure periods of masking and tracking for each system and passed over two prominent surveyed terrain features: Slate Peak to the northwest, and Pilot Knob to the west (see Attachment 1). The aircraft flight paths are shown in Attachment 1.

The EA-6B was configured with a J-band jamming pod steered to always radiate directionally toward the FSA. This signal was specifically

14

tailored so as not to interfere with any of the tracking systems, but rather to function as a high power directional beacon for the FSA to determine when RF energy could be seen by the ground-based receiver. The FSA receiver was omni-directional.

(2) RAW DATA. The raw data collected included:

- TSPI data for each aircraft at 1 second intervals

- Time tagged video of weapon radar and FSA displays

- Time tagged video of all weapon optics

- Time audio recording of radar operator voice network including acquisition and drop track calls

The desired set of data was the unmask (ACQ) and mask (DRP) points for all aircraft at various altitudes for each system. The set of these points would be used to define the empirical boundaries of the actual RTM envelope for each site, and would be used as truth data by which to evaluate the three models. ACQ and DRP events were manually correlated to associated optics video to discriminate only those events positively associated with terrain masking (i.e., eliminate tracking problems from clutter, slew rate, operator confusion, etc.). All surviving ACQ and DRP events (~250) were entered into a spreadsheet, and also into TAMPS as three-dimensional route points.

(1) INITIAL ANALYSIS AND DATA FILTERING. TAMPS' vertical profile function (Attachment 1) was used to view the terrain between the aircraft and the ground site for each data point to get a first cut at how the point

15

compared to optical LOS. In this initial analysis several observations were made:

1. The radar line of sight for the tracking radars associated with J-17 and I-5 was near indiscernable from the optical line of sight. All radar ACQ points occurred coincident with or just after optical LOS was observed through the associated weapon optics. Most DRP points were coincident with optical masking, and none extended more than 1 second beyond the point where the aircraft was visually observed to be masked. These data points, which were the most numerous collected, seem to indicate that **an optical line of sight is a better approximation of the realistic engagement envelope of tracking and missile guidance radars**. This finding is not surprising when considering their narrow field of view, requirements for precision cueing for acquisition, and need to maintain a high data update rate. Since these points were virtually indistinguishable from the optical LOS, they were not used toward resolving the accuracy of the radar range equations (RRE) used by the three models which each assume radar refraction effects beyond the optical LOS.

2. The ACQ and DRP points for the surveillance radars (A-2 and E-12) fell well inside the modeled RTM envelopes, and usually within the optical LOS as well. The surveillance radars used in this test were older generation systems with 6-10 second circular scan periods and operator displays which required extensive manual interpretation. The delays introduced by the scan period and operator recognition of tracks probably

16

explain these results. These points remained in the spreadsheet database, but are probably not indicative of the capabilities of newer generation EW/GCI/ACQ radars, and were not used in this study.

3. It soon became apparent that the most promising system for finding points out to the classic radar LOS was the FSA. Initial investigation using the TAMPS vertical profile tool proved this out. Thirty-seven FSA ACQ and DRP points were identified as near or beyond optical LOS, and were highlighted for use by all the test teams against the TAMPS, AFMSS, and IMOM model predictions. These results are the subject of the balance of this report.

a. IMOM Accuracy Determination Procedure

Once a track passed the screening for reliability of field test data and passed on to NPS, the true latitude and longitude of the a/c radar track acquisition (or drop) point was established and plotted. An IMOM simulation was then run at NPS using the characteristics of a typical generic search radar which was taken to be located at the Lat/Long location of the actual test site radar. The target for this IMOM analysis was assumed to be one with a fixed RCS of 10 square meters on the actual flight path of the target. The resulting IMOM rings display would then be examined and superimposed on the same plot as that previously showing the target location determined with the radar data. That single ray of the IMOM plot on the bearing of the Lat/Long position of the a/c would be highlighted. The end of the rays' length (for maximum range of detection) would be marked on the plot and the Lat/Long recorded.

17

The distance between the two plotted points, the point where the target was first detected (or dropped) by the radar, and the second point where IMOM predicted this would occur, was compared. This distance was defined as the IMOM "error", assuming that the actual field test data for this occurrence was "truth". This information is summarized and presented in Table 1.

5. SUMMARY OF DATA COMPARISON

Choosing the runs where the confidence level was high enough that all systems in the test range were operating satisfactorily, an outline of the analytical steps taken by NPS is summarized below:

a. Establish the time the FSA equipment at the radar site received the J-band signal from the EA-6B that was in view.

b. Confirm the validity of this sighting by examining videos of the optical receiver at that site at that time.

c. Run the IMOM printout for a radar at the Lat/Long of the chosen site and printout two displays: ring display and vertical beam display.

d. The inputs to the IMOM run consist of:

      1) Radar site location

      2) Characteristics of generic search radar

      3) a/c RCS of 10 square meters

      4) Terrain resolution 3 arc-seconds

Table 1: Terrain Masking Accuracy Comparison

Run#	Reference	Signal Cut-Off Location	Calculated Range @ Cut-Off		Linear Discrepancy IMOM to Actual	
		Actual Lat - Long (All "N") (ALL "W")	IMOM	Actual*	nmiles	%
A	161129	360409 1165120	47.3	47.3	0	0
B	161315 ** Error - Aircraft in Climb	360254 1165442	44.9	44.9	2.7	5%
C	161405 ** Error - Aircraft in Climb	360703 1165342	48.8	50.2	3.9	7%
D	161553	360348 1165059	47.1	47.1	0	0
E	163003	355909 1165301	42.3	42.3	0	0
F	163043 ** Error - Aircraft in Climb	355823 1165013	43.2	46.0	2.8	3%
G	164009	352401 1170431	14.6	14.6	0	0
H	164025	352318 1170301	15.9	15.9	0	0
I	164114	352137 1165814	19.9	19.9	0	0
J	164210	352455 1165655	20.9	20.7	0.2	1%
K	164226	352426 1165812	19.8	19.8	0	0
L	164514	352347 1170516	14.0	14.0	0	0
M	165026	354424 1170454	24.9	27.5	2.6	11%

N	165920	352352 1171309	7.6	7.6	0	0
O	170245	353812 1171032	17.1	16.2	0.9	6%
P	170333	353938 1170523	20.9	21.9	1.0	5%

** Error - Aircraft in Climb

Q	170606	352716 1165744	20.4	20.4	0	0
R	170633	352508 1165625	21.3	21.3	0.5	2.5%
S	170731	352120 1165640	21.2	21.2	0	0
T	170742	352133 1165738	20.4	21.0	.6	3%
U	170851	352556 1165604	21.6	21.6	0	0
V	171156	352352 1171327	7.3	7.5	0.2	2.5%
W	171210	352349 1171529	5.7	5.5	0.2	5%
X	171226	352349 1171759	3.6	3.6	0	0
Y	171506	353740 1171057	16.5	16.5	0	0

** If you connect the two rings at 34 degs and 35 degs, target on the mark

Z	171606	353918 1170417	21.3	21.3	*	*

** Error - Aircraft in Climb

AA	171624	353756 1170341	20.6	20.6	*	*

** Error - Aircraft Maneuvering (Beginning Descent)

BB	171734	353244 1170052	19.7	19.7	*	*

** Error - Aircraft Maneuvering

CC	171757	353100 1165952	19.7	19.7	0.5	1%
DD	171835	352809 1165821	20.1	20.1	0	0

EE	171919	352451 1165640	21.1	21.1	0.5	3%
FF	172142	352414 1170012	18.1	18.1	0	0
GG	172954	354227 1170134	25.0	25.0	*	*
	** Error					
HH	173048	353837 1170018	23.1	23.1	*	*
	** Error					
II	173459	352425 1165850	19.2	19.2	0	0
JJ	173508	352509 1165850	*	*	*	*
	** Error - Wrong Aircraft					
KK	173747	352351 1171322	7.4	7.7	0.3	1%
LL	174106	353759 1171052	16.8	16.8	0	0
MM	174214	353935 1170426	21.4	21.4	*	*
	** Error - Wrong Aircraft					
OO	174222	353854 1170410	21.0	21.0	*	*
	** Error - Wrong Aircraft					

* No Data Point

** Error – Type Determined by VX-9

Actual = Point of Radar/IMOM Site to transition Location

Comparison determined from measurements on Fig. numbers 1 & 2

e. Prepare a superimposed Lat/Long plot on the IMOM ray plot of the radar site location and the location of the FSA indicated acquisition (or drop) point.Select the IMOM ray on the bearing from the radar site to the a/c target.

f. Determine the 'end' of that ray, indicating the range at which the target should appear (or disappear).

g. Plot the Lat/Long of the end of that ray.

h. Measure the linear distance from the point plotted in e to that plotted in g.

This linear distance is then considered the "error" of the IMOM predictive algorithm.

6. ACCURACY ANOMALY ON JULY 10

An unusual anomaly appeared in the results from the last 15 runs on the July 10th field test. The accuracy analysis summary of the field test results under consideration are pictured in Table 1. In particular, attention is focused on the results of the last 15 runs toward the end of the day. We note that in the first 25 runs of the day, there was an average error of about 2%, with only one even approaching a 10% error. Then the next three runs had an error in excess of 100%. This bimodal distribution continued until the end of the last 15 runs, with the 'better' runs having an error distribution much like the first 25.

This appears to be an illogical pattern indicating that perhaps there was something else coming into play in these last 15 runs that was not present in the earlier 25 runs. It could be hypothesized that some test equipment failure may have been introduced unexpectedly into the tests that resulted in the sudden 'out of the ballpark' results. In fact, in looking at the GPS pod problems that forced the rejection of the entire first days data,

it is believed that these problems may have begun to appear late in the second days test sequence, causing the errant behavior in test results.

7. RELATED TOPICS

a. Earth 4/3 Radius Assumption

In order to simplify the conceptual plotting of information in line of sight radar predictions, engineers often approach the mathematical modeling of the propagation of radar waves over the earth's surface by applying certain simplifications. One of these very commonly used procedures, called the "4/3 earth approximation" has been incorporated in the IMOM computer code. During the course of this study, the question arose as to whether or not the printed data displayed by IMOM is equivalent to the results that would have been obtained by having calculated direction ranges using simply basic theory of propagation models.

Wave propagation of radar transmission over the earth's surface can be approached by imagining the earth to be an ideally smooth sphere. Then the straight line from a point at a height h above the earth is tangent to the earth's surface as illustrated in Figure 1.
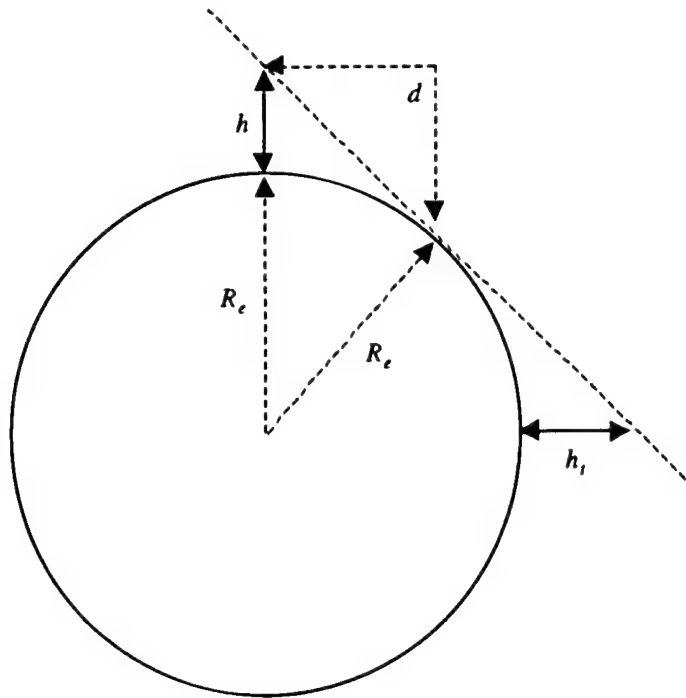
Figure 1: Tangent line.

The distance d to the tangent point is one side of a right triangle, and its length is calculated from the equation

$$d^2 = (R_e + h)^2 - R_e^2 \tag{1}$$

from which d can be solved for

$$d = (2R_e h + h^2)^{1/2} \tag{2}$$

If the height h is very small compared to R_e (with R_e being the earth's radius) this approximation is always the case and then d can be found by simplifying Equation (2) to

$$d = (2R_e h)^{1/2} \tag{3}$$

Substituting the earth's radius as 21×10^6 feet, and expressing h in feet and d in nautical miles (NM), then this equation simplifies to

24

$$d = 1.07h^{1/2} \qquad\qquad (4)$$

This is the distance to the tangent point from a position h feet above the surface of a perfectly round earth. The distance d_t, to a farther point along this tangent line at height h_t above the earth's surface can be determined by adding a second term, as shown below:

$$d_t = 1.07\left(h^{1/2} + h_t^{1/2}\right) \qquad\qquad (5)$$

The radar line of sight distance differs only in the bending of radar waves over the earth's surface. This bending extends the radar horizon, just as optical wave bending extends the optical horizon. A commonly accepted way to account for this increase radar line of sight is to increase the earth's radius in the above equation by a factor of 4/3rds. Making this change, and using ha to represent the radar antenna's height, the radar line sight then becomes:

$$\text{Radar LOS} = 1.23\left(h_a^{1/2} + h_t^{1/2}\right) \qquad\qquad (6)$$

This is the basic equation to estimate radar line of sight in NM for any antenna or target height in feet. Note that if both heights are expressed in meters, the constant changes from 1.23 to 2.23 with LOS still measured in NM. Furthermore, in diagramming these relationships one can now represent the earth as a flat surface rather than a small portion of a sphere, thus simplifying the conceptual aspects to the problem.

The earth "mask" therefore, can now be considered to be at the radar line of sight. Any target beyond this radar LOS will be assumed to be outside the radar coverage. Masking around a radar on a perfectly round earth would show as a circle of radius LOS, as depicted in Figure 2.

To confirm whether this theory is in agreement with the predictions that IMOM provides, a simple series of IMOM plots were run and the maximum radar detection range was then determined by measuring the length of the IMOM plotted rays. These values were then compared with similarly calculated values derived from substitutions into the basic Equation (6) from above.
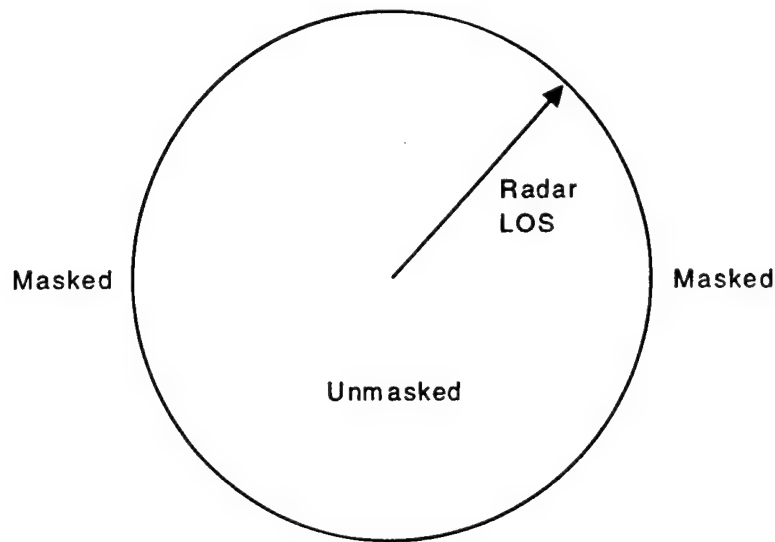
Figure 2: Masking for a perfectly round earth.

The IMOM radar was chosen as one electronically generic to the types located in sites J-1E-12, A-2, I-5, and J-17. A platform target with an RCS of 10 square miles was selected and placed at three selected altitudes: 500 feet, 5000 feet, and 10,000 feet. The resulting comparison table is shown in Table 2.

Table 2

Platform Altitude	Range of Detection	
(feet)	calculated	from IMOM plot
500	31.95 NM	32.0 NM
5000	91.42 NM	91.4 NM
10,000	127.45 NM	127.5 NM

The IMOM ray and vertical beam plots used to measure these values are shown in Figure 3 and Figure 4, respectively, in the attachments. These results do indeed confirm that the IMOM program does agree with the 4/3 earth theory predictions derived from the basic equations.

b. IMOM Defense Mapping Terrain Resolution

There are two possible terrain resolutions, 3-arc second and 15 arc-second, that can be selected when employing the DMA terrain data in IMOM plots. NPS experimented with using both resolutions. From a running time to obtain a solution point of view, there is no question that the 15 arc-second is faster. IMOM could calculate a ring display in less than a minute using 15 arc-second inputs, while it took on average nine minutes to calculate a ring display in 3 arc-second data. In both cases a SUN SPARC 10 workstation was employed with an 80 MHz processor (of course if a 300 MHz processor had been used, there would have been a considerable saving in run time).

However, this angular resolution difference when translated into ground truth measurements was considerable. A 3 arc-second resolution yields a 300 foot ground resolution, while the 15 arc-second resolution degrades to a 1500 foot view. This

difference was considered too great to allow us to select the choice which offered the most convenient (shorter) time when one considers that entire mountain tops at China Lake can be missed within a distance of 1500 feet. So, despite the longer run times required, all data used in this study employed the 3 arc-second DMA terrain data.

c. Generic IMOM Radar Selection

Since the IMOM plots required the input of the electrical characteristics of a specific radar, and our test set up on the ground used four separate radars, NPS chose to use a composite radar of a generic nature, that was then fed into IMOM for the purposes of producing predicted results. The specifications of this generic system were based on a typical high power value of 270 kilowats, good receiver minimum detectable signal capability of −100 dBm, and with an antenna pattern having beam elevations ranging from 2 to 83 degrees from the horizontal.

It should be kept in mind that the latitude and longitude determination of all aircraft platforms at the time of either track acquisition or track drop, were actually determined by the signals either received or dropped from the frequency spectrum analyzer (FSA) at the radar site. This receiver was being employed (with visual detection back-up confirmed from the recorded videos) as an LOS detector of transmissions from the J-band transmitter pod on the EA-6B platform. So in no case were these target locations based on responses from any of the radars being used during the tests.
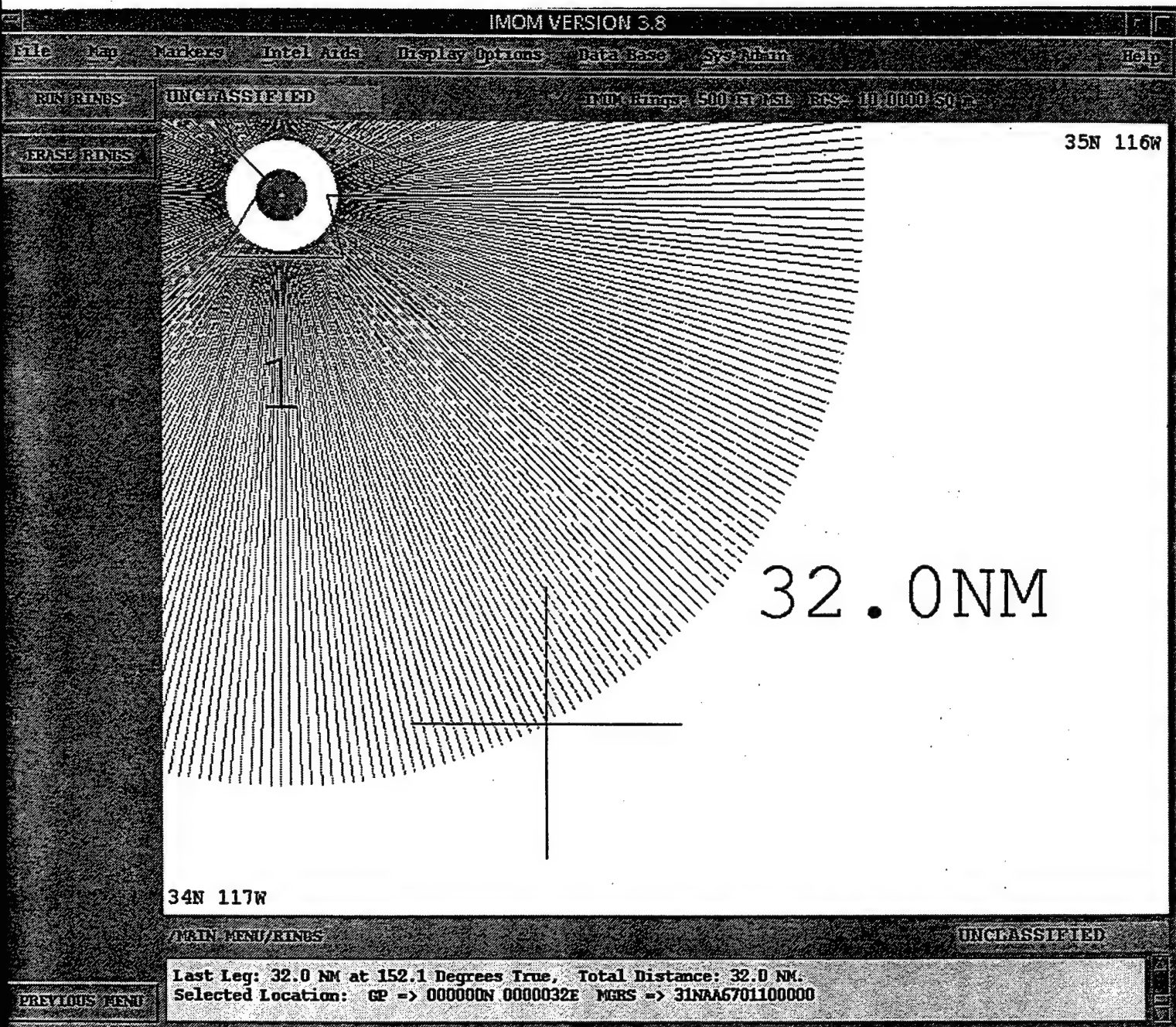
Figure 3: Ray plot, 32.0 NM.
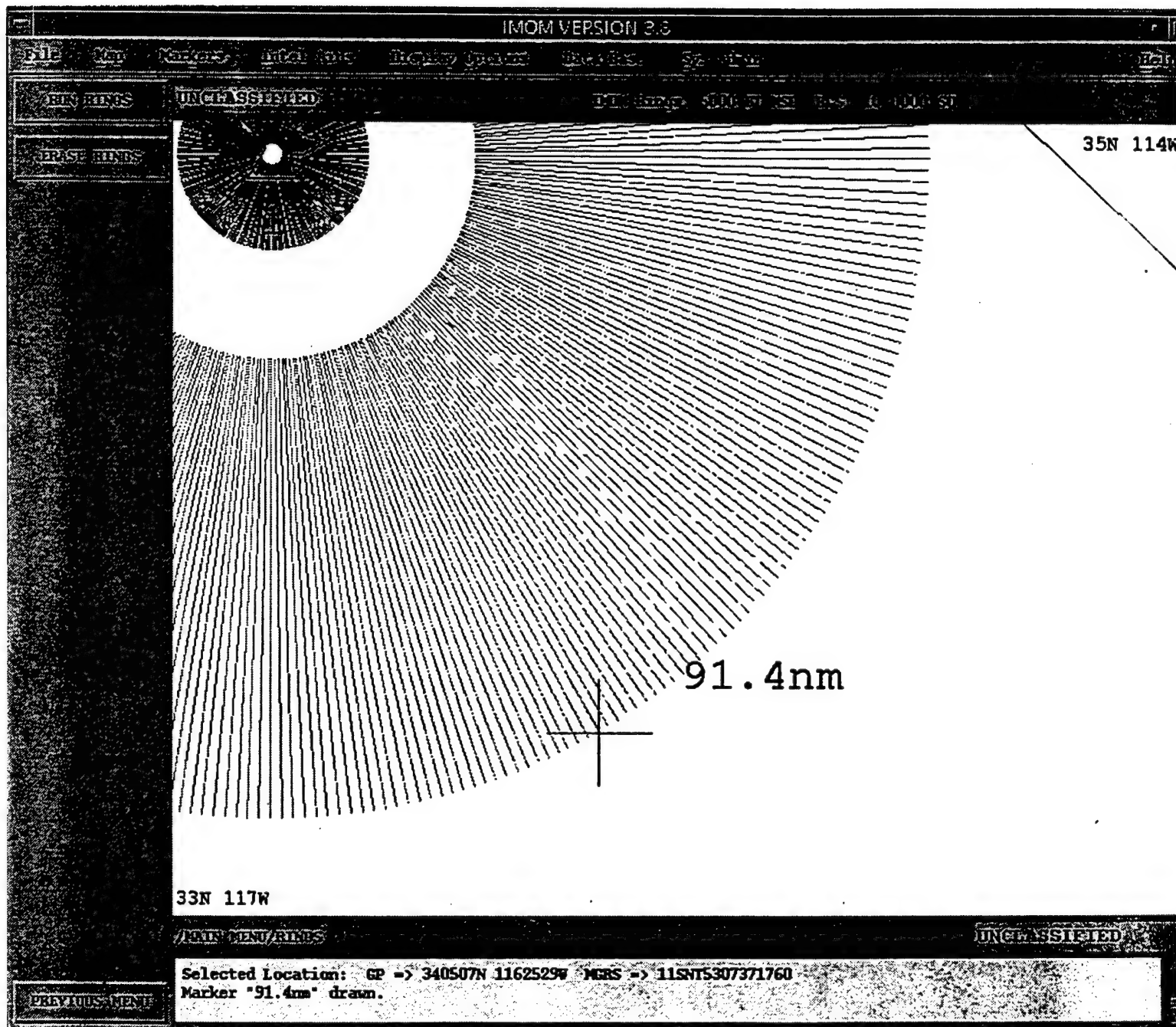
Figure 3: Ray plot, 91.4 NM.
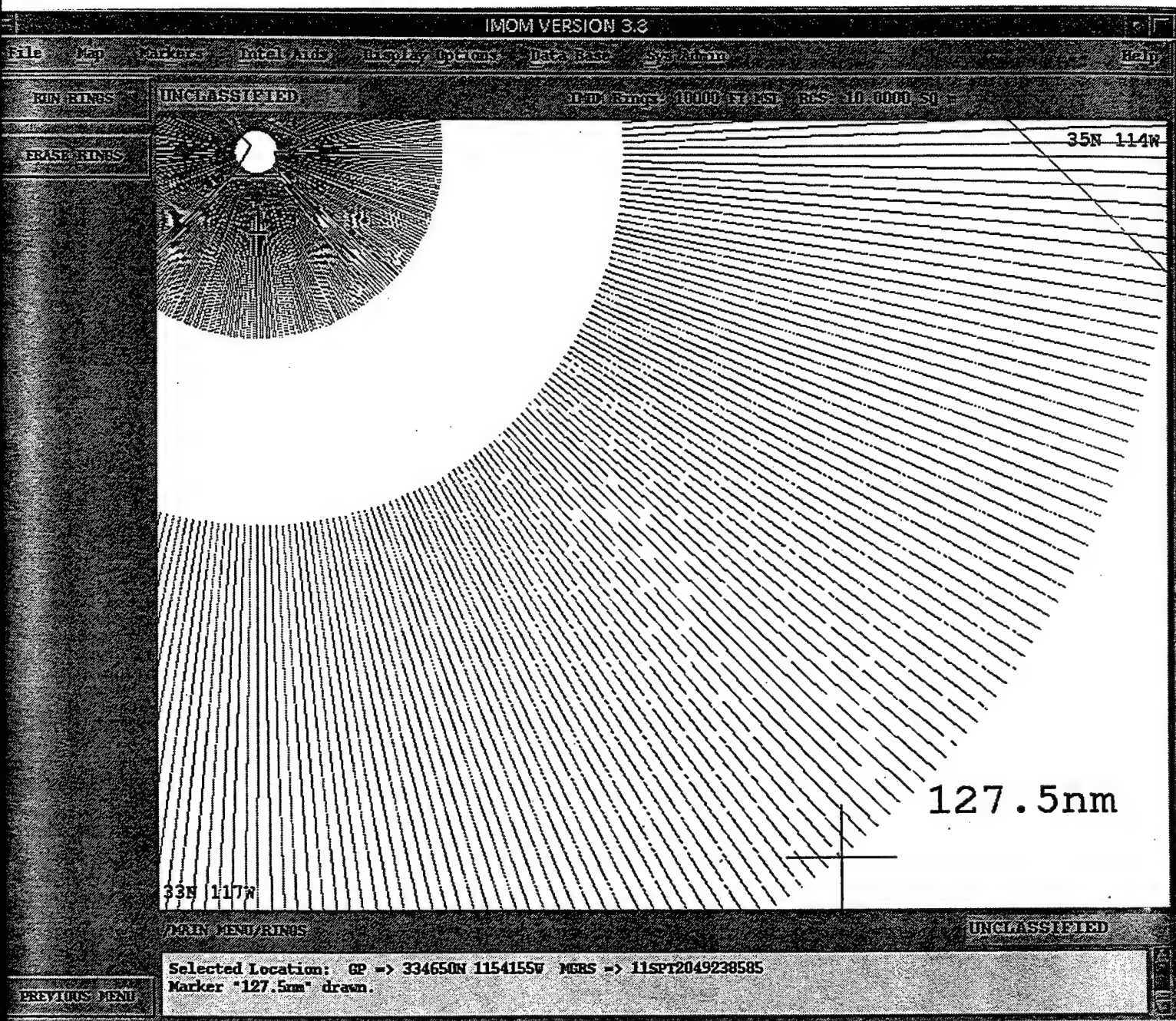
Figure 3: Ray plot, 127.5 NM.
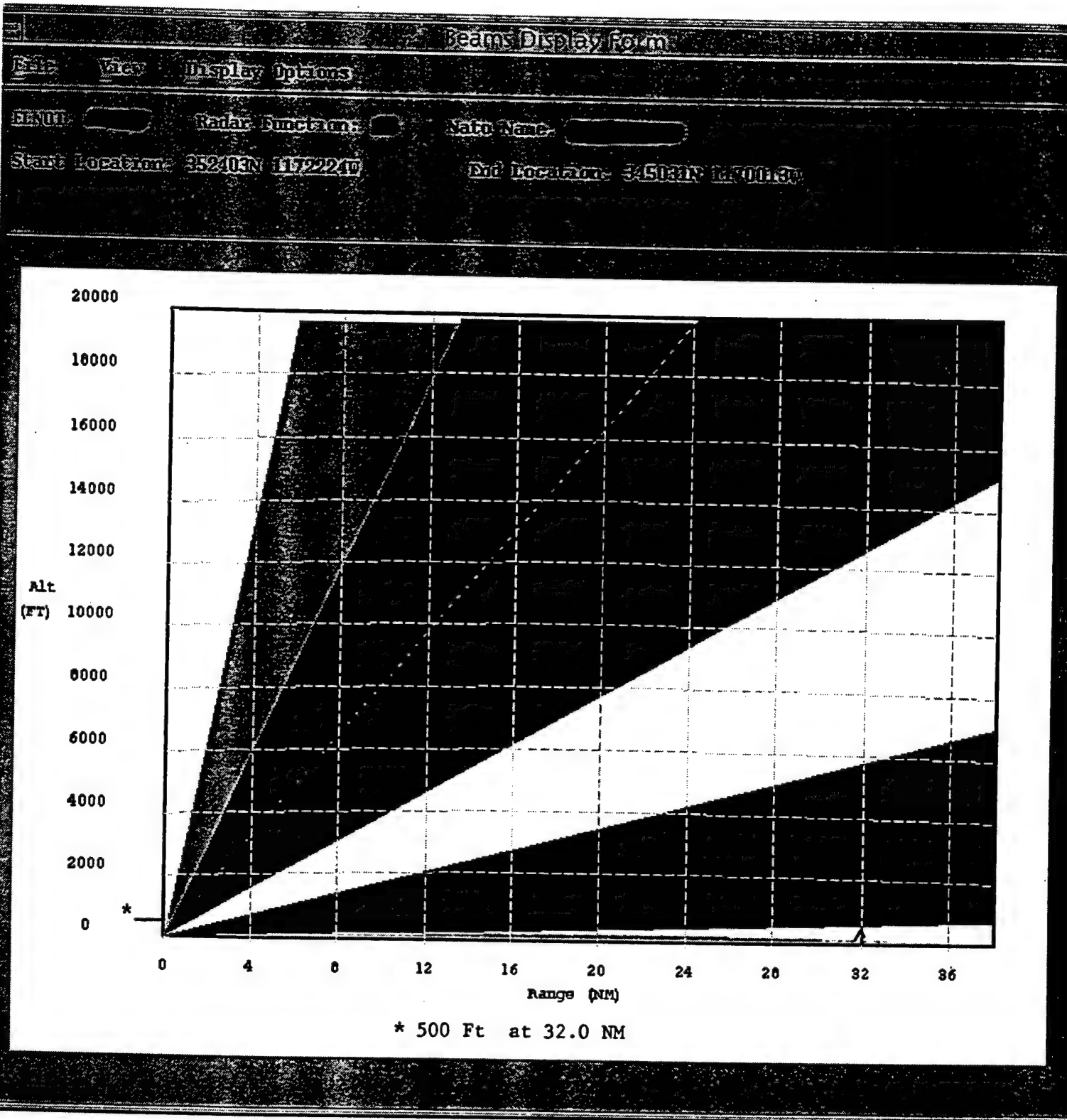
Figure 4: Vertical plot, 500 ft at 32.0 NM.
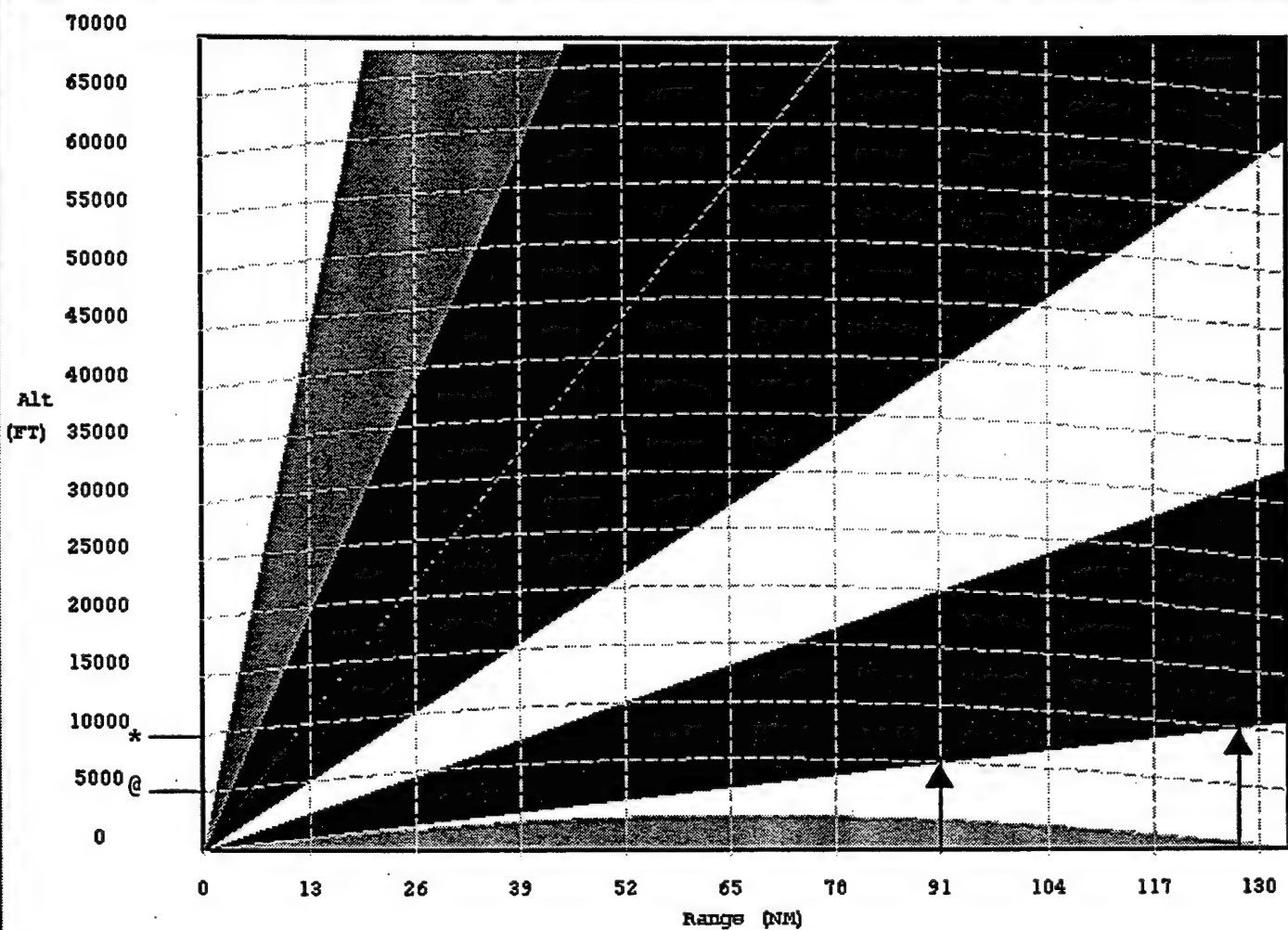
Figure 4: Vertical plot, 5000 ft at 91.4 NM and 10,000 ft at 127.5 NM.

33

8. CONCLUSION

Taking into account the anomaly of the July 10th data as was described in Section 6, we can calculate the total average error of the IMOM results compared to field test results from several points of view. We can, for example as choice [a], first employ all the data gathered from all 40 runs. Secondly, as choice [b] we can break the data down into two different categories. First, simply using all the data with no regard to any judgement on the quality of the data. Or second, we can apply some judgement to the data based on what appears to be an anomaly found in the test process, which appears to be not attributable to the performance of the predictive ability of the IMOM program. With these possible logical choices for analysis (examining Figure 5) we find of the second choice in [b] the results to be: 32 data points = 2.38% average error. The eight points that resulted in readings with errors in excess of 100% were so far from any reasonable reality in fact, that it was deemed highly probable that these errors were caused by some problem unrelated to the IMOM model calculations. These errors could have resulted from possibly (but not exclusively) a GPS malfunction (again), or an error in the translation of data between the various platforms and the test sites. It is the considered opinion of the NPS research team that the most probable ability of the IMOM modeling system in predicting the affects of RTM in a mission planning scenario is best represented by the accuracy displayed in choice b above.

Figure 5: IMOM accuracy distribution of July 10th FSA runs at NAWC China Lake (error anamoly indicated).

ATTACHMENTS

1. VX-9 – NPS – AFIWC RTM Study

2. Terrain Masking Plots

ATTACHMENT 1

VX-9-NPS-AFIWC RTM Study

VX-9 ⊕ NPS ⊕ AFIWC
RTM Study

REVISED 980318 by VX-9
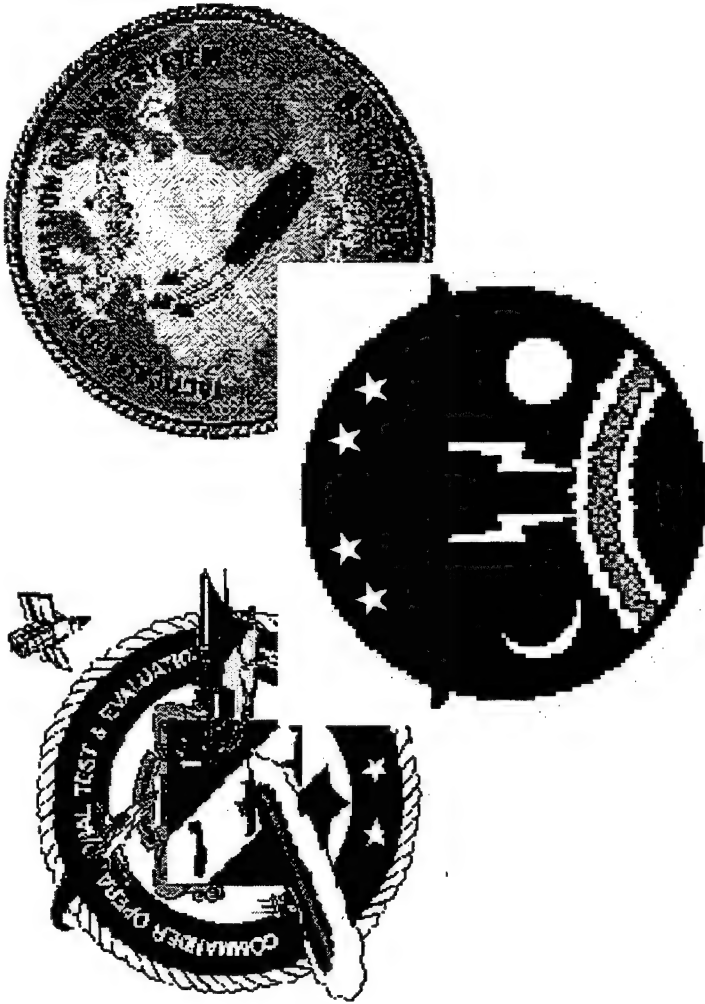
Outline

- **Objectives**

- **Test Range Setup**

- **Flight Test Data**

  – Collection, Filtering

- **TAMPS Products/Problems**

  – RTM, Vertical Profile

Objectives

- Validate accuracy and utility of TAMPS, IMOM, and AFMSS RTM models

- Examine accuracy of 4/3 Earth radius LOS equations

- Explore differences in LOS for passive vs. active detection (one way vs. two way propagation)

R-2524 Echo Range Emitters
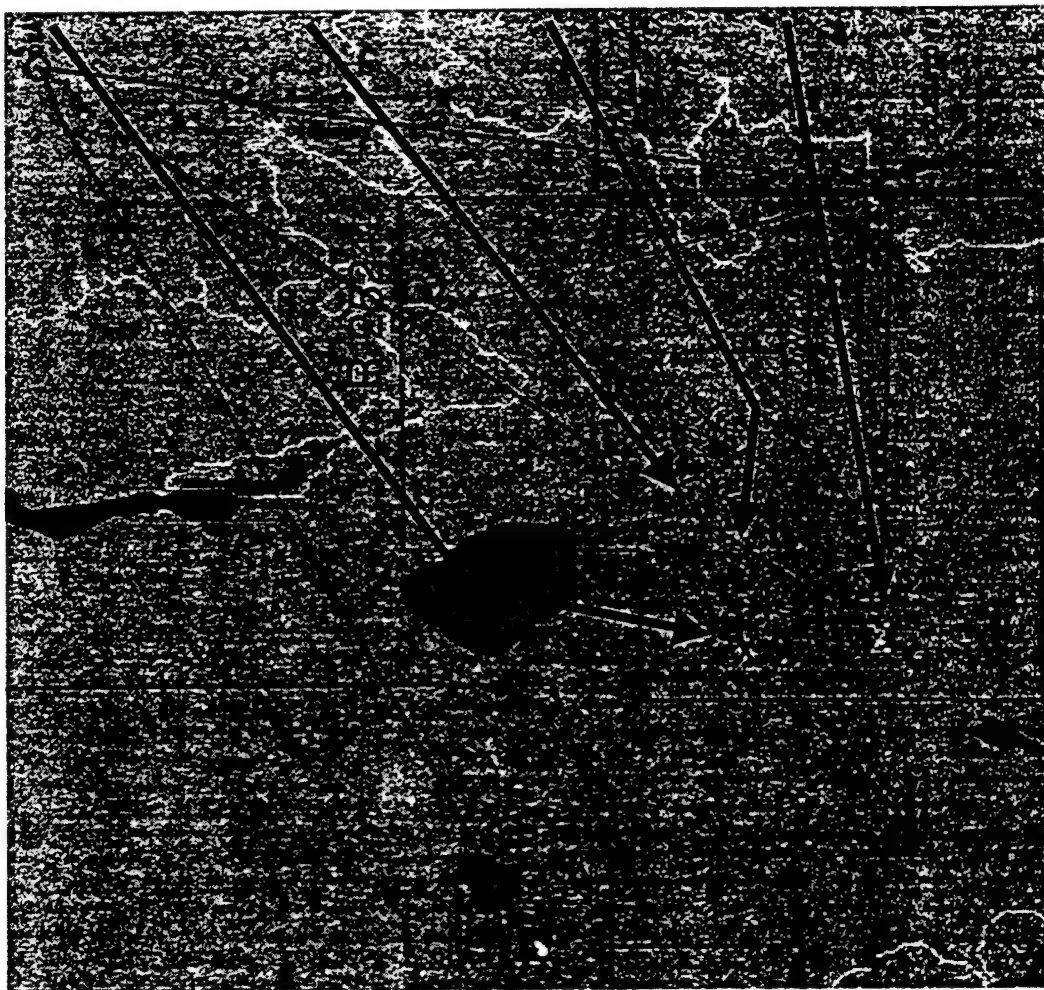
- A2
N35:31:05
W117:19:16
2501'

- J17
N35:32:31
W117:15:54
2332'

- I5
N35:31:23
W117:18:18
2480'

- E12, J1, FSA
N35:24:04
W117:22:25
3224'

Major Obstructing Terrain Features

ID	LATITUDE LONGITUDE	ALT: MODE	CR: MODE	HD: S TRU TRU M MAG MAG C
0	35:41:15N 117:41:26W	0 A	000 346	000 346
1	36:05:38N 116:47:59W	-242M	060 046	060 046
2	35:48:00N 117:03:02W	310dM	215 201	215 201
3	35:57:16N 117:11:31W	5534M	213 19	215 199
4	35:24:04N 117:22:25W	3195M	214 200	214 200
5	35:23:40N 117:13:36W	5337M	092 078	092 078
6	35:23:20N 116:55:00W	3093M	092 070	092 078

DEATH
MINT
STRAW
NATO
KNOB
STONE

Straw Peak
Pilot Knob

Aircraft Track Waypoints

ID	LATITUDE LONGITUDE	ALT: MODE	CR: TRU MAG	HD: TRU MAG	S M C
0	35:41:15N 117:41:26W	0 A	000 346	000 346	
1 DEATH	36:05:38N 116:47:59W	-242M	060 066	060 046	
2 MINT	35:48:00N 117:03:02W	3106M	215 201	215 201	
3 STRAW	35:37:16N 117:11:3?W	5534M	213 199	213 199	
4 NATO	35:24:04N 117:22:25W	3195M	214 200	214 200	
5 KNOB	35:23:4?N 117:13:36W	5337M	092 078	092 078	
6 STOKE	35:23:20N 116:55:?0N	3093M	092 078	092 078	
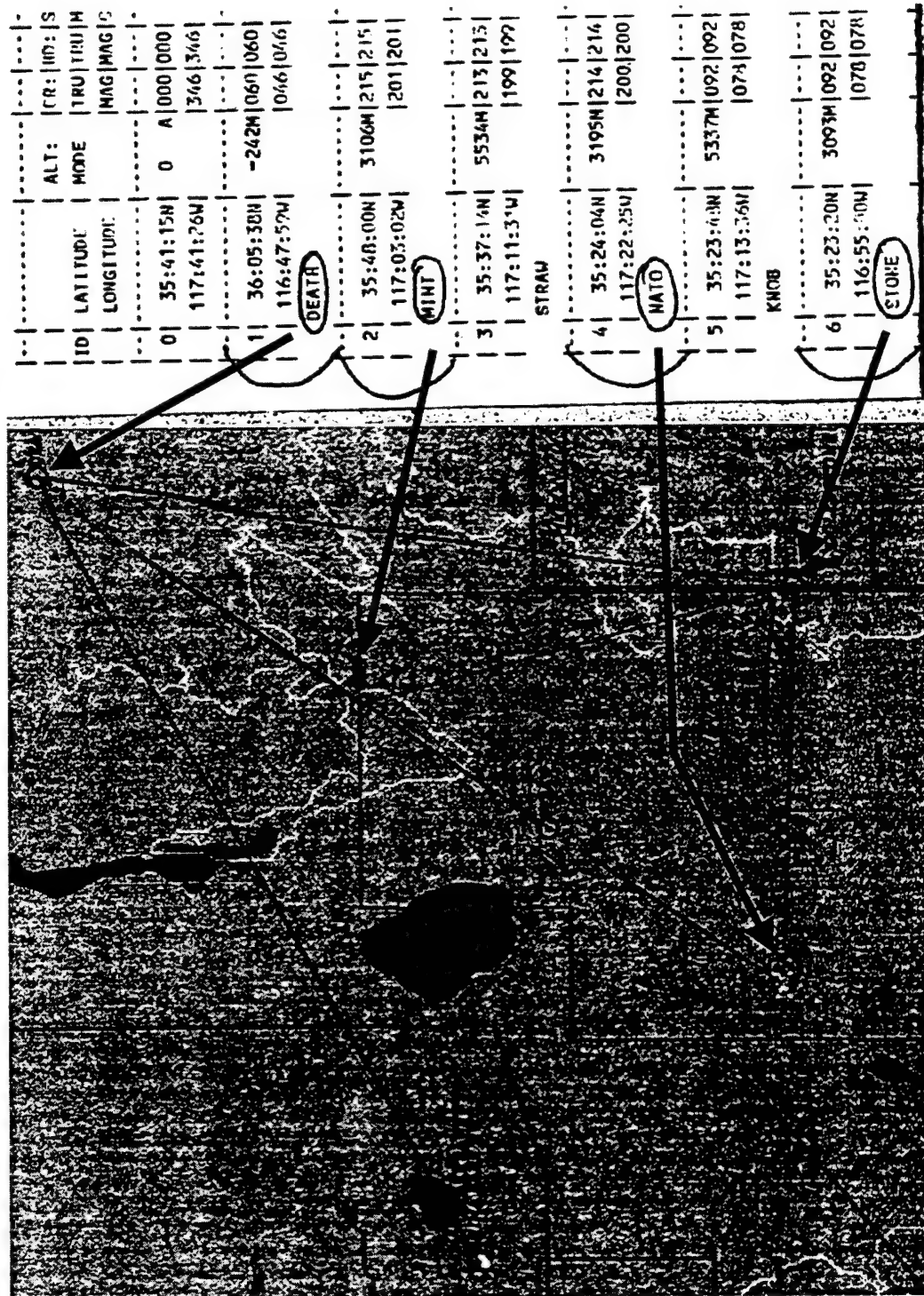
Data Run Ground Tracks
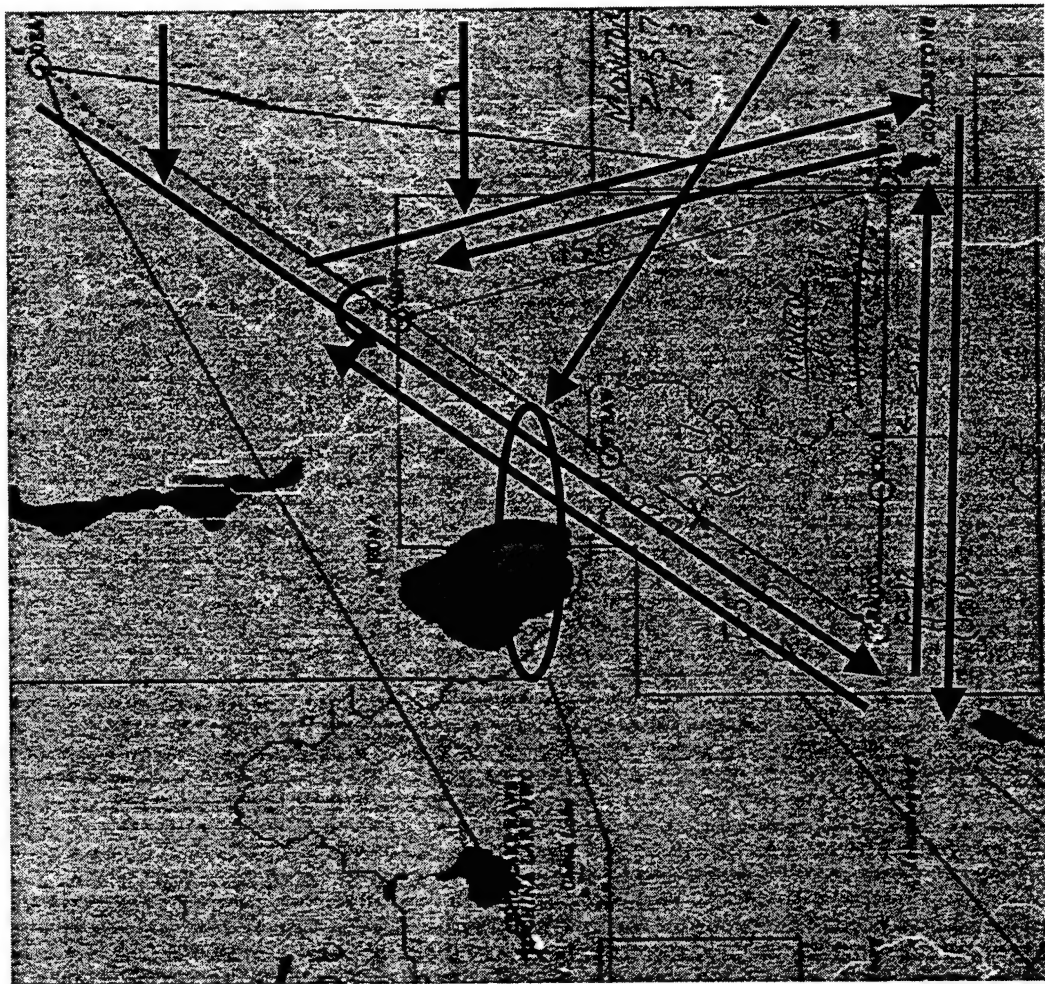
- Track flown exclusively by EA-6B

- Track flown by EA-6B, FA-18, and AH-1W (CW and CCW directions)

- Hover operating area for AH-1W

Data Collection/Filtering

- High precision 3D location data (lat/long/alt) at for FA-18 and EA-6B from fully encrypted GPS telemetry pods on A/C. (EA-6B pod worked only on 7/10/97)

- High precision 3D location data for AH-1W from Nike tracking radars.

- Threat systems and frequency spectrum analyzer (FSA) acquisition (ACQ) and drop track (DRP) times deduced from time-tagged operator voice audio, scope video, and weapon optics video.

- All data correlated to nearest second in time.

- ACQ and DRP events manually correlated to associated optics video to discriminate only those events positively associated with terrain masking (i.e., eliminate tracking problems from clutter, slew rate, operator confusion, etc.)

- All surviving ACQ and DRP events (~250) entered into Excel spreadsheet and also into TAMPS as 3D route points.

- TAMPS vertical profile function used to cull out 37 "interesting" points which appeared to be at or beyond optical LOS.

- Excel spreadsheet and 37 vertical profiles distributed to NPS and AFIWC.

44

TAMPS Vertical Profile
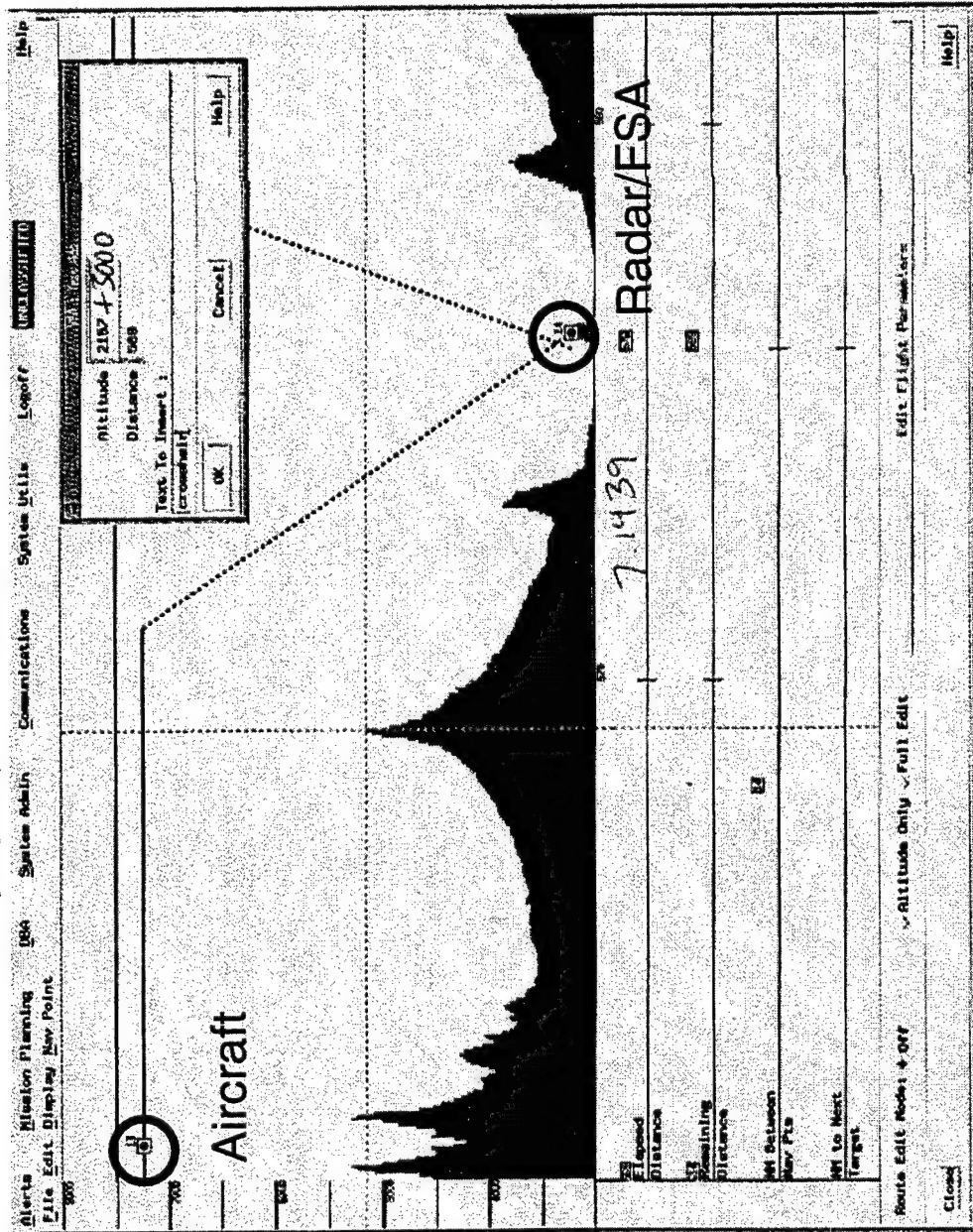
- DTED slice along azimuth between site and aircraft

- Used to determine terrain elevation and downrange distance of obstructing point (crosshair)

- Plot does not reflect curvature of Earth

- 37 data points chosen for further analysis based on this plot indicating near or beyond optical LOS

164009   FSA

Aircraft

Radar/FSA
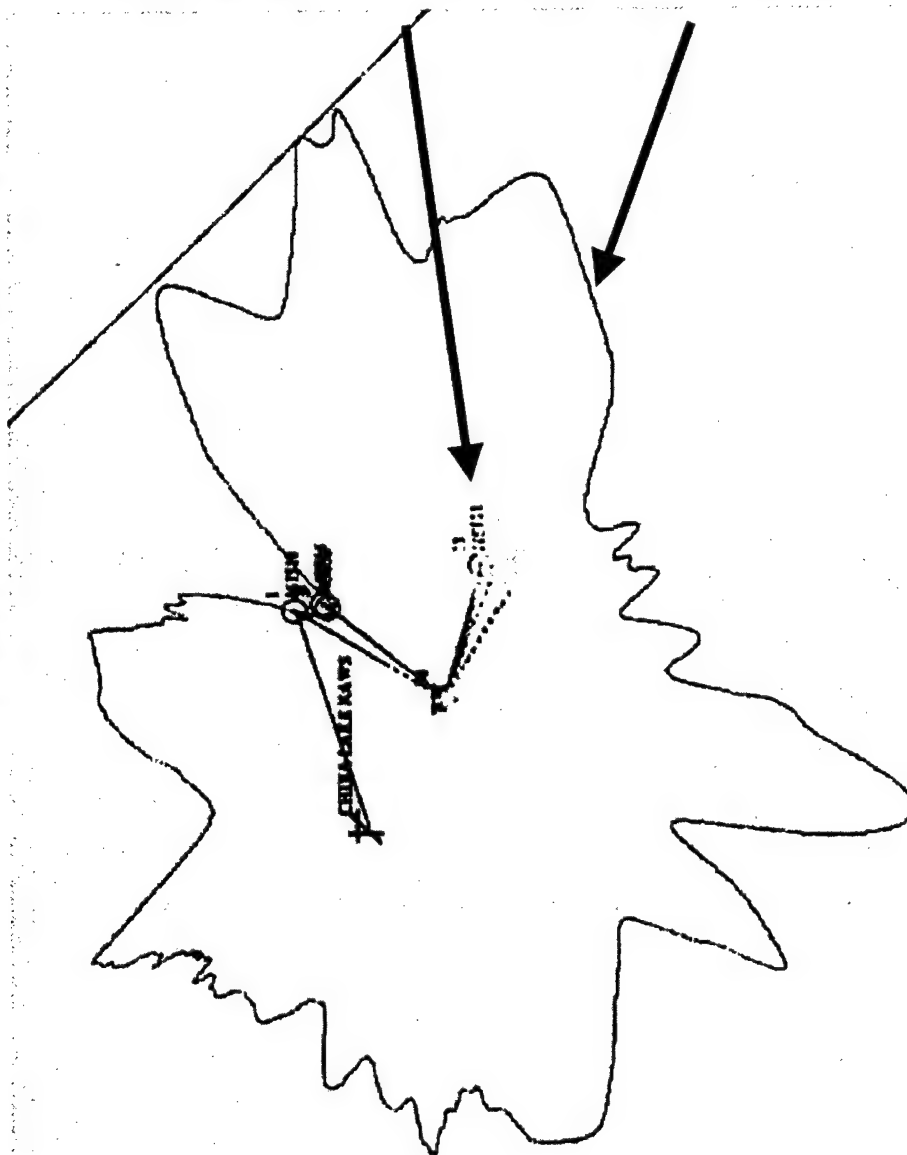
TAMPS RTMs

- Circles are plots of actual aircraft location when acquired or dropped by A-2.

- Circles in white are points where aircraft was detected at 7200' MSL.

- TAMPS RTM unmask envelope for A-2 at 7200' MSL is displayed as a detection line (preferred over rays).

A-2 7200 MSL

7-10-97

Flight Test Data vs. TAMPS
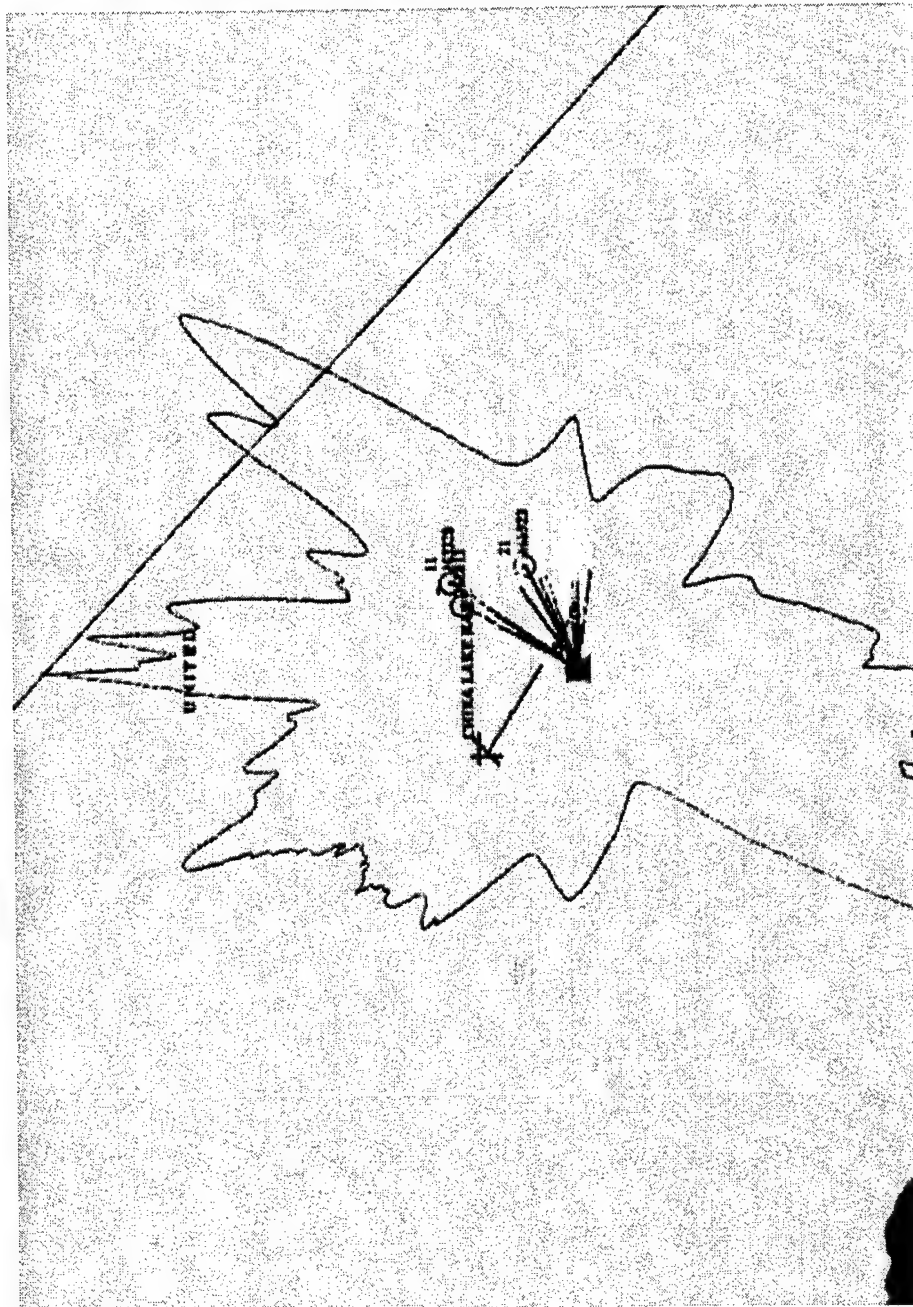
This plot of E-12 data as well as the previous slide reflect TAMPS' consistent pattern of depicting unmasking ranges well beyond those observed in flight testing for all systems. Disparities as great as 300% were observed and led to early decision to shift analysis effort to IMOM and AFMSS.

Other TAMPS Anomalies
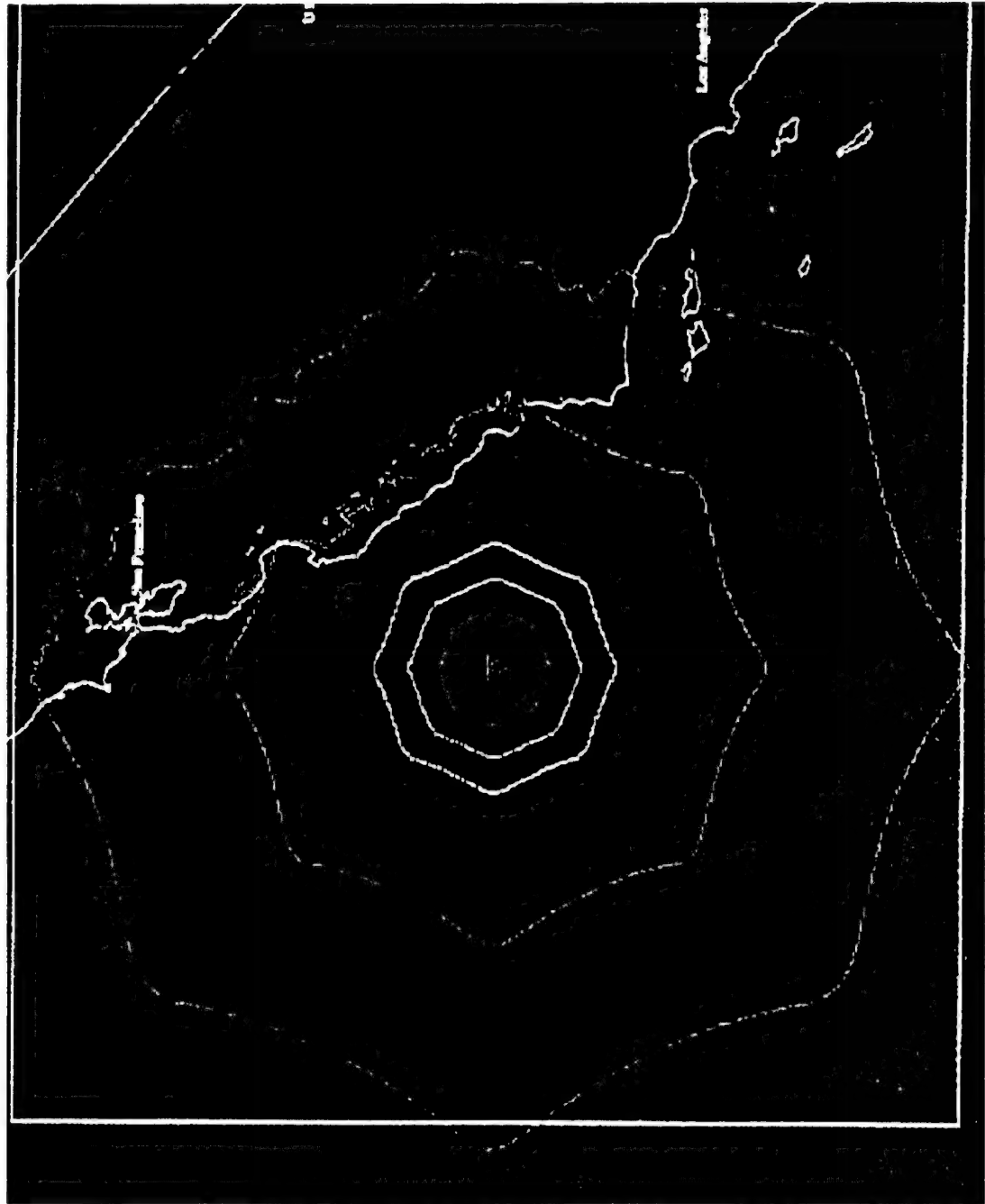
- TAMPS plotted RTMs over water, where DTED elevation was universally zero, as stylized octagons instead of circles. This was another indication that the algorithms were fundamentally flawed.

- Ranges were also still 30-35% longer than 4/3 earth radius LOS.

ATTACHMENT 2

Terrain Masking Plots

FIG. A-1

47.3 nm @ 37.3° True

Beams Display Form

File   View   Display Options

ELNOT: Radar Function: Nato Name:

Start Location: 352403N 1172224W   End Location: 361751N 1164050W

* 10552 FT
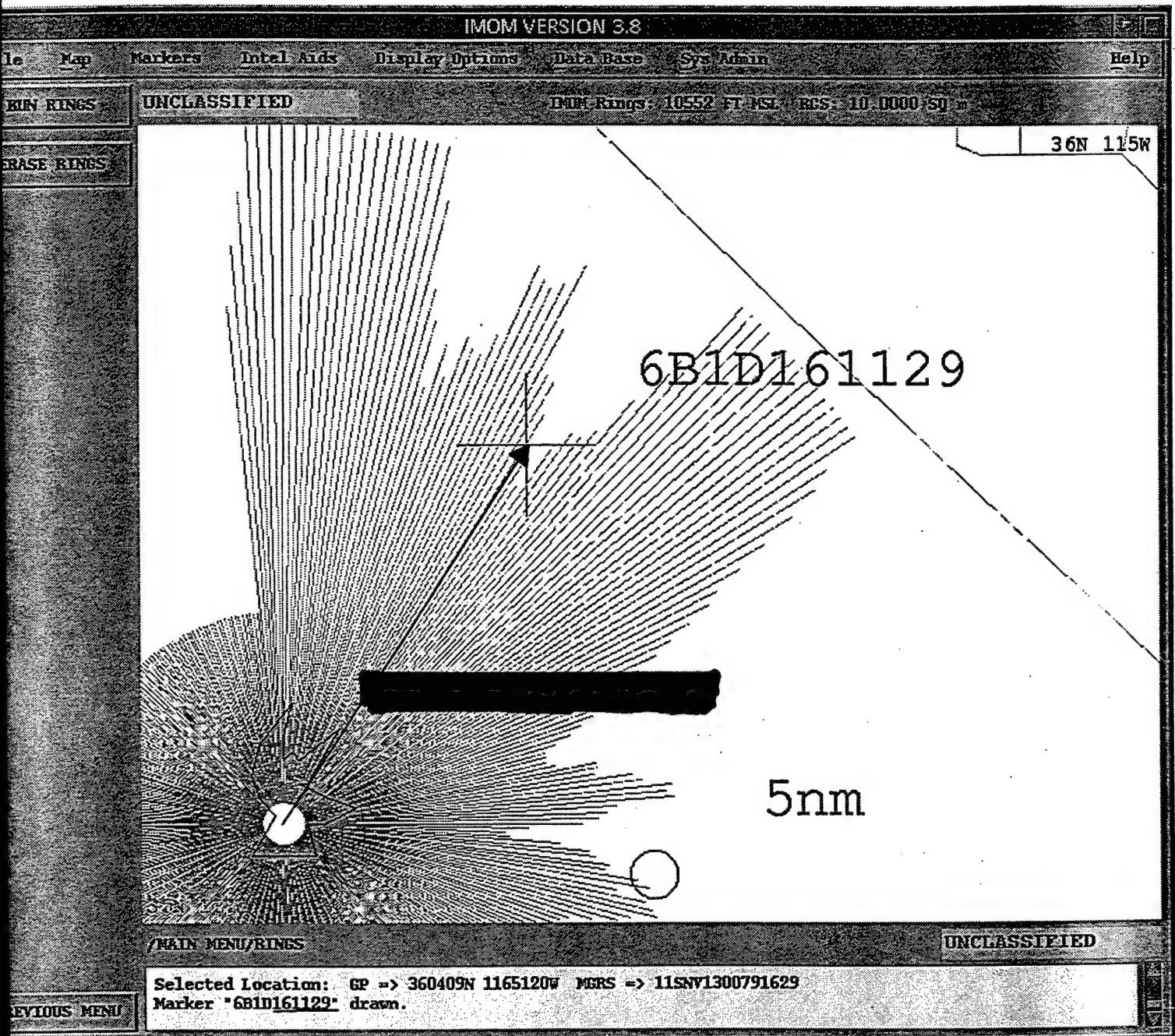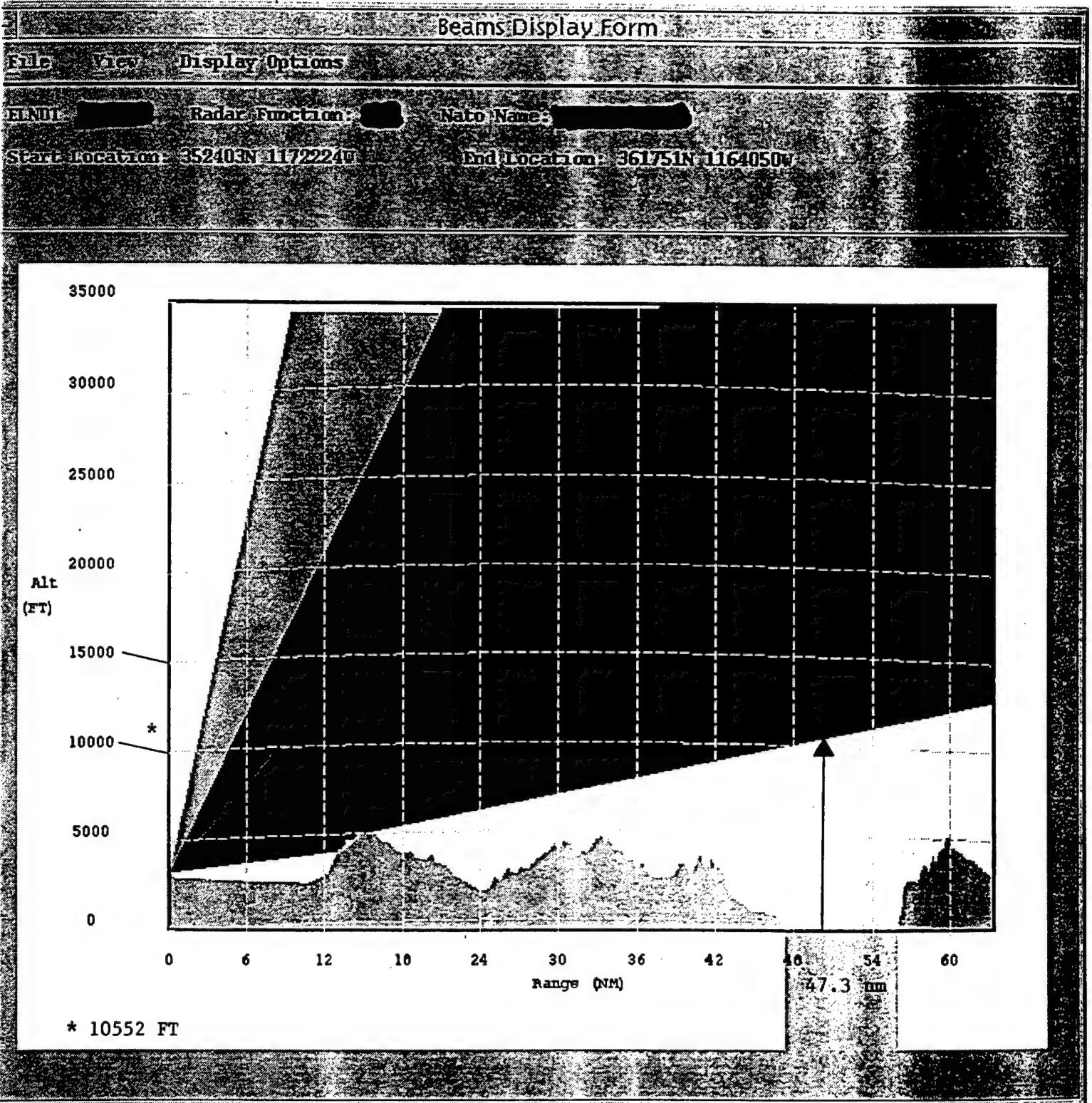
FIG. B-1
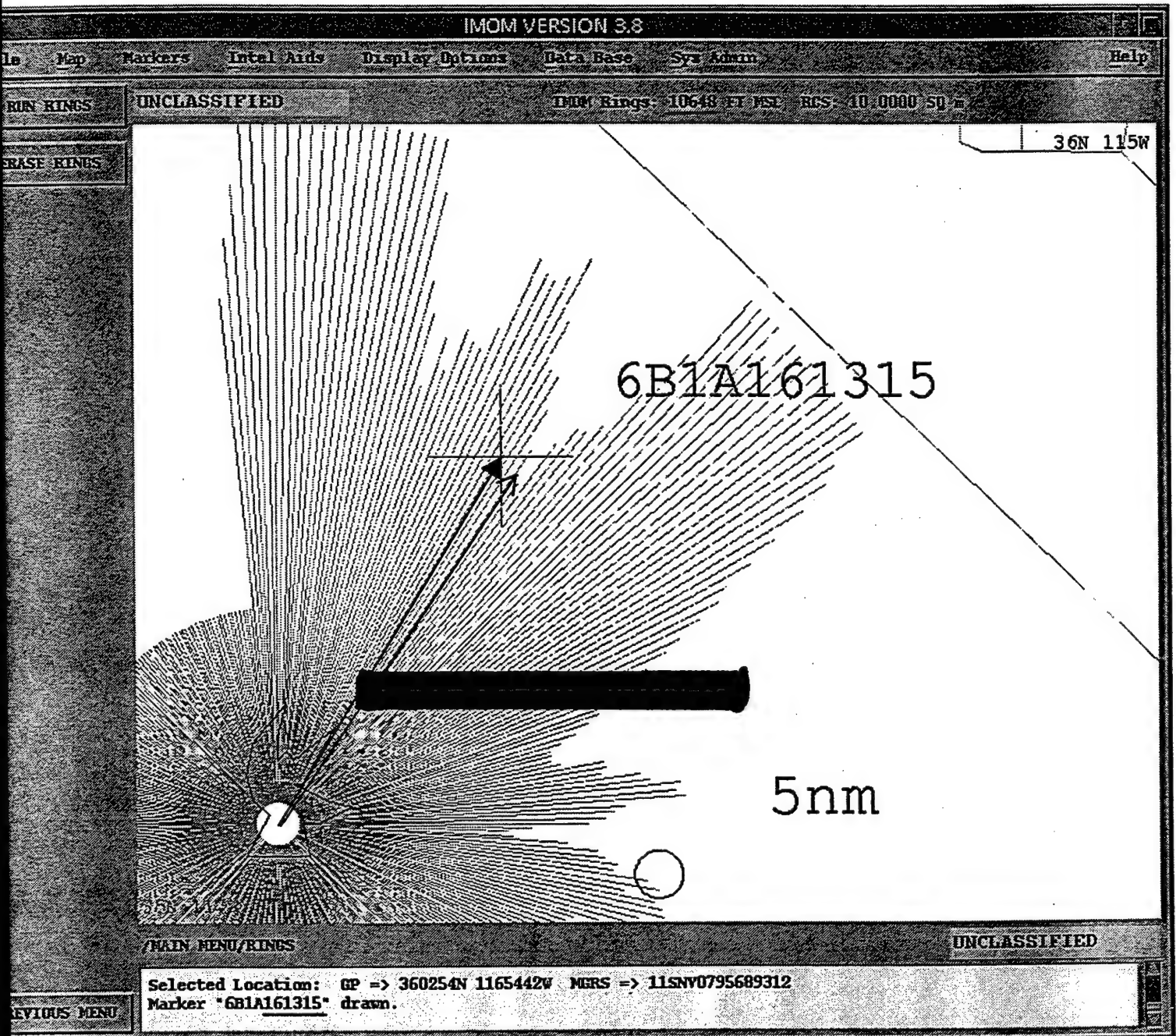
44.9 nm @ 30.2° True
(2.7nm)

FIG. B-2
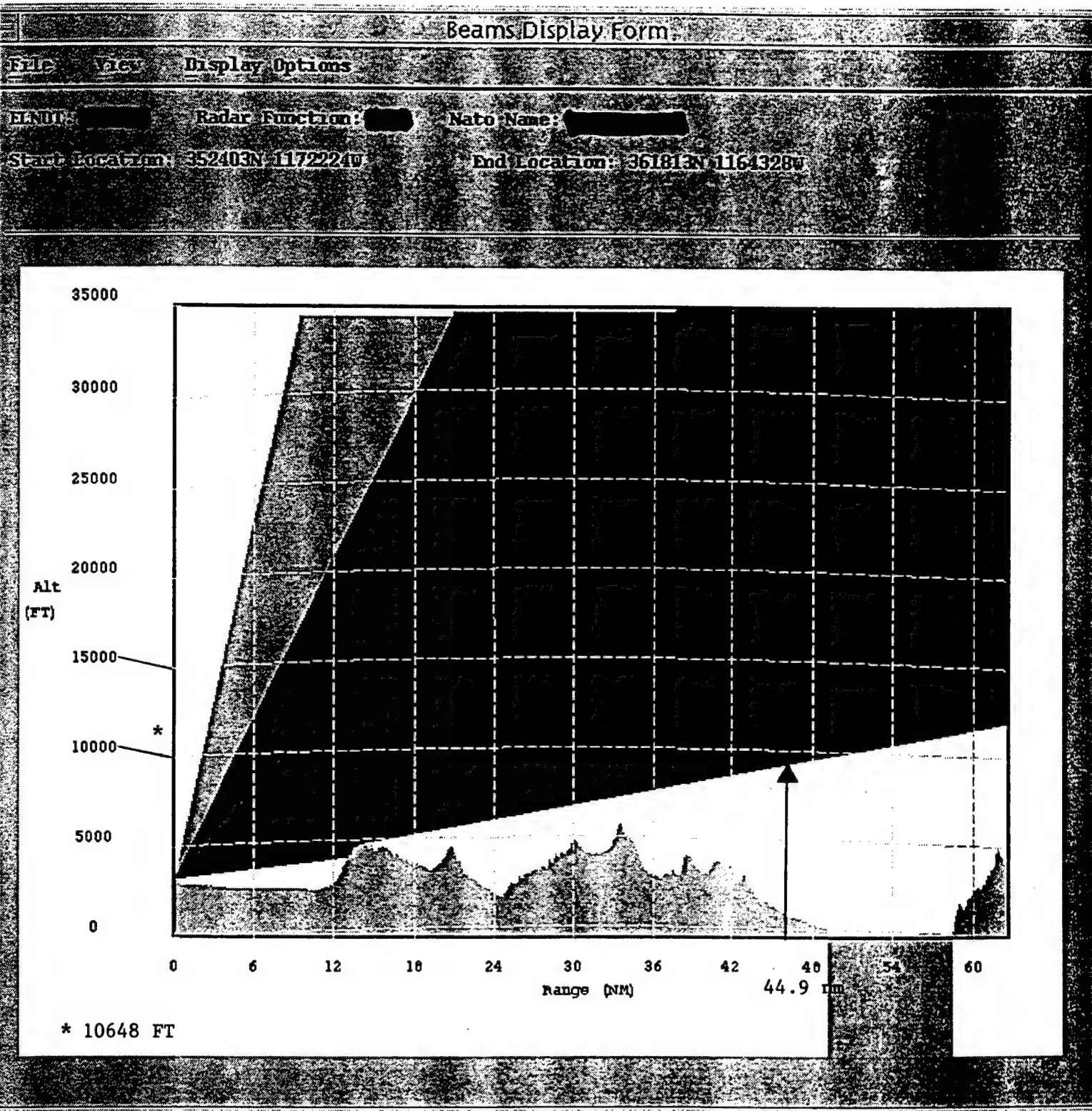
FIG. C-1
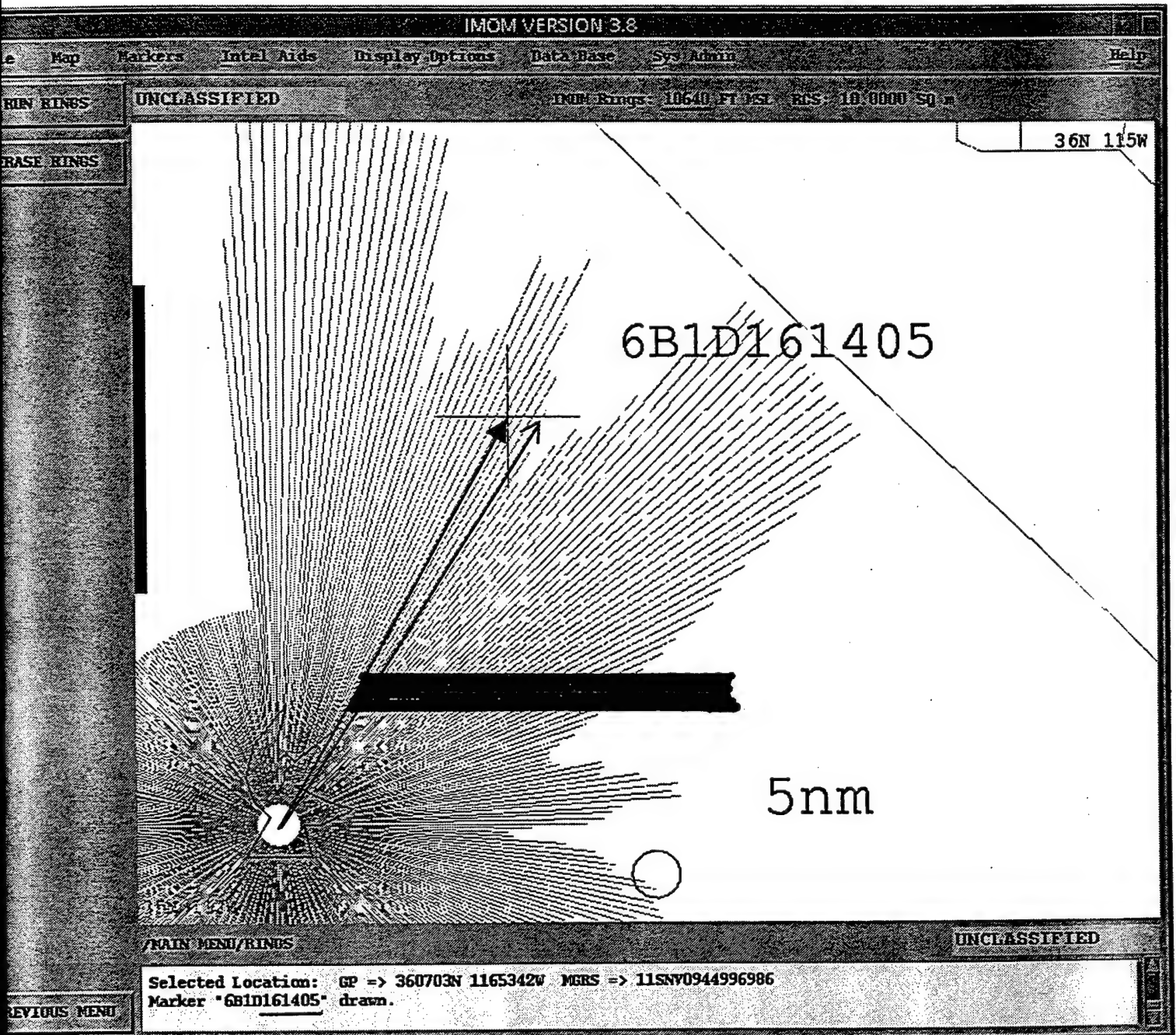
48.8 nm @ 28.5° Trüe
(3.9nm)

FIG. C-2

6B1D161405
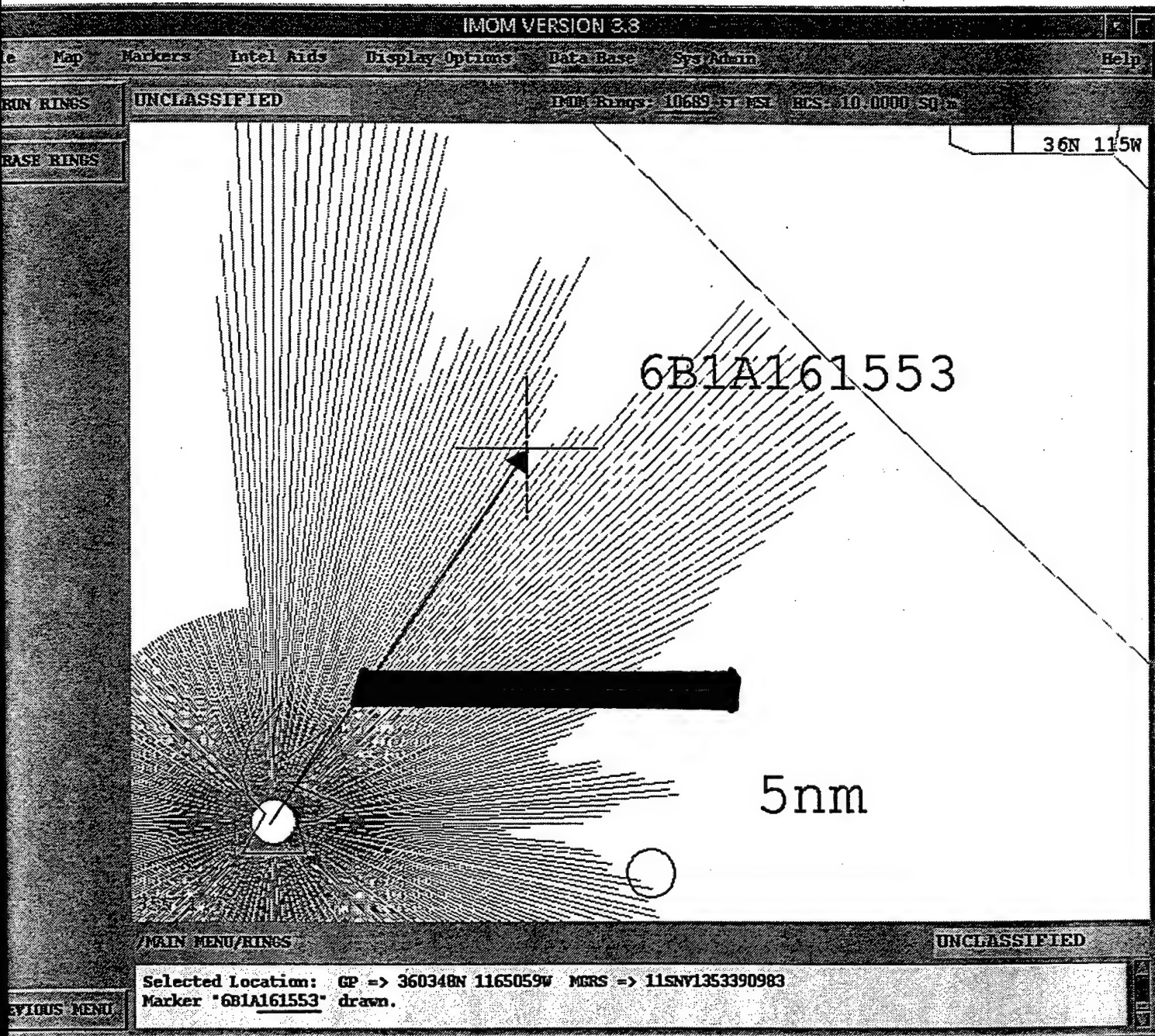
54

FIG. D-1

47.1 nm @ 32.6° True

FIG. D-2

56

FIG. E-1

42.3 nm @ 34.3° True

57

FIG. E-2

Beams Display Form

File   View   Display Options

ENU   Radar Function   Nato Name

Start Location: 352403N 1172224W   End Location: 360852N 1164501W

* 10484 FT
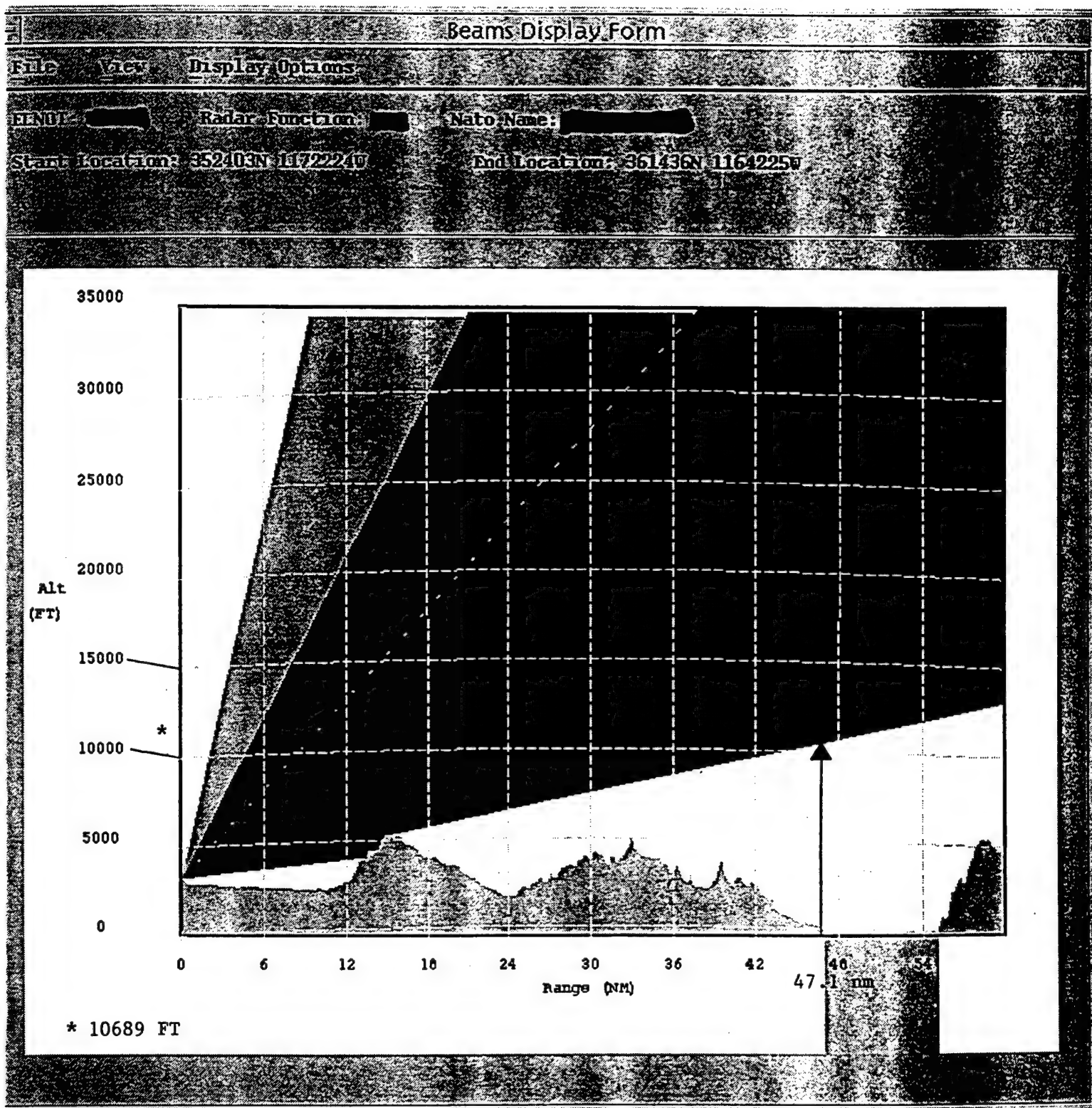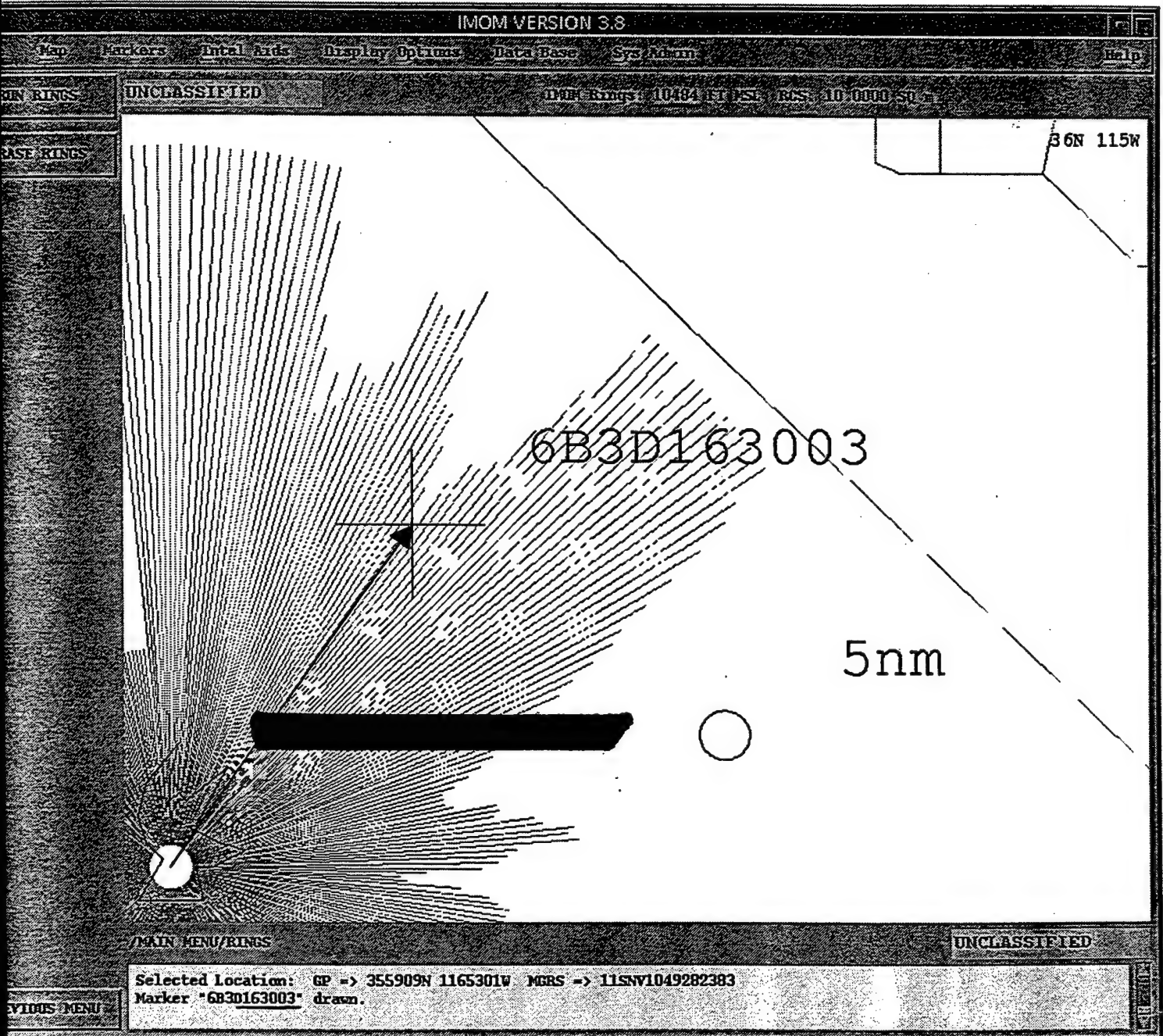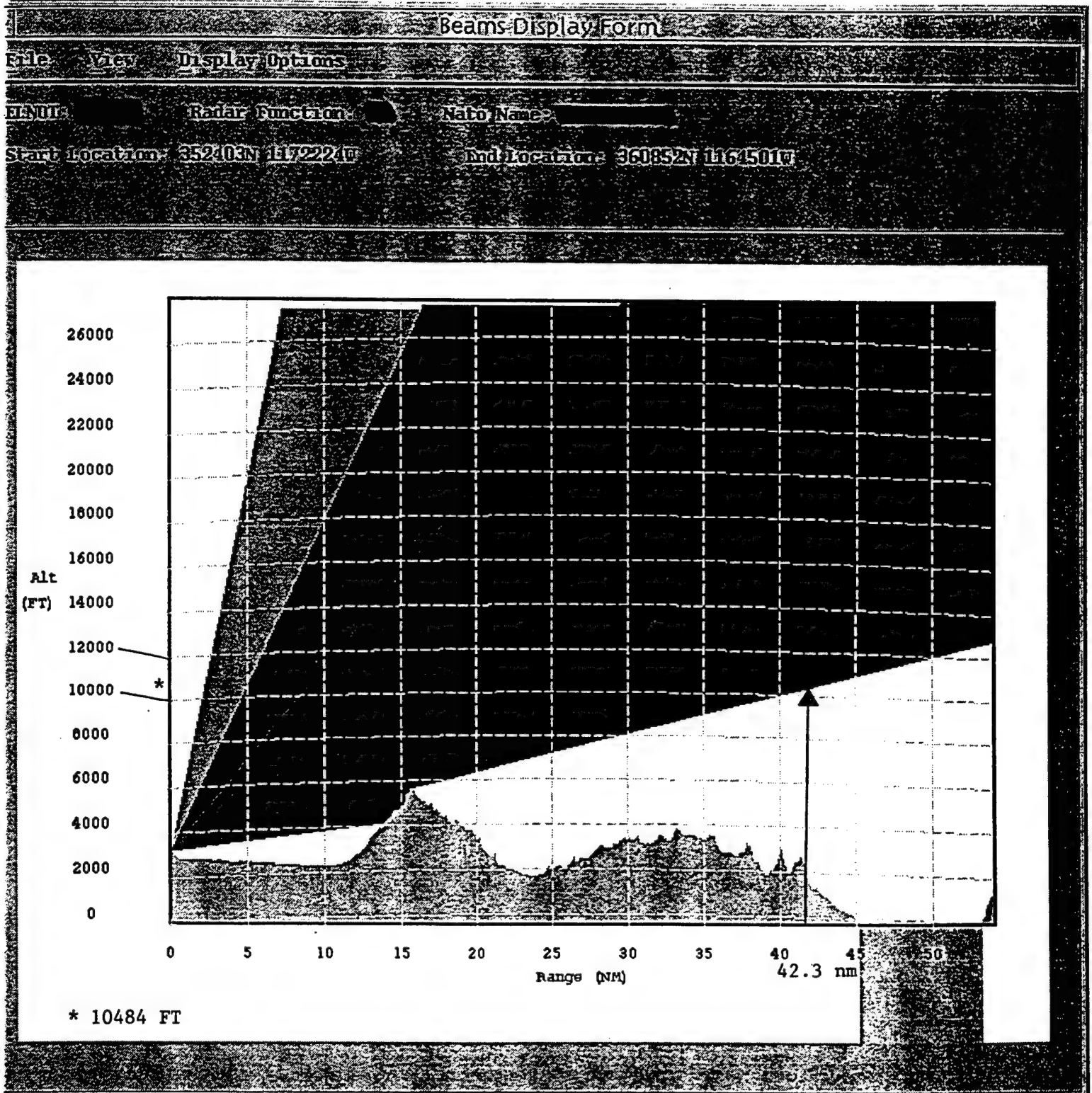
6B3D163003
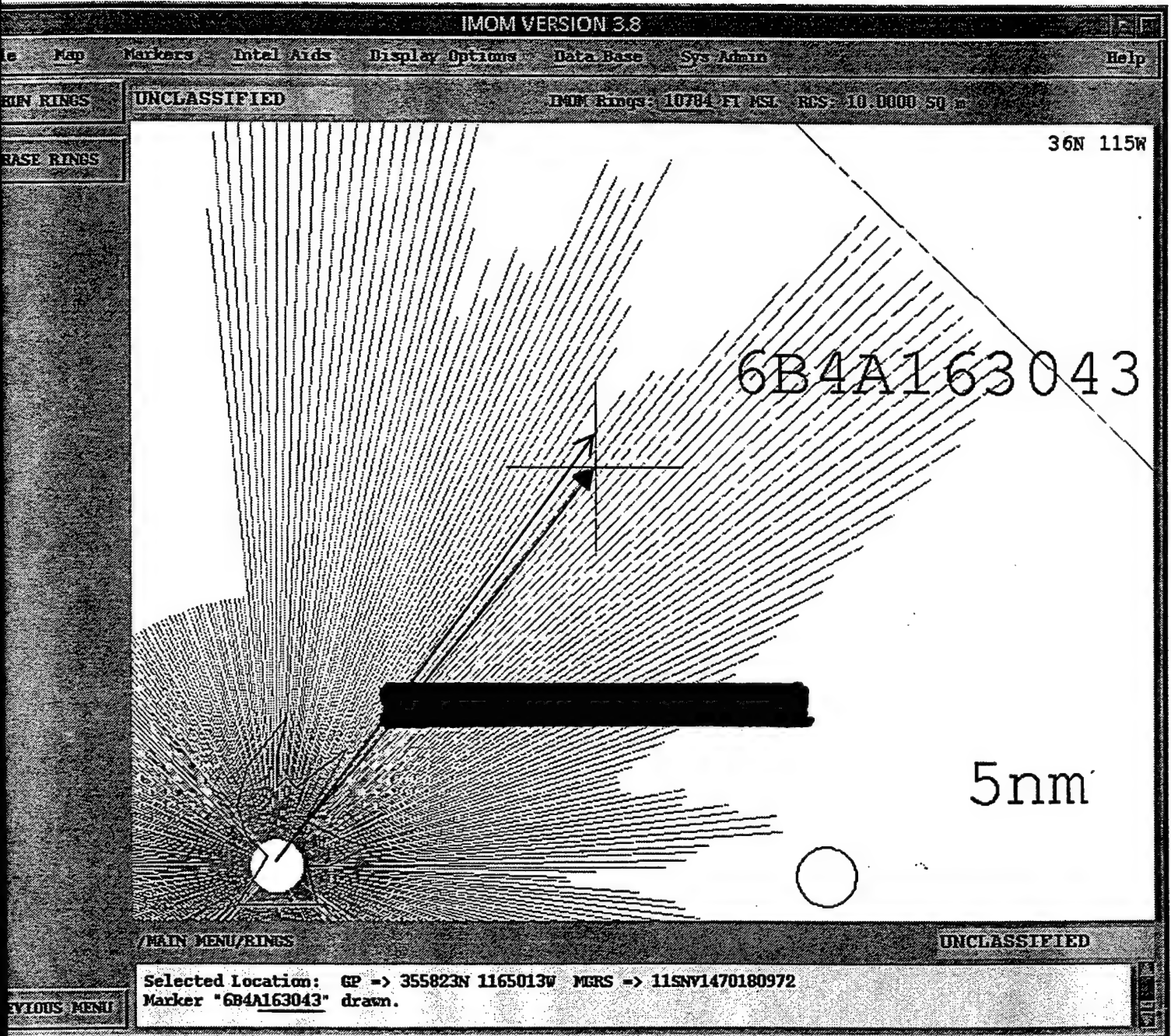
43.2 nm @ 37.3° True
(2.8nm)

FIG. F-2

Beams Display Form

File   View   Display Options

ELNOT: Radar Function: Nato Name:
Start Location: 352403N 1172224W   End Location: 360706N 1164201W

* 10784 FT

6B4A163043

60

FIG. F-3

le   View   Display Options

ENOT: Radar Function: Nato Name:

art Location: 352403N 1172224W   End Location: 360641N 1164655W

* 10784 FT

6B4A163043

61
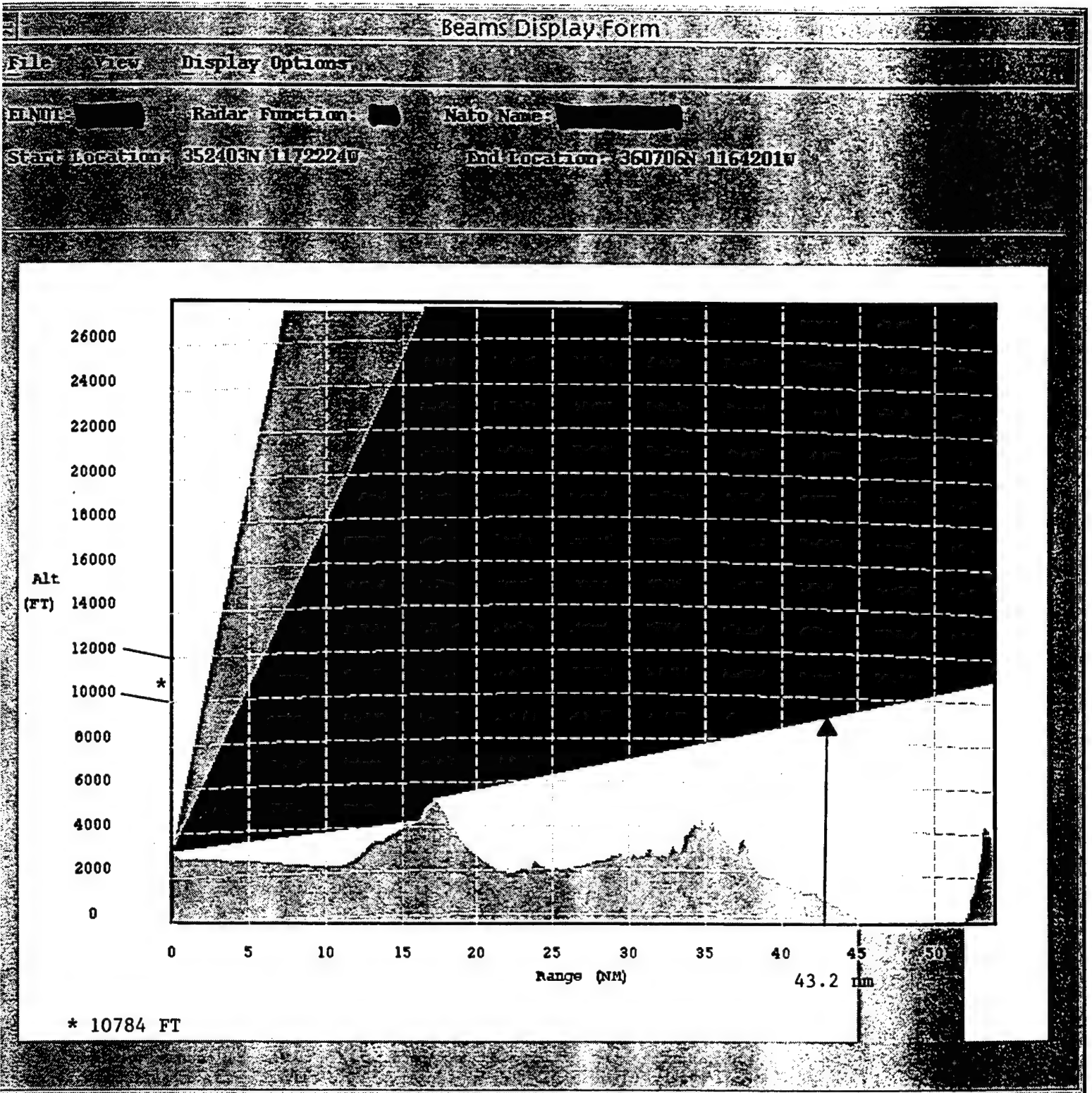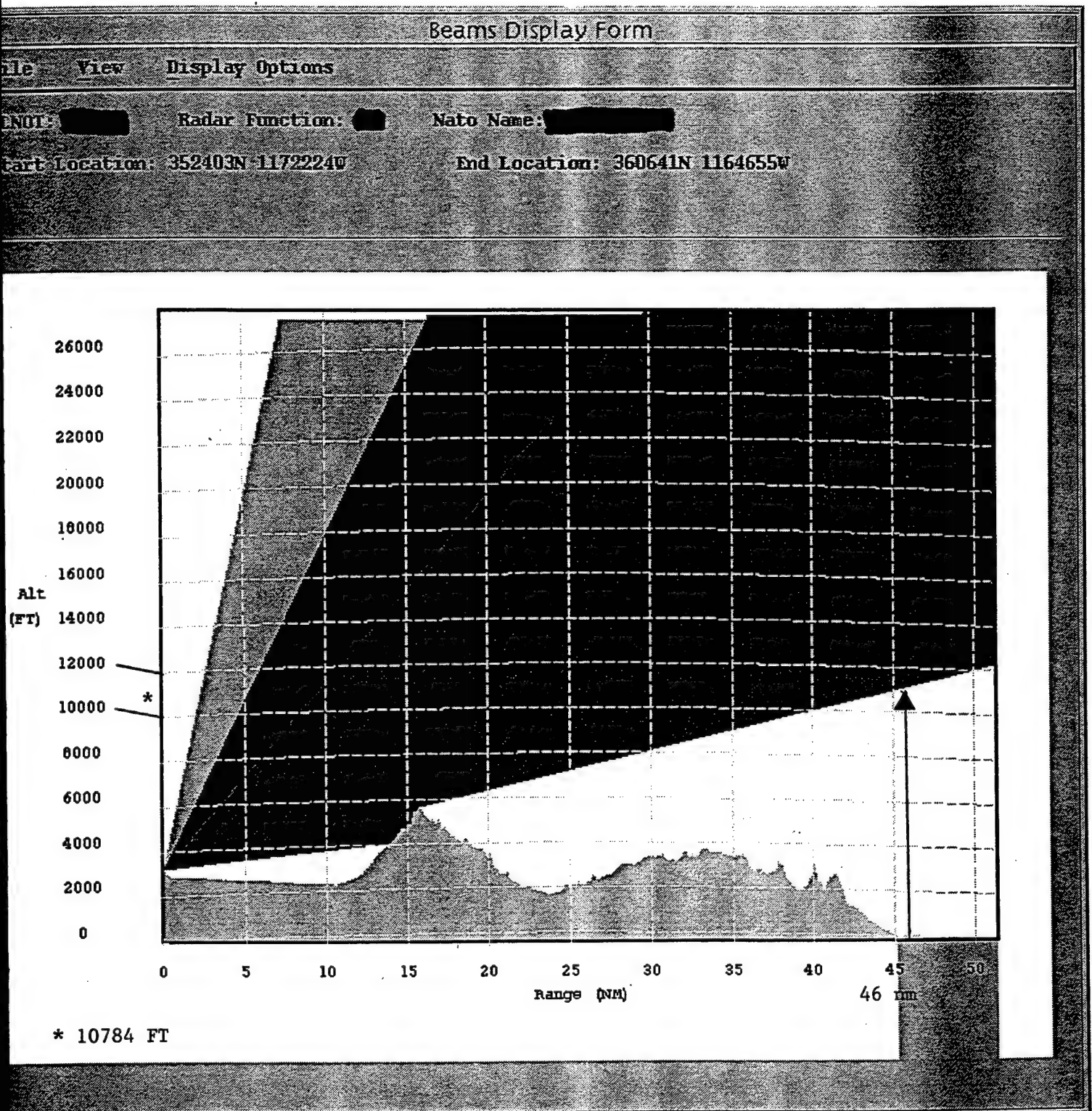
FIG. G-1

14.6 nm @ 90° True

FIG. G-2

Beams Display Form

View   Display Options

NOT: Radar Function: Nato Name:

Start Location: 352403N 1172224W   End Location: 352406N 1165525W

Alt
(FT)

*

Range (NM)   14.6 nm

* 7249 FT

6B5D164009

63

FIG.H-1

15.9 nm @ 92.5° True

64

FIG. H-2

Beams Display Form

File   View   Display Options

UNIT: ▮▮▮▮   Radar Function: ▮▮   Nato Name: ▮▮▮▮▮▮▮

Start Location: 352403N 1172224W   End Location: 352303N 1165854W

* 7326 FT
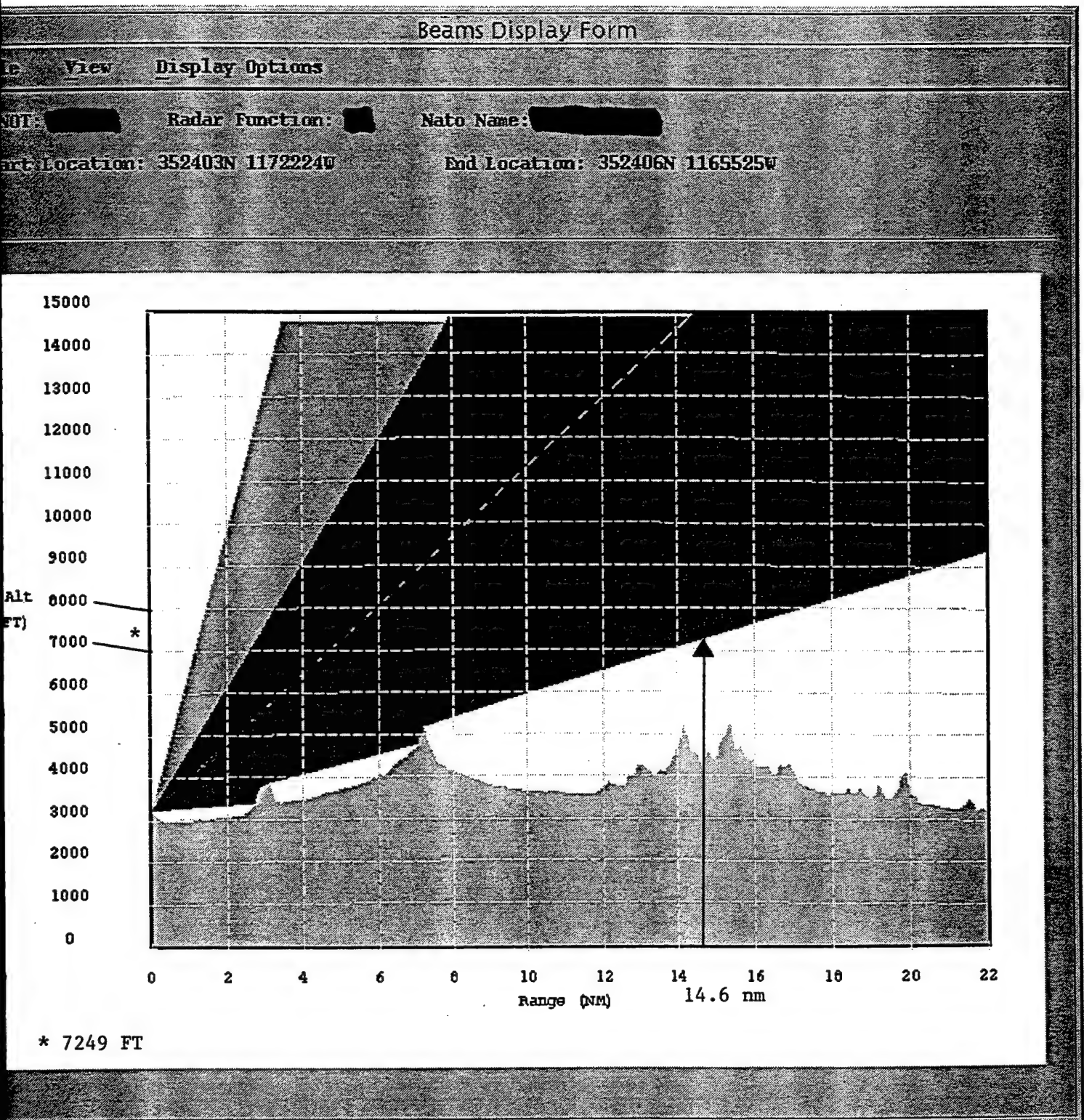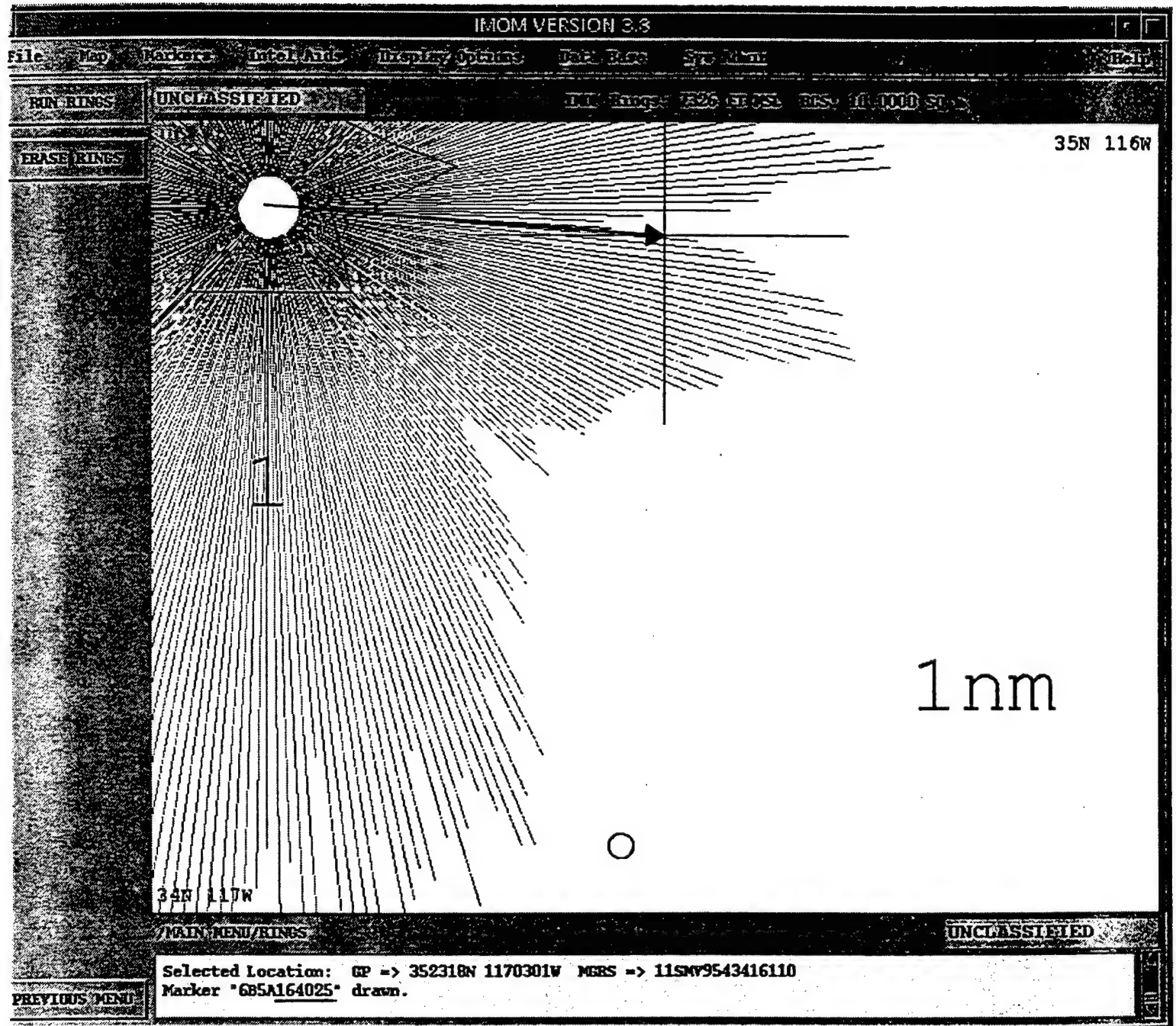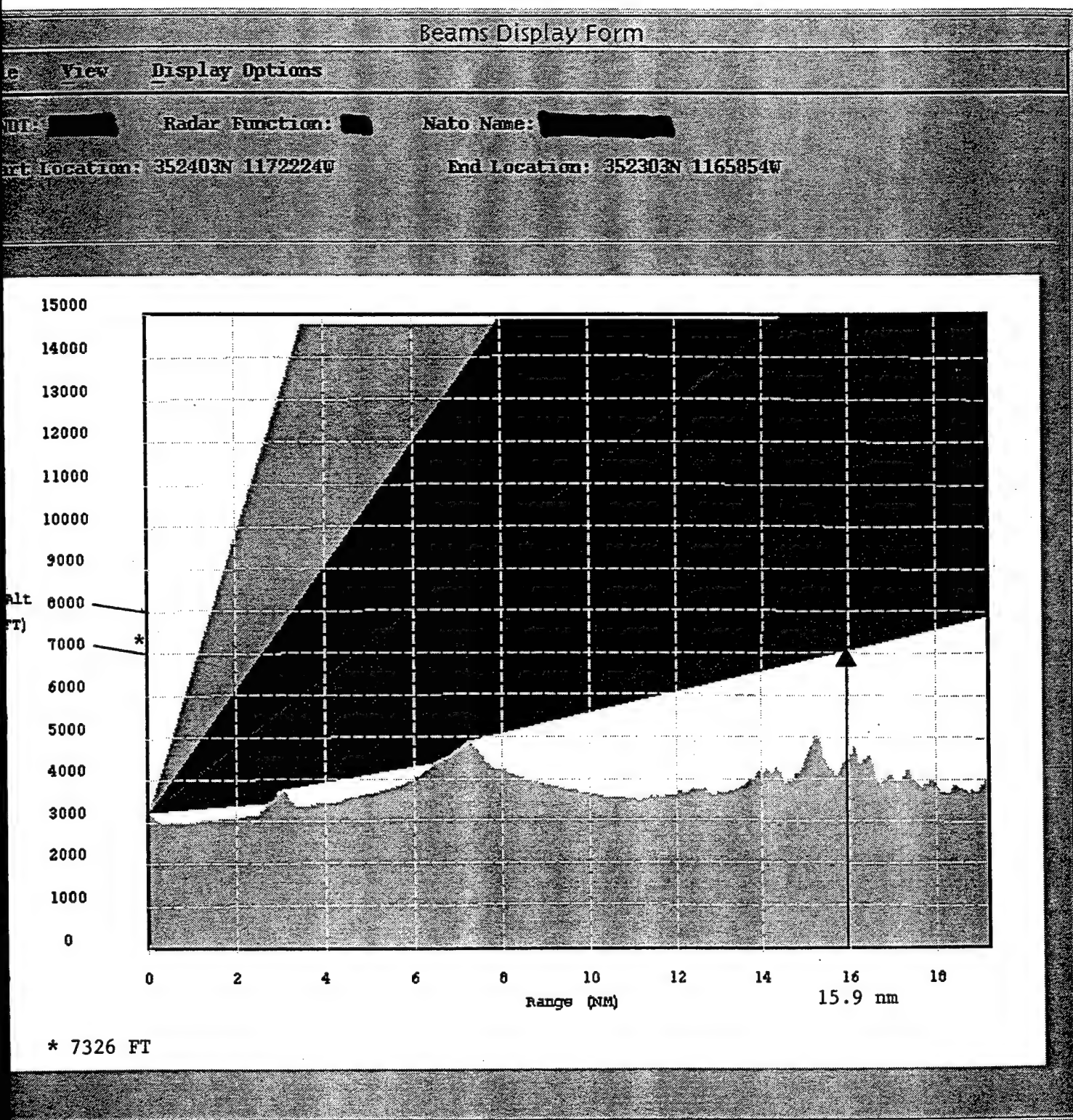
6B5A164025

FIG. I-1

19.9 nm @ 97° True

FIG. I-2

Beams Display Form

File   View   Display Options

NOT: [redacted]   Radar Function: [redacted]   Nato Name: [redacted]

Start Location: 352403N 1172224W   End Location: 352101N 1165323W

* 7289 FT
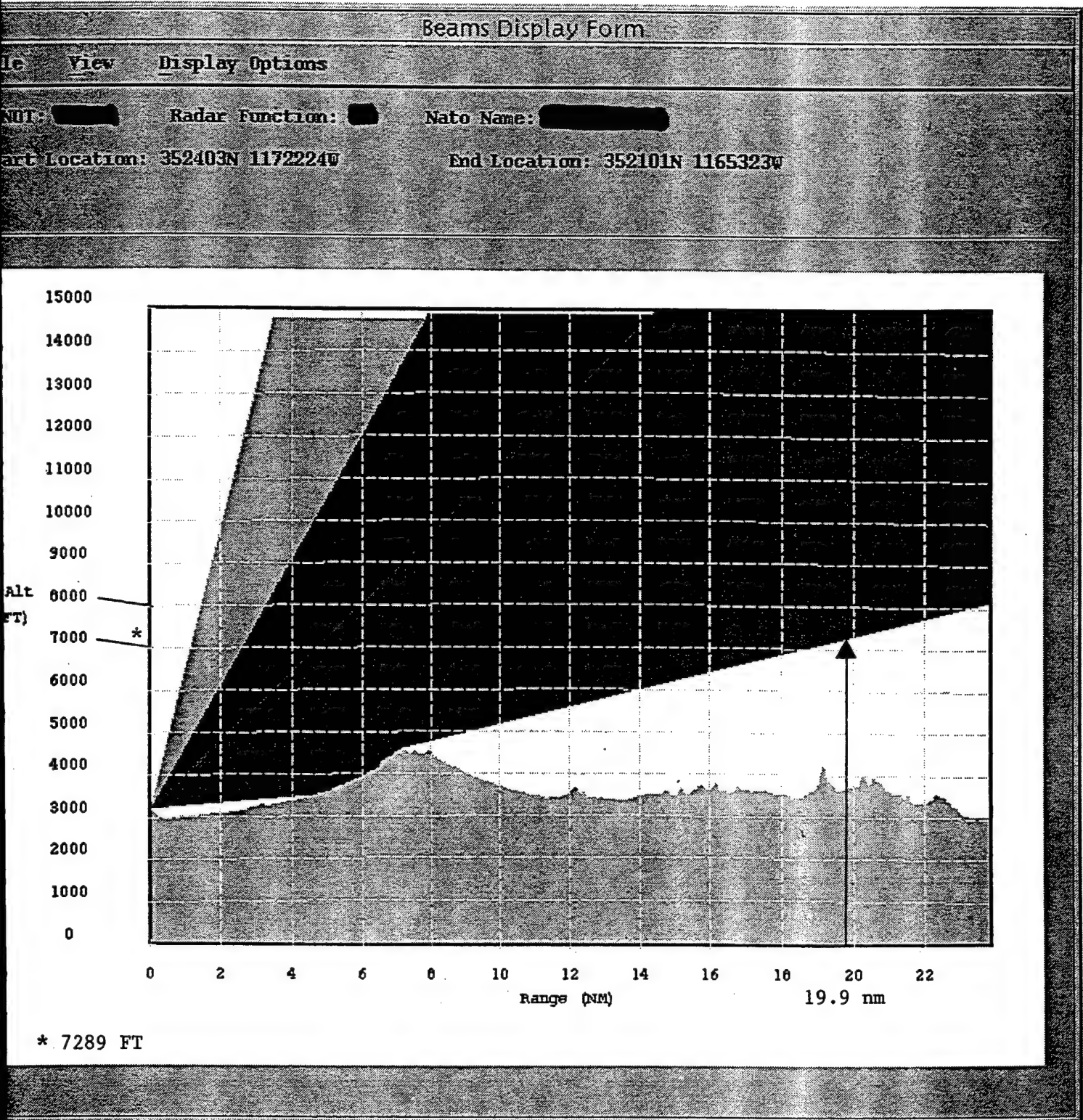
FIG. J-1

20.9 nm @ 87.6° True
(.2nm)

FIG. J-2

Beams Display Form

View   Display Options

NDT: ██████   Radar Function: ██   Nato Name: ████████

Start Location: 352403N 1172224W   End Location: 352509N 1165145W

Alt (FT)

*

* 7443 FT

Range (NM)   20.9 nm

6B5A164210

69
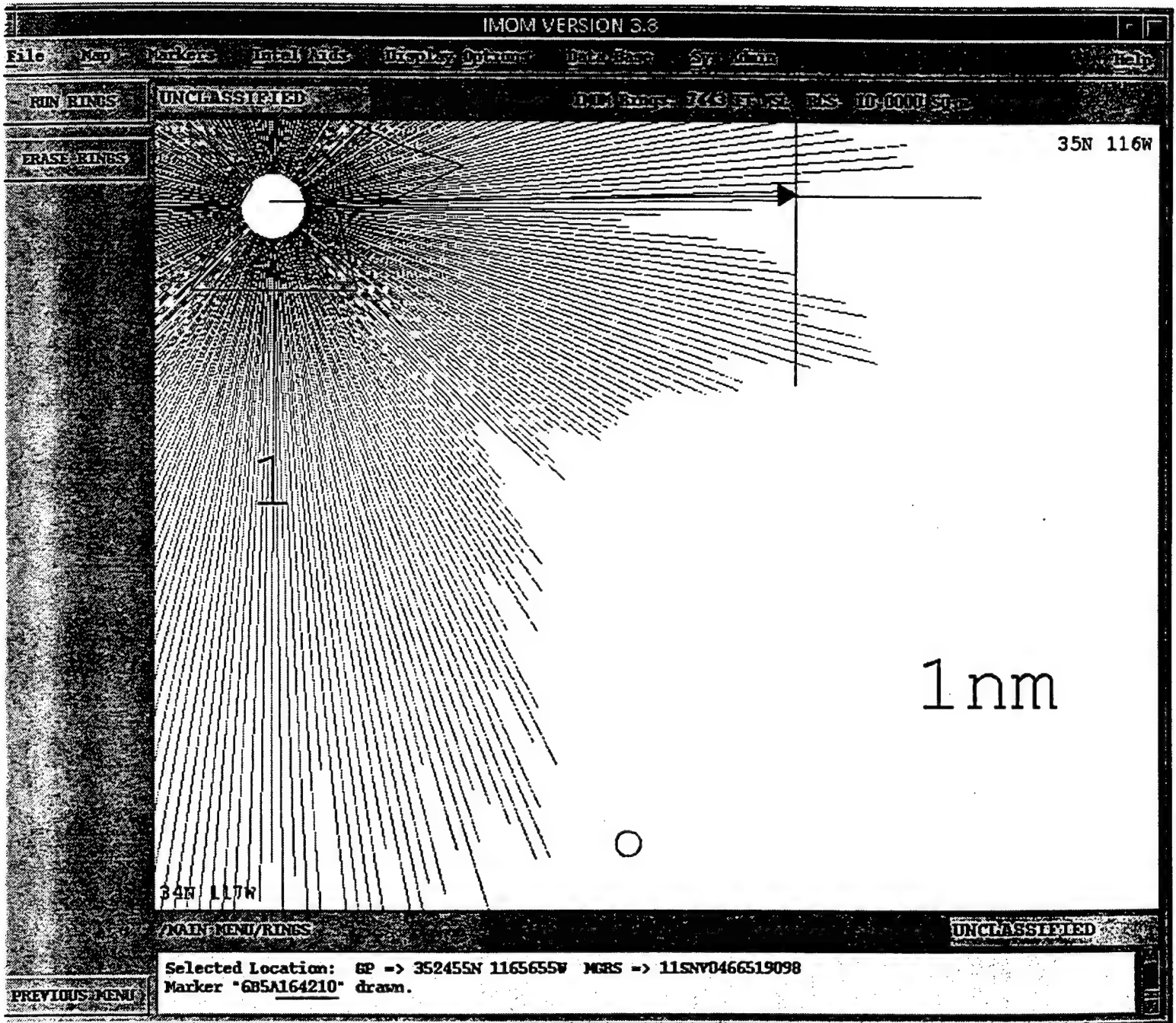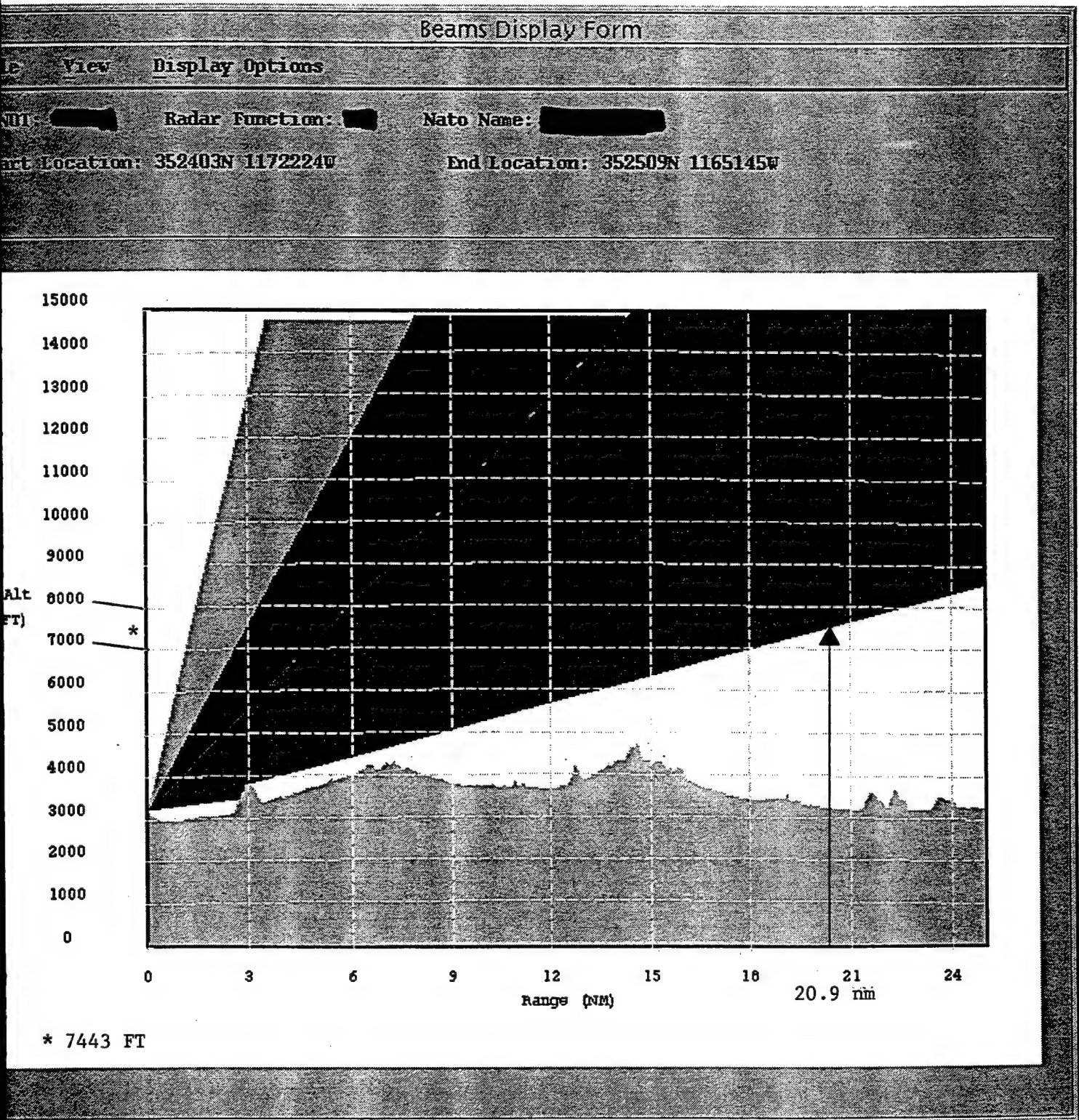
FIG. K-1

19.8 nm @ 88.8° True

FIG. K-2

Beams Display Form

File   View   Display Options

UNIT: ▮▮▮▮   Radar Function: ▮▮   Nato Name: ▮▮▮▮▮▮▮

Start Location: 352403N 1172224W   End Location: 352420N 1165051W

* 7392 FT
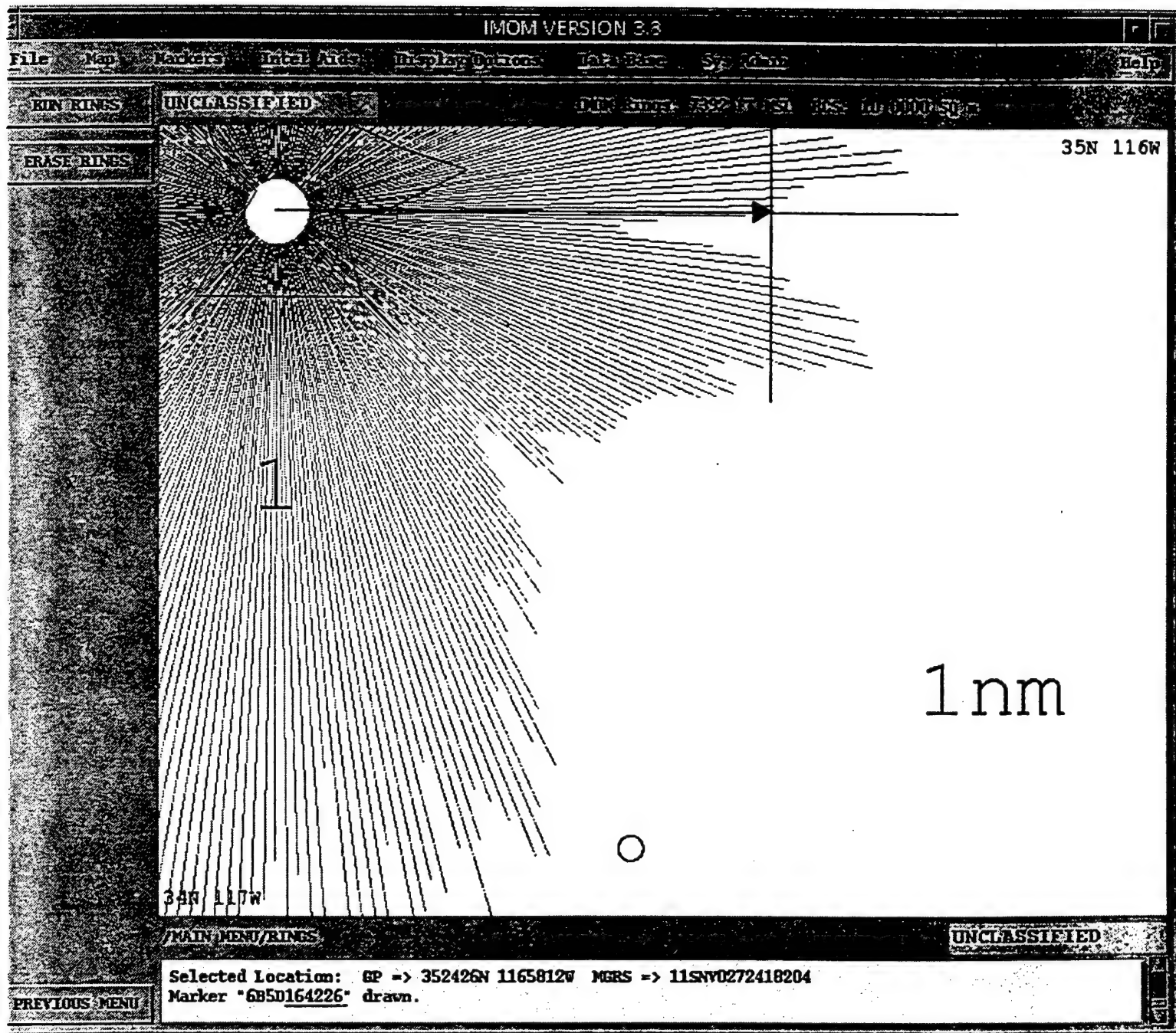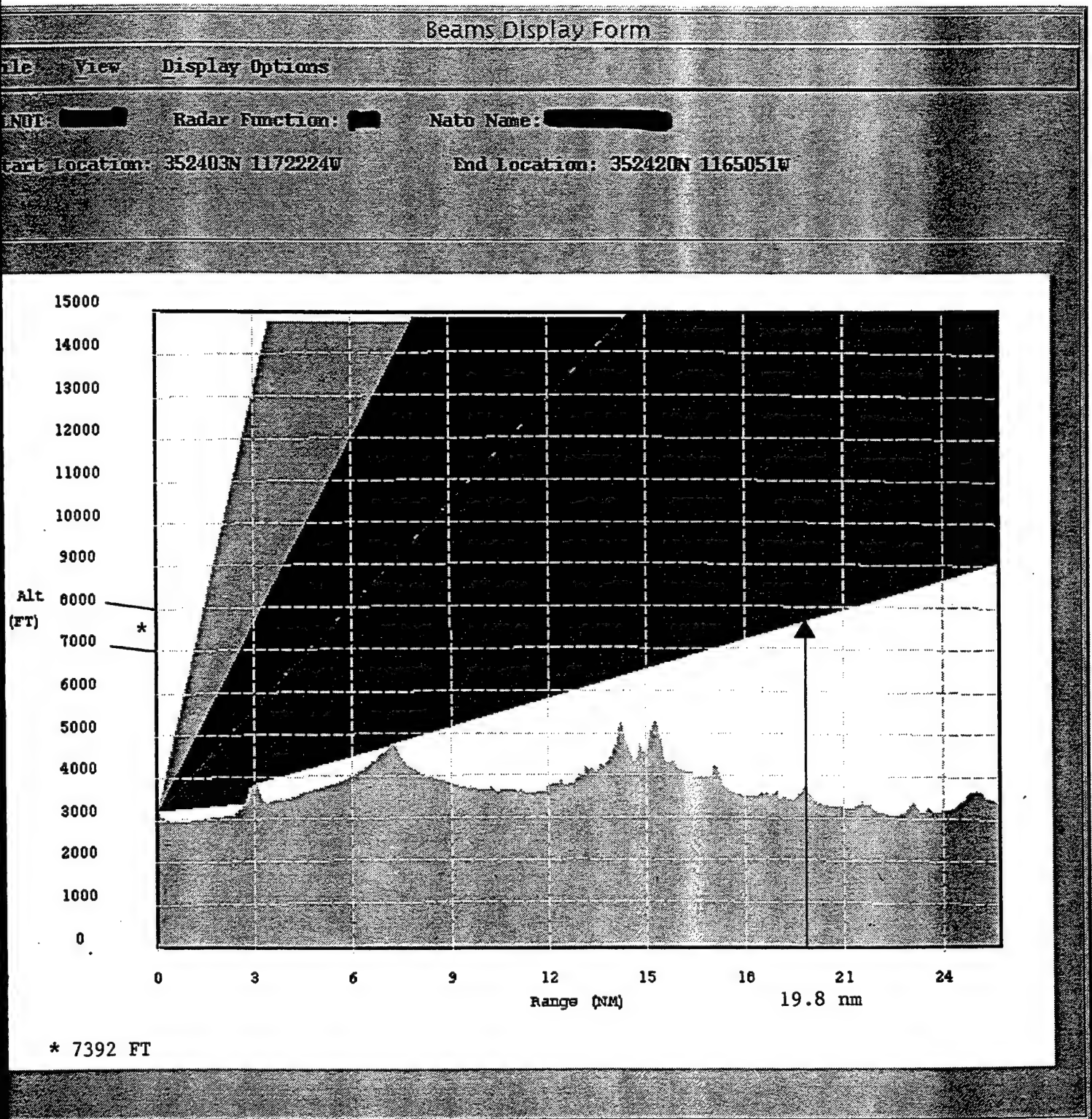
FIG. L-1
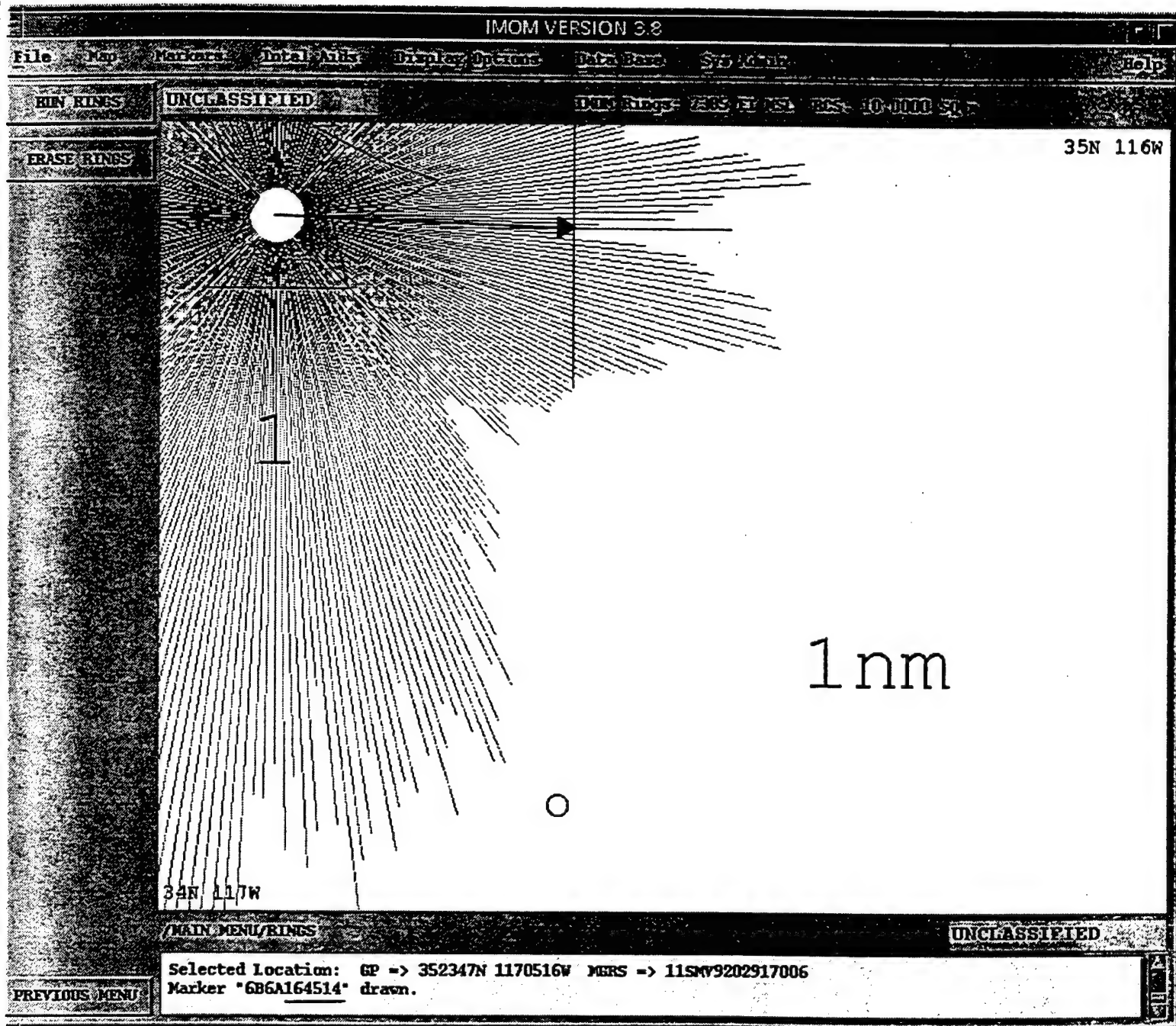
14.0 nm @ 91.1° True

FIG. L-2

* 7385 FT

6B6A164514

73
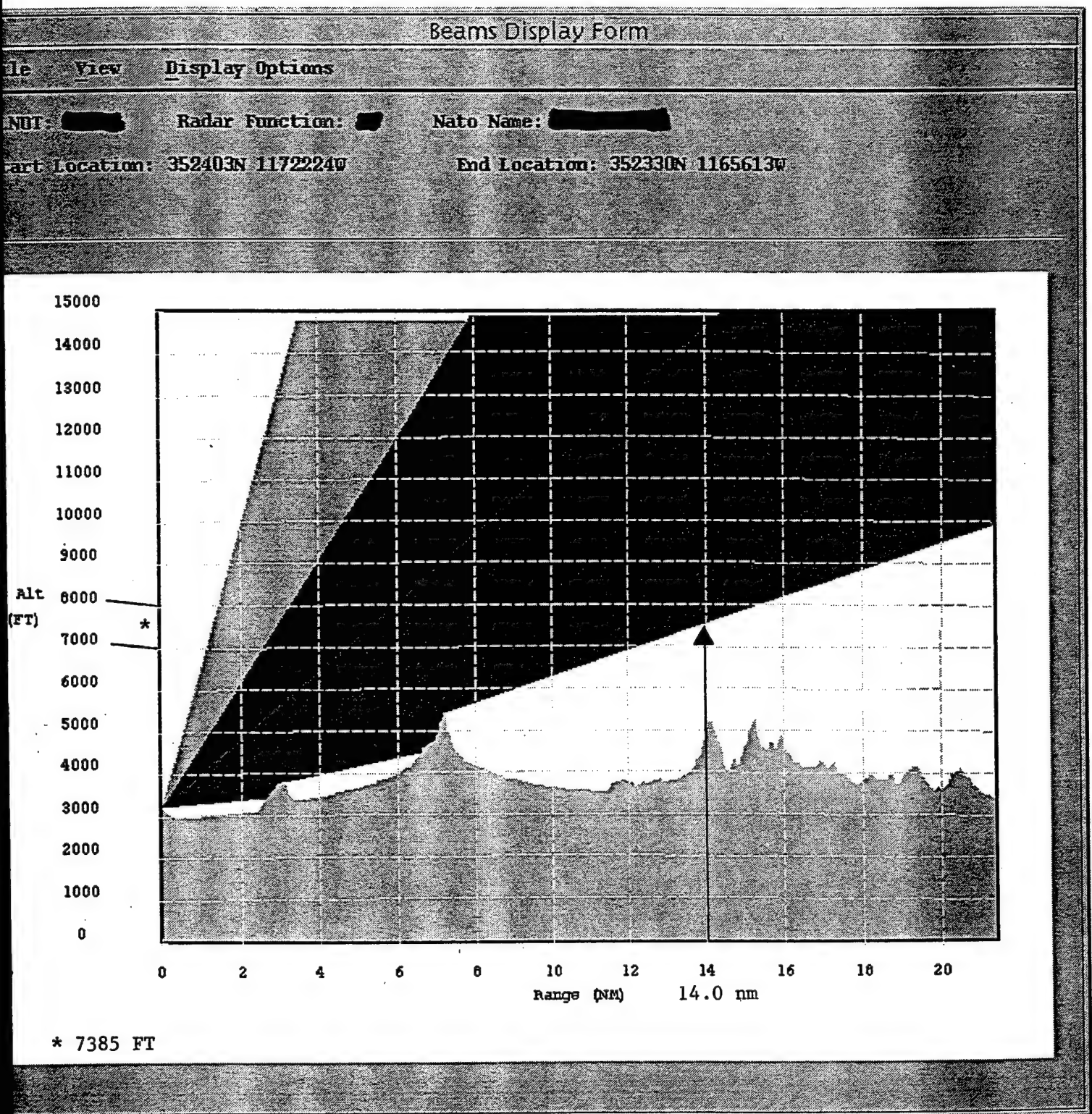
FIG. M-1
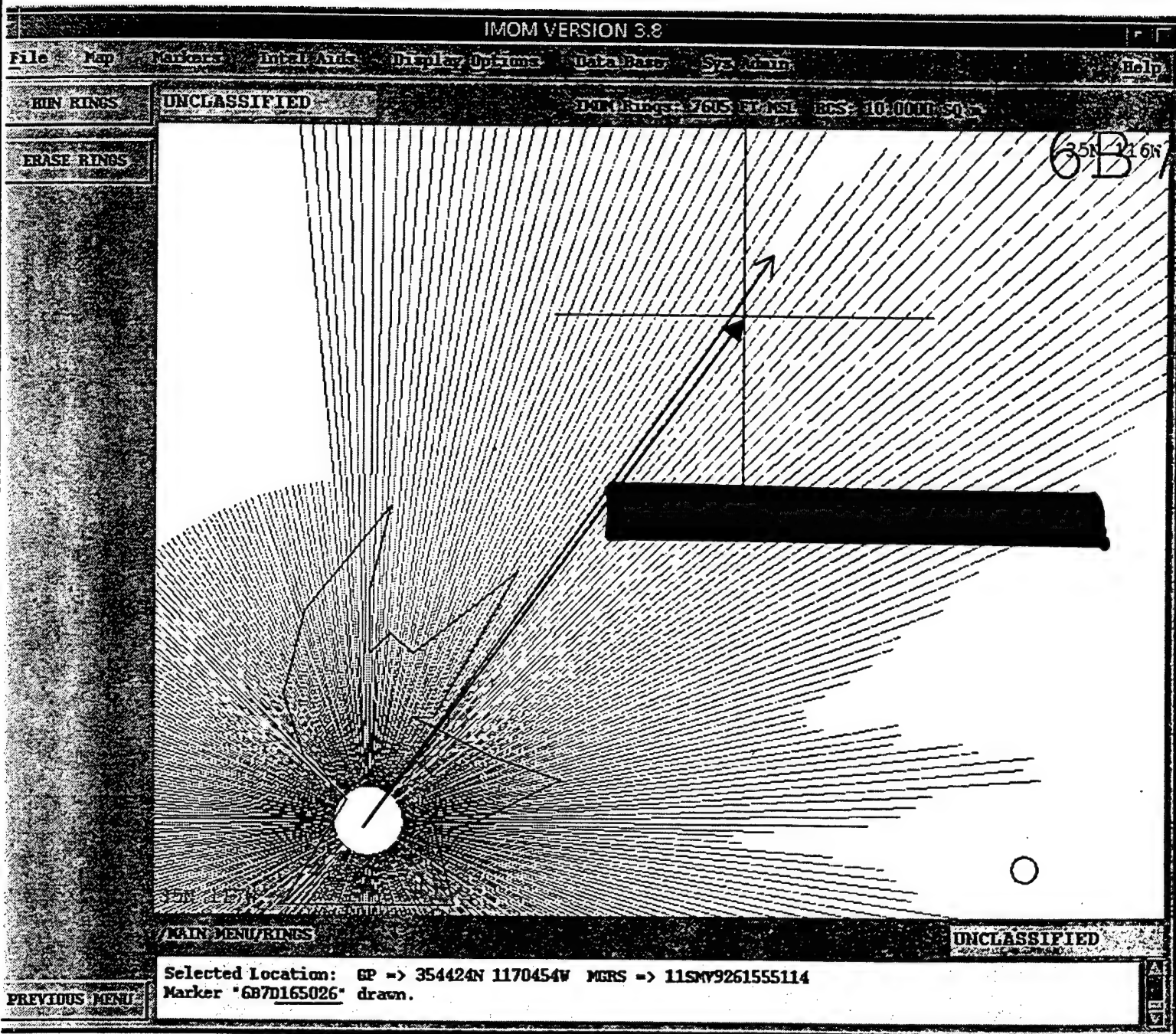
24.9 nm @ 34.8° True
(2.6nm)

FIG. M-2
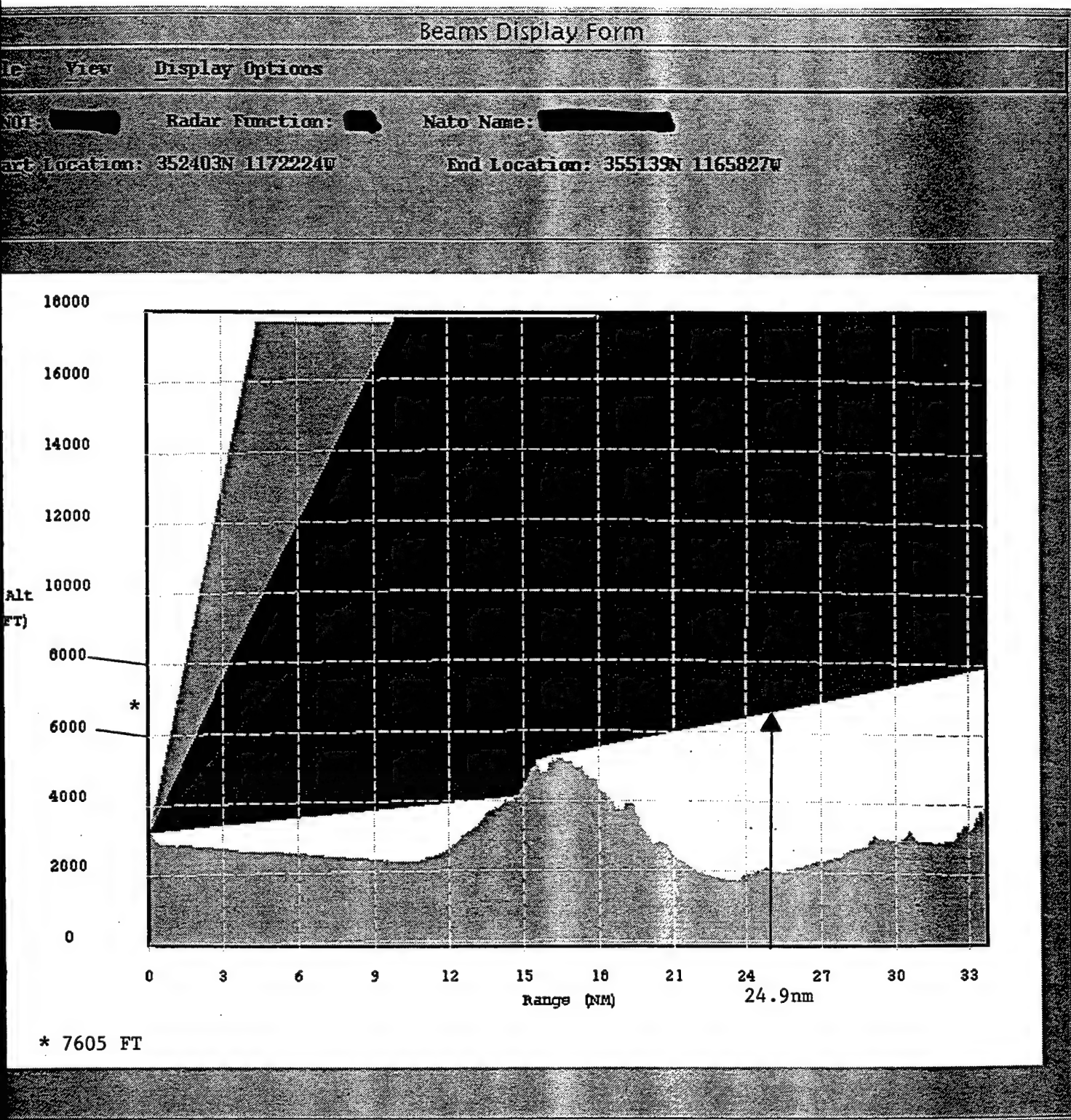
Beams Display Form

File   View   Display Options

NOI: Radar Function: Nato Name:

Start Location: 352403N 1172224W   End Location: 355139N 1165827W
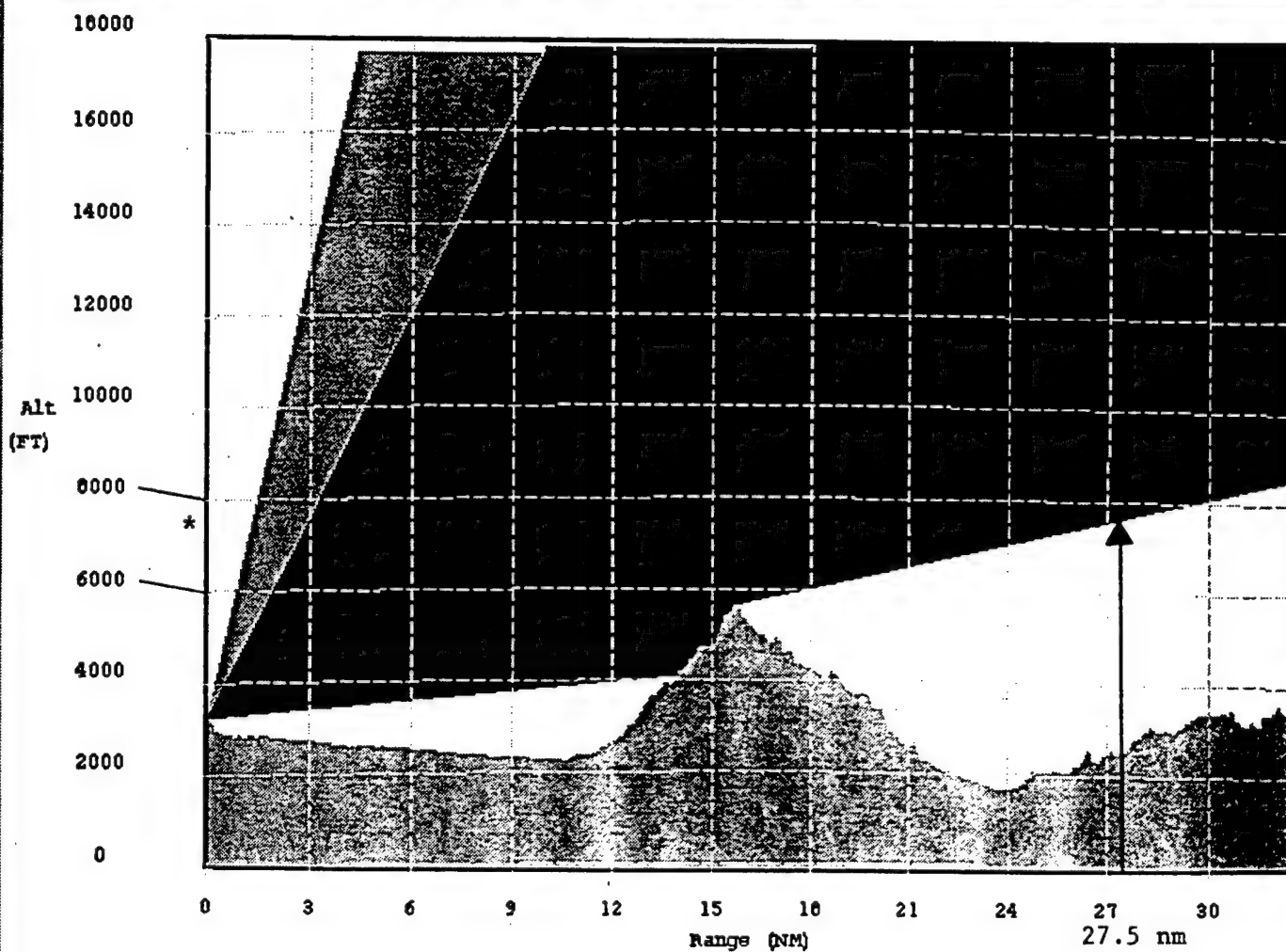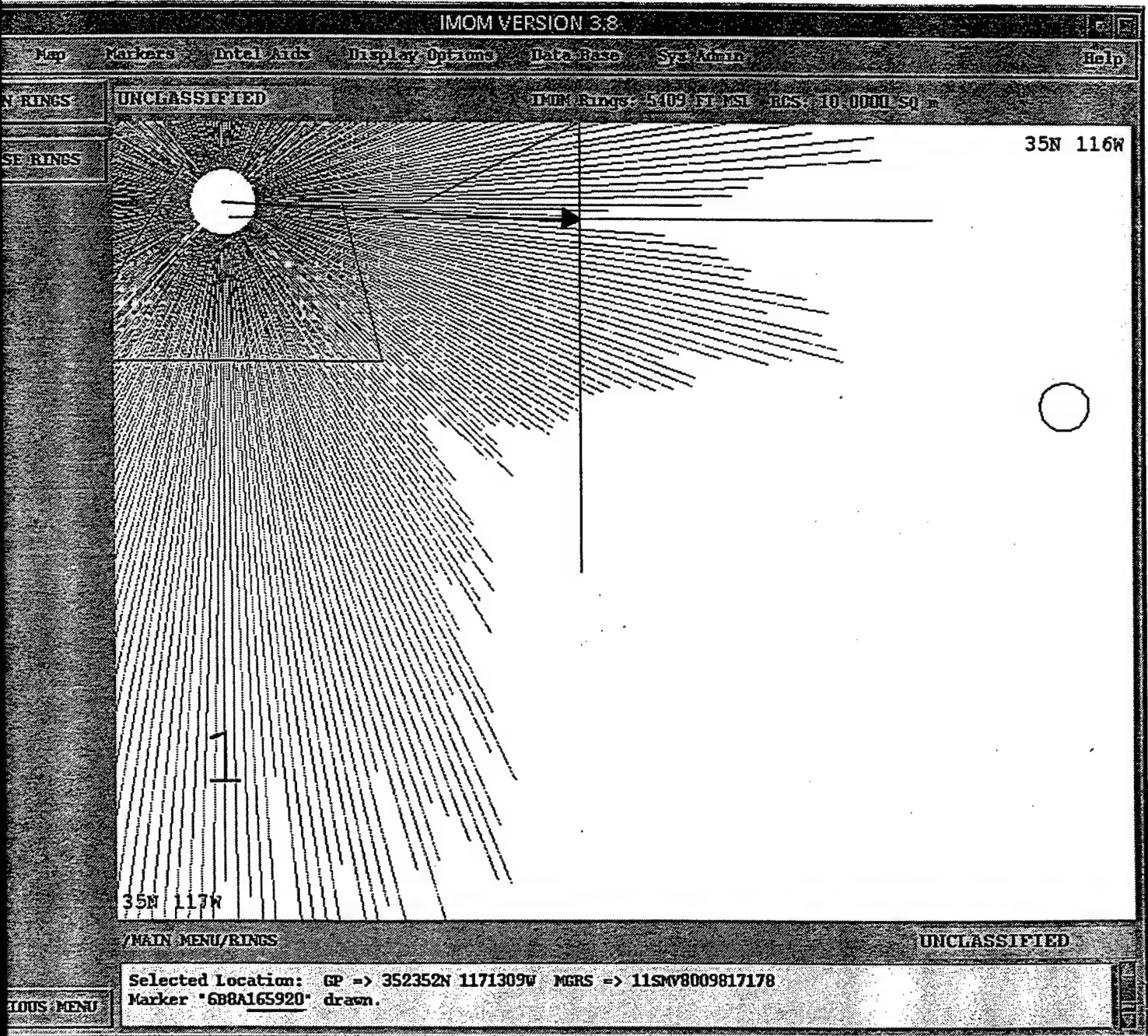
* 7605 FT

FIG. M-3

6B7D165026

7.6 nm @ 91.3° True

FIG. N-2
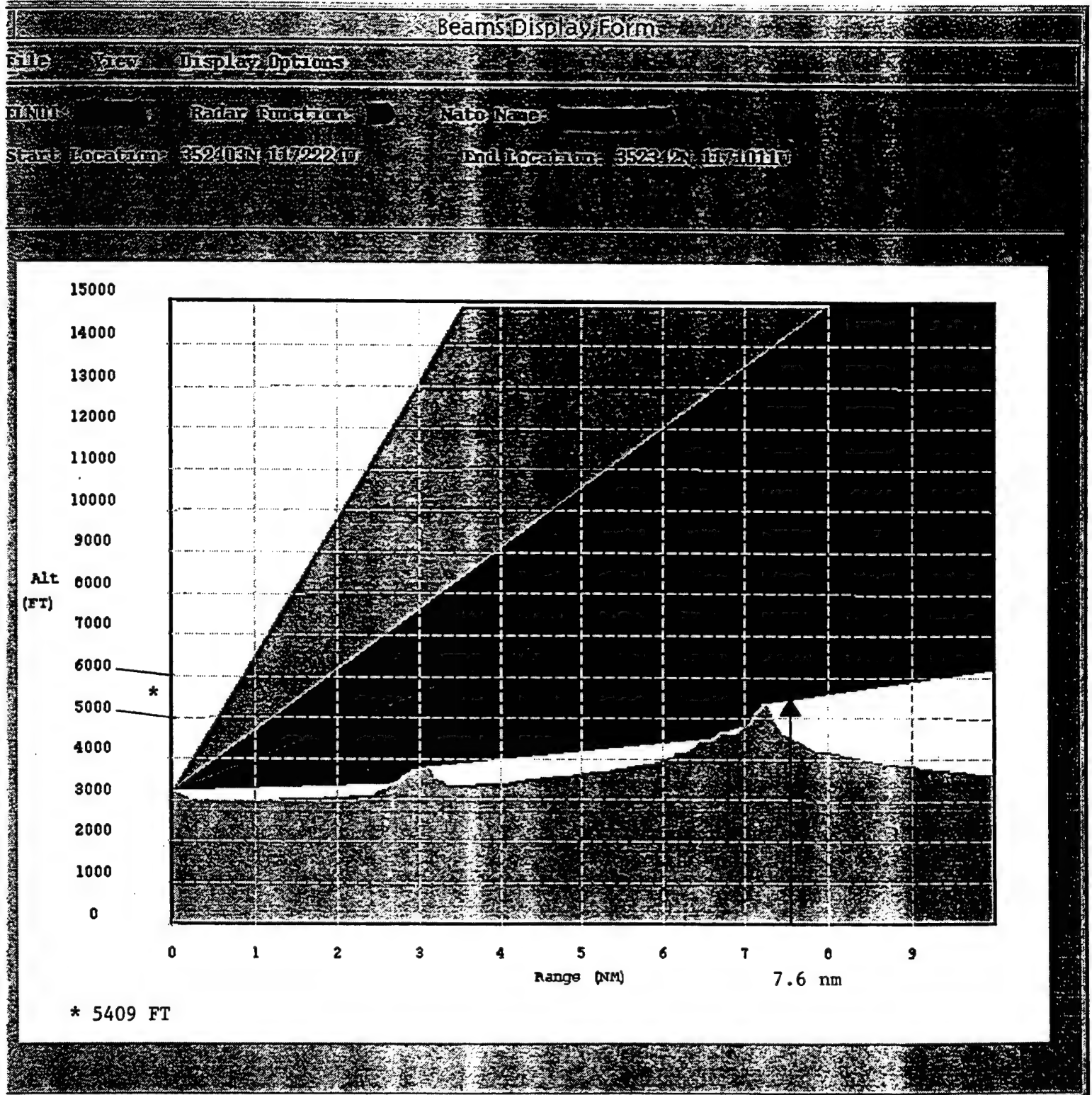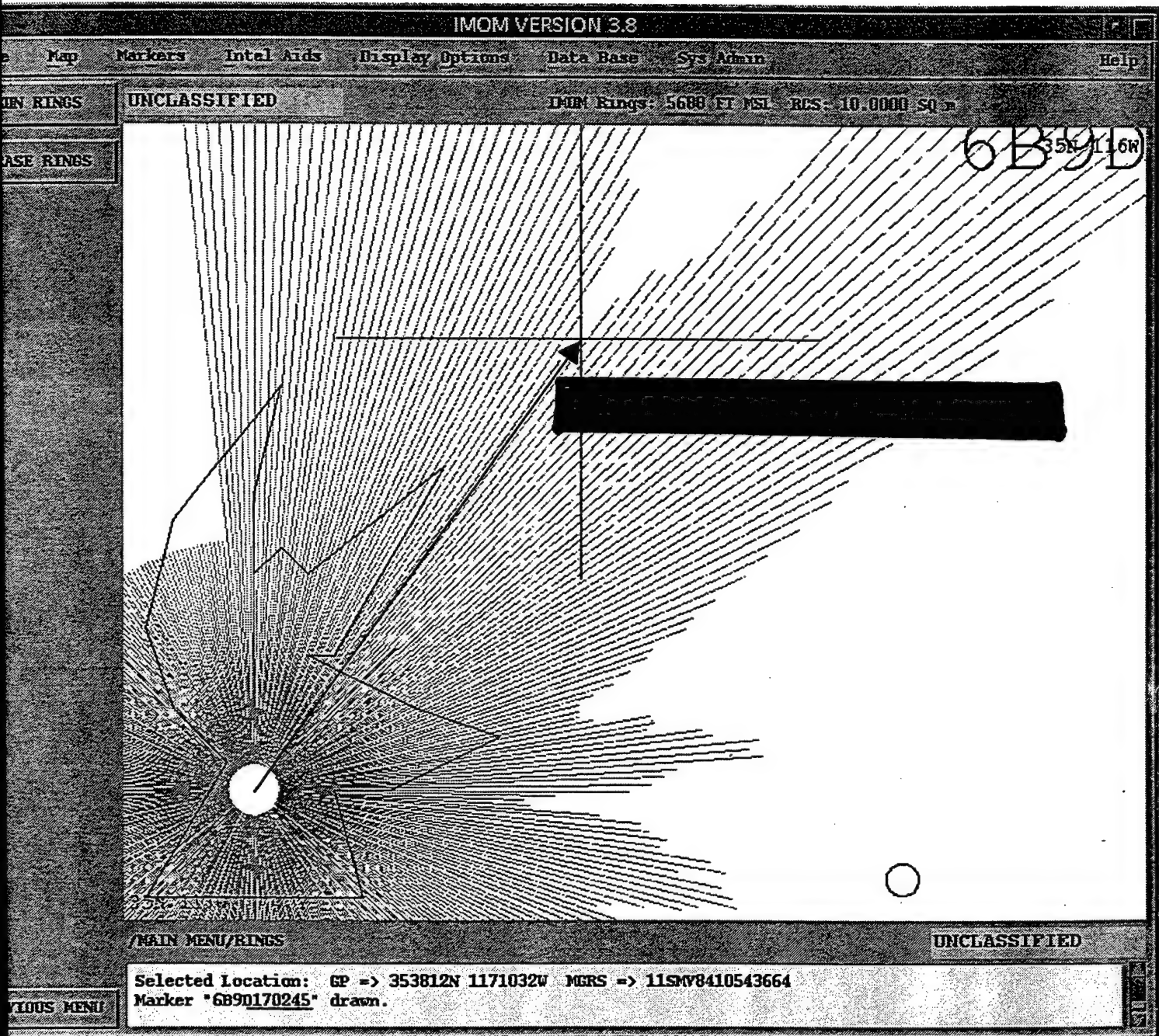
Beams Display Form

File   View   Display Options

Unit   Radar Function   Nato Name

Start Location: 352403N 1172224W   End Location: 352342N 1174101W

* 5409 FT

6B8A165920

FIG. O-1

17.1 nm @ 34.6° True
(.9nm)

FIG. O-2

Beams Display Form

File View Display Options

ELNOT: ⬛   Radar Function: ⬛   Nato Name: ⬛⬛⬛⬛

Start Location: 352403N 1172224W   End Location: 354050N 1170814W

* 5688 FT
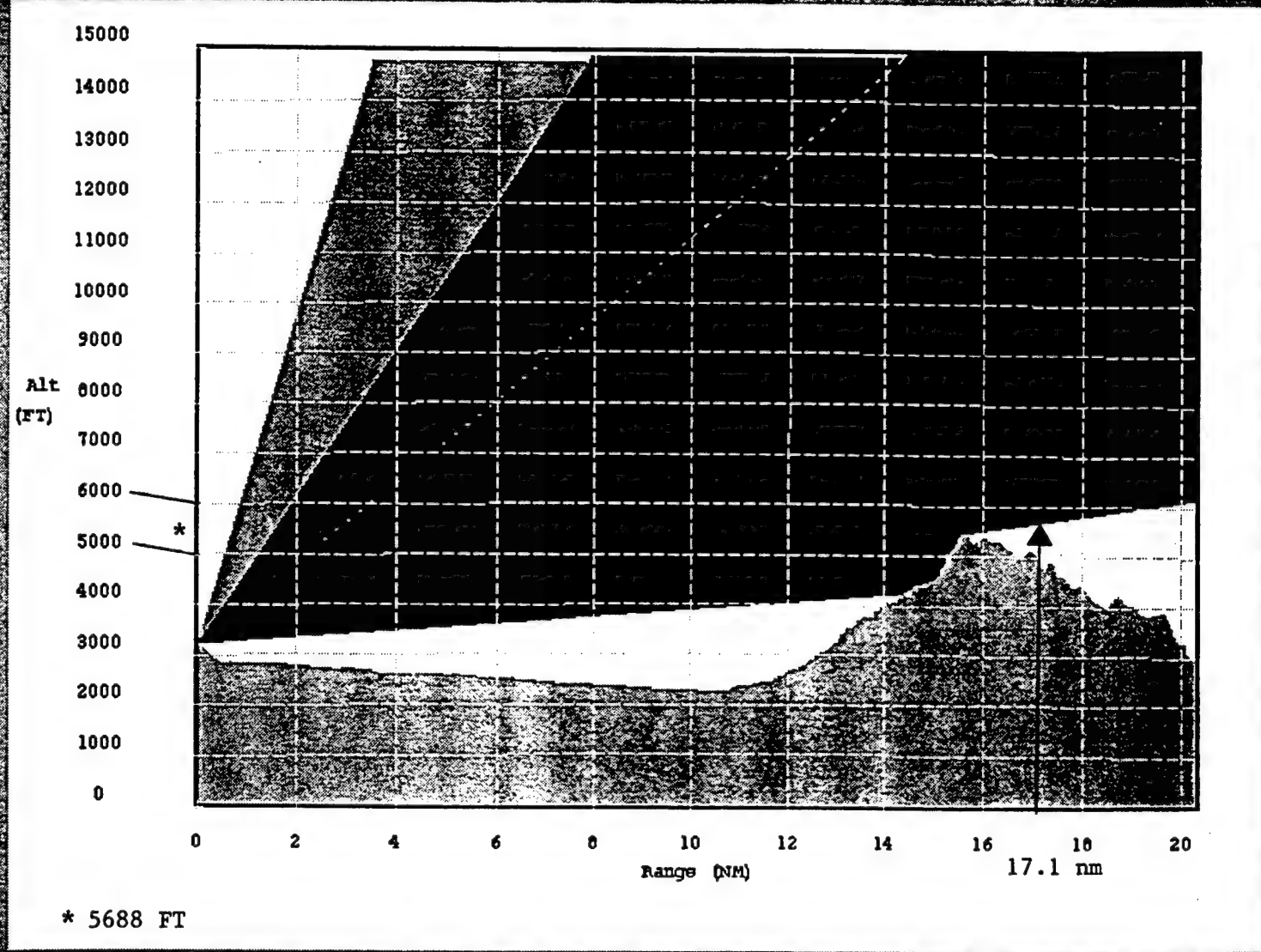
6B9D170245
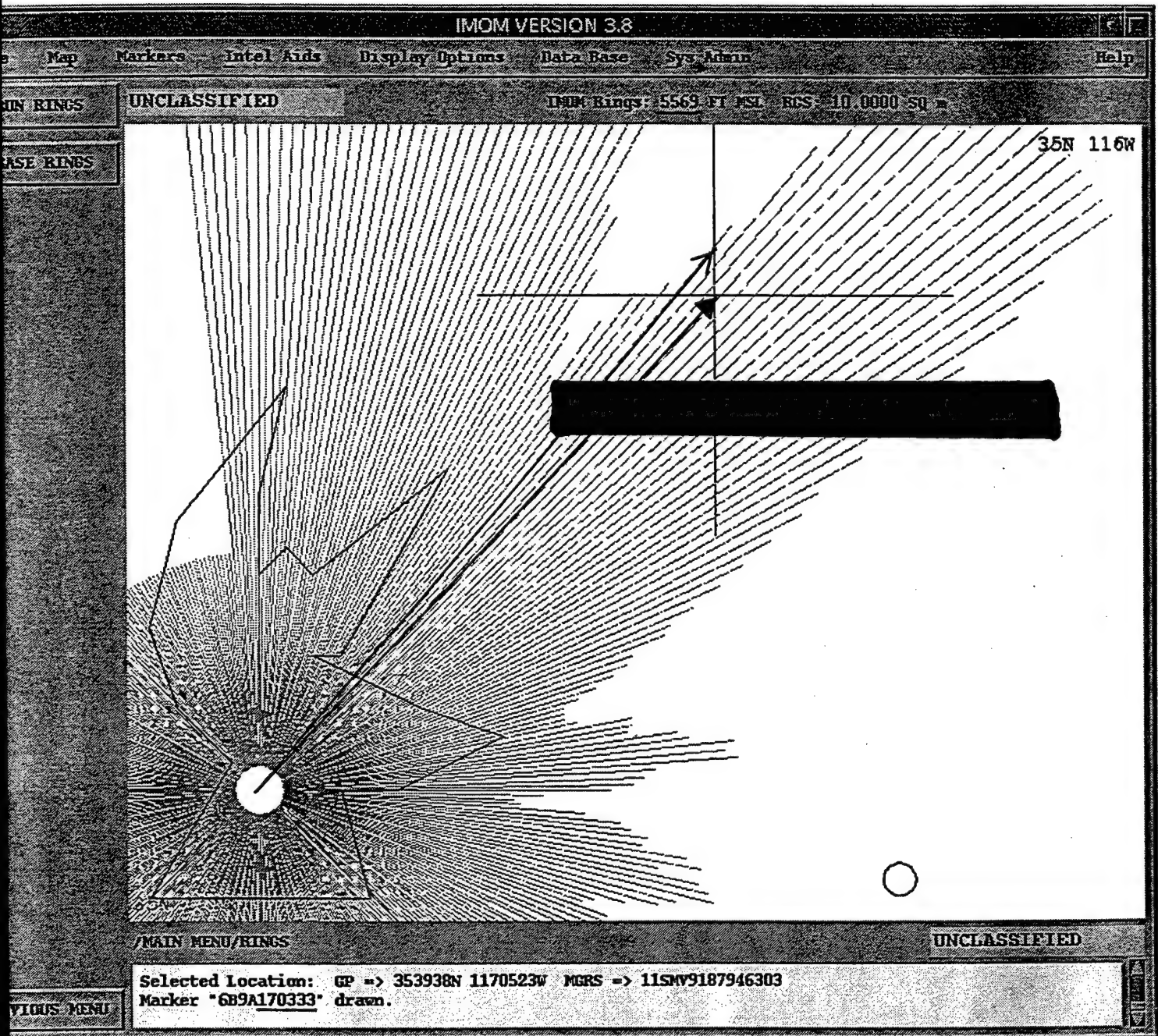
20.9 nm @ 41.6° True

(21.9 nm @ 39.0°)

FIG. P-2

Beams Display Form

File   View   Display Options

ELNOT: Radar Function: Nato Name:

Start Location: 352403N 1172224W   End Location: 354303N 1170139W

* 5569 FT

6B9A17033

FIG. P-3

Beams Display Form

File   View   Display Options

INDT: Radar Function: Nato Name:

Start Location: 352403N 1172224W   End Location: 354344N 1170257W

* 5569 FT

Range (NM)   21.9 nm
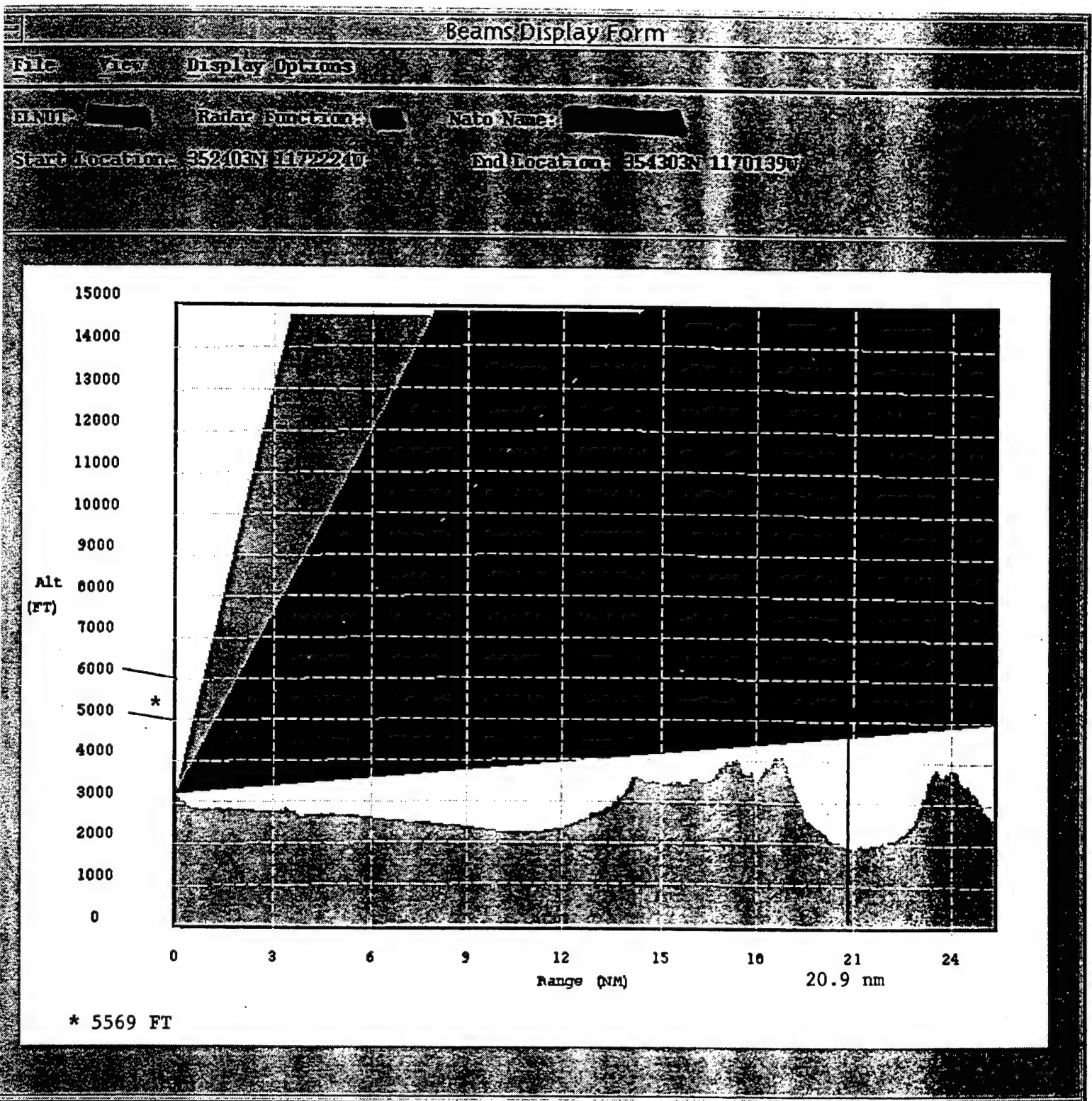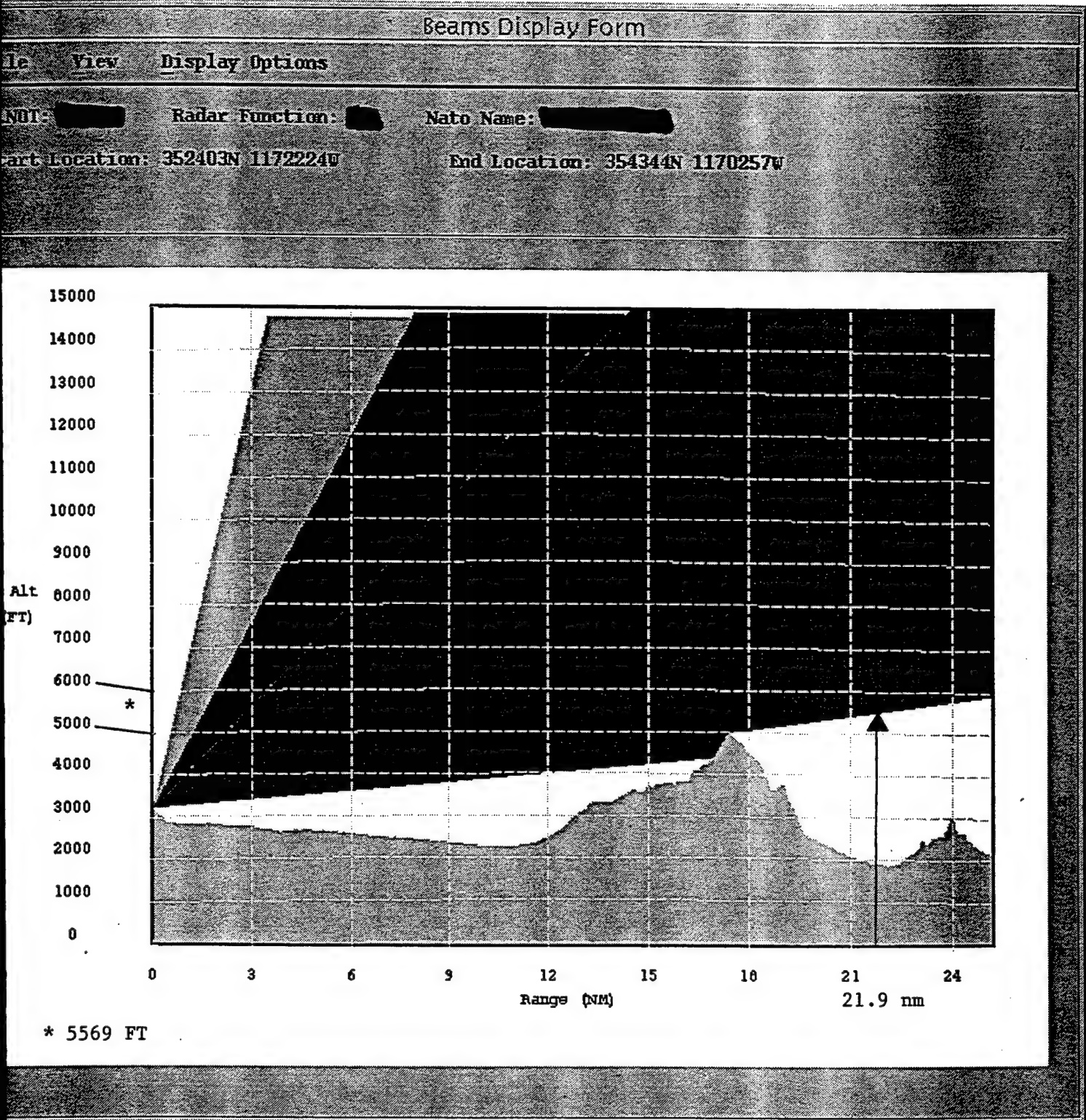
5B9A17033

83

FIG. Q-1
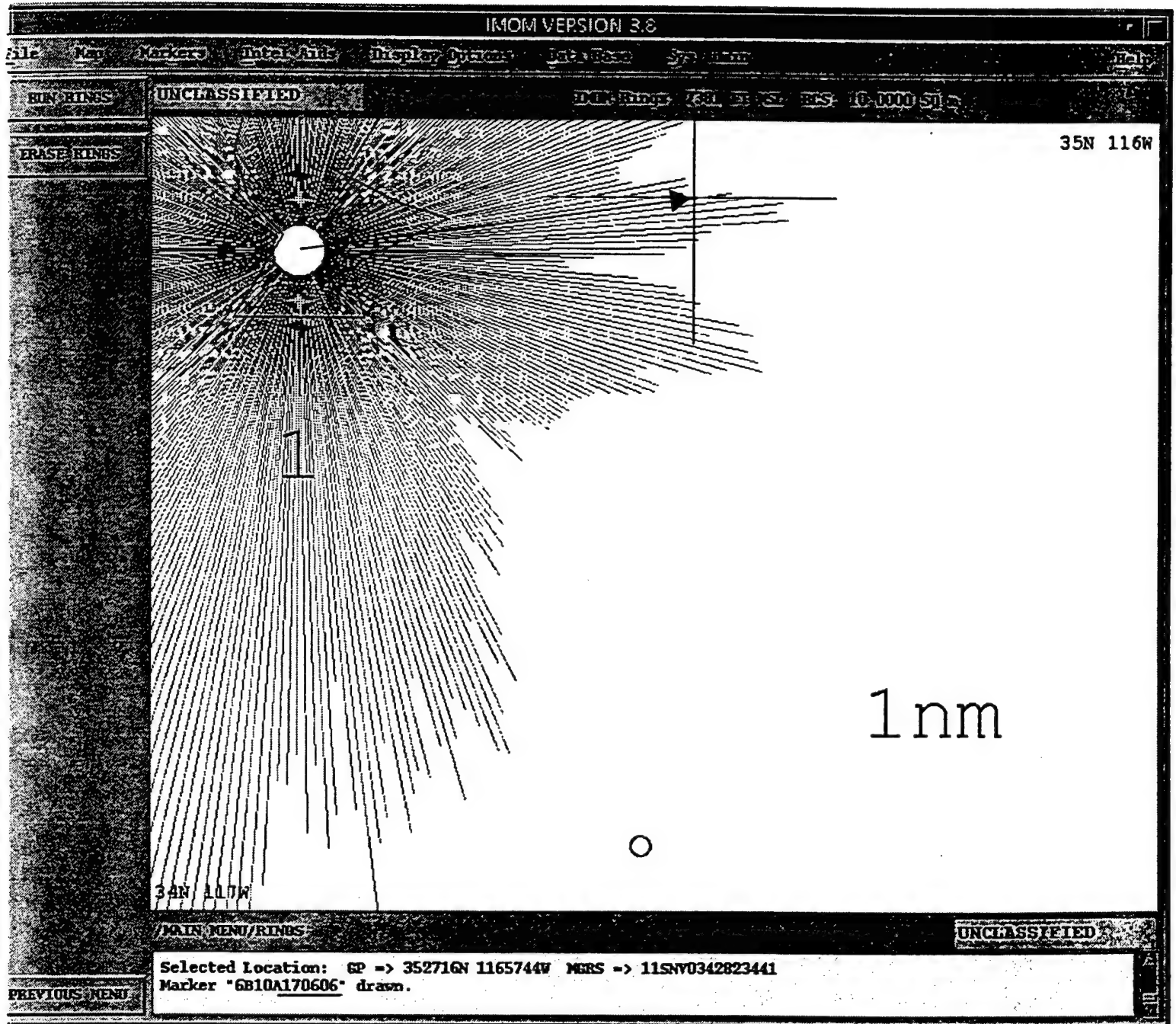
20.4 nm @ 80.6° True

FIG. Q-2
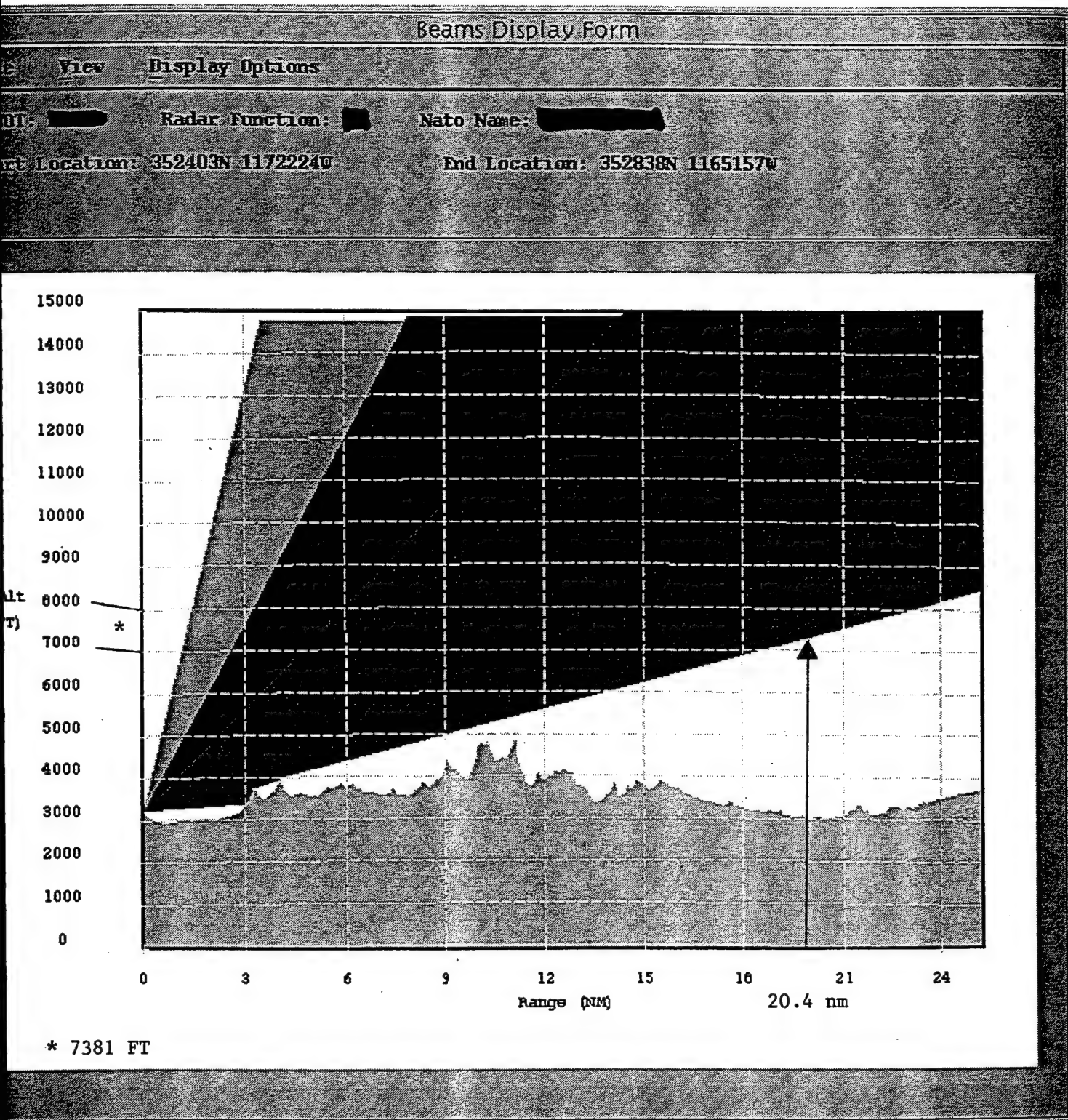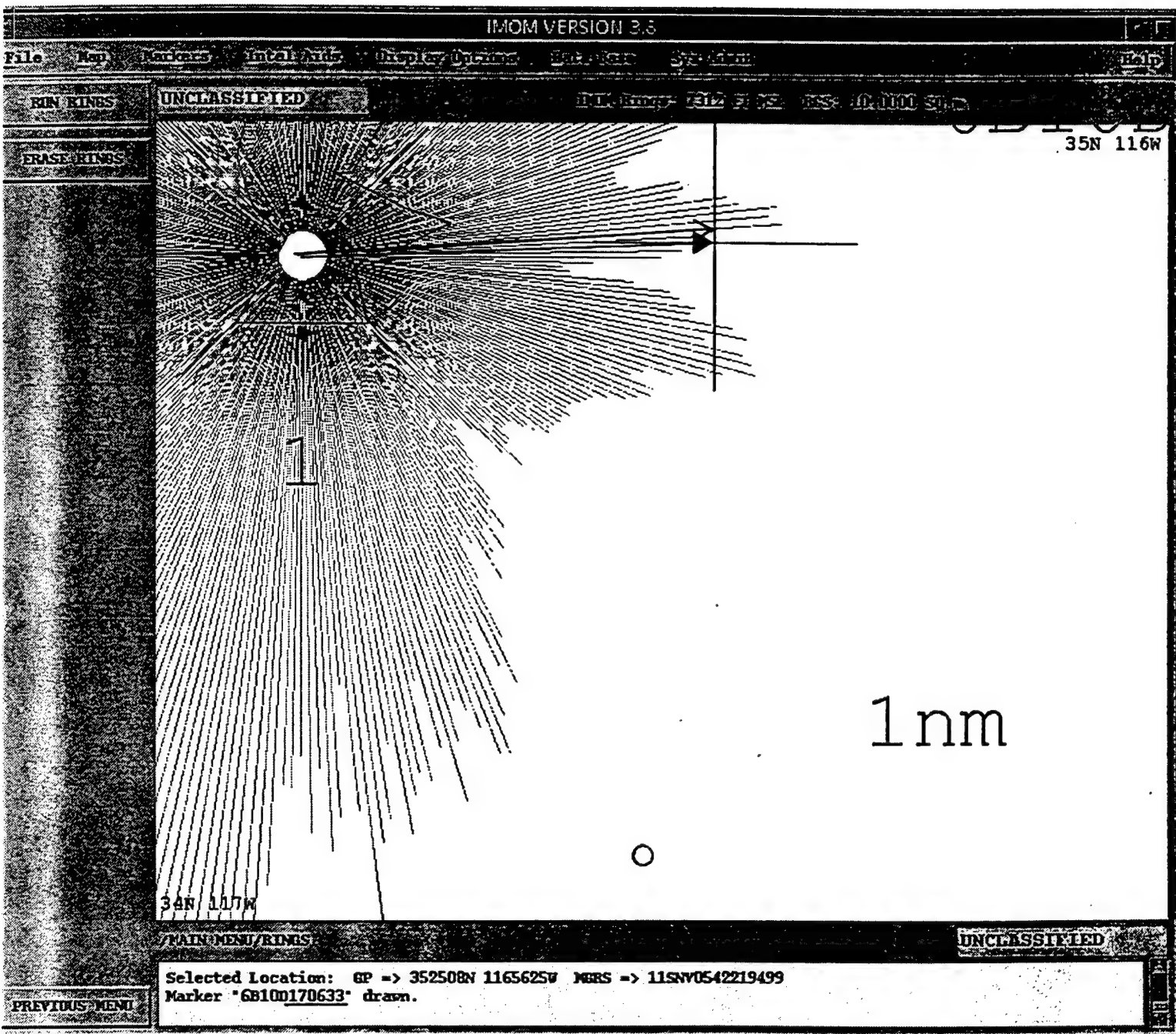
21.3 nm @ 87.1° True

(21.3 nm @ 85.4° True)

(.5nm)

FIG. R-2

* 7312 FT
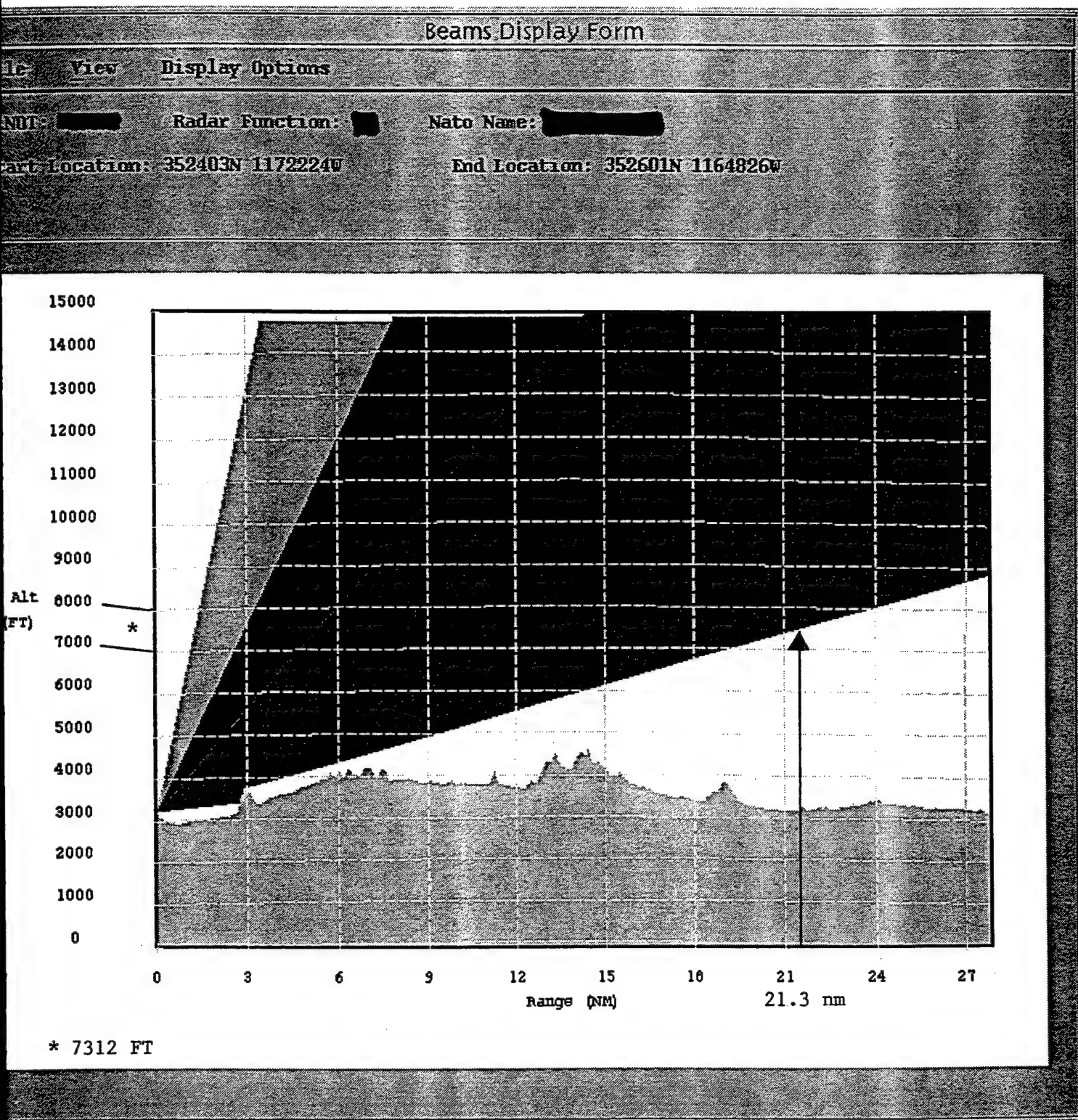
6B10D170633

FIG. S-1

21.2 nm @ 97.8° True

88

FIG. S-2

* 7505 FT
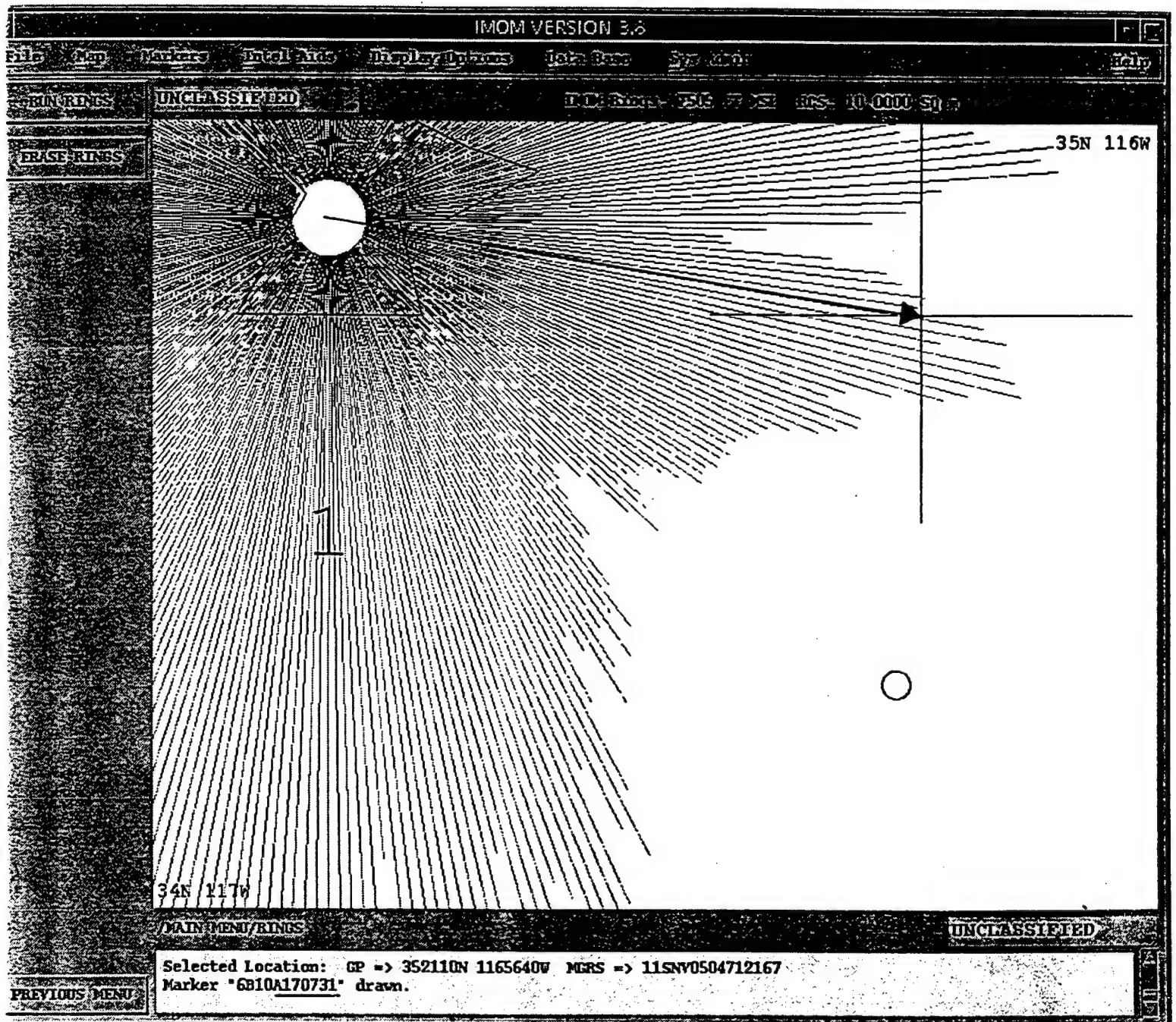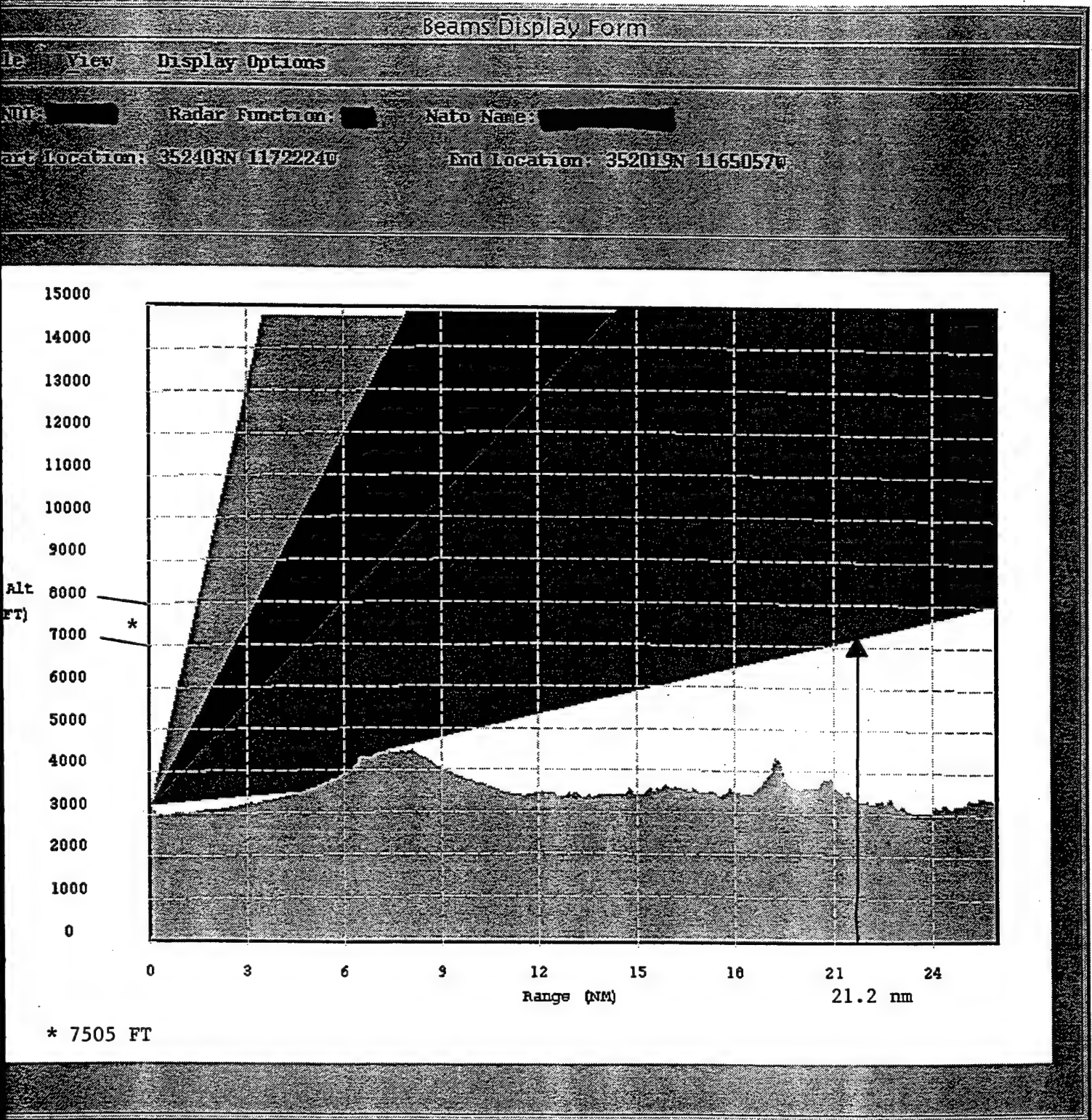
6B10A170731

20.4 nm @ 96.9° True
(.6nm)

FIG. T-2

Beams Display Form

View   Display Options

Radar Function: Nato Name:

Start Location: 352403N 1172224W   End Location: 352046N 1164921W

* 7464 FT
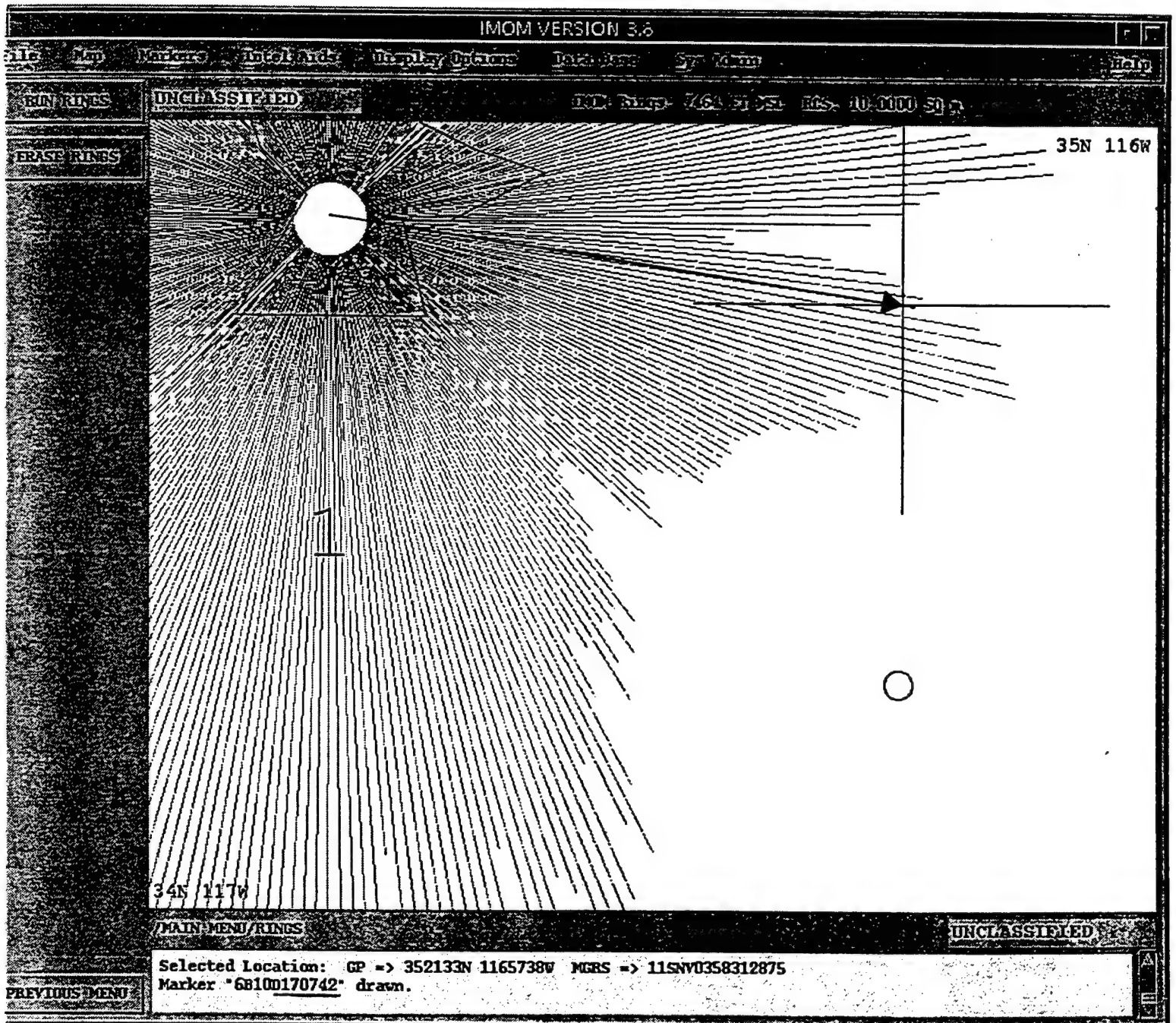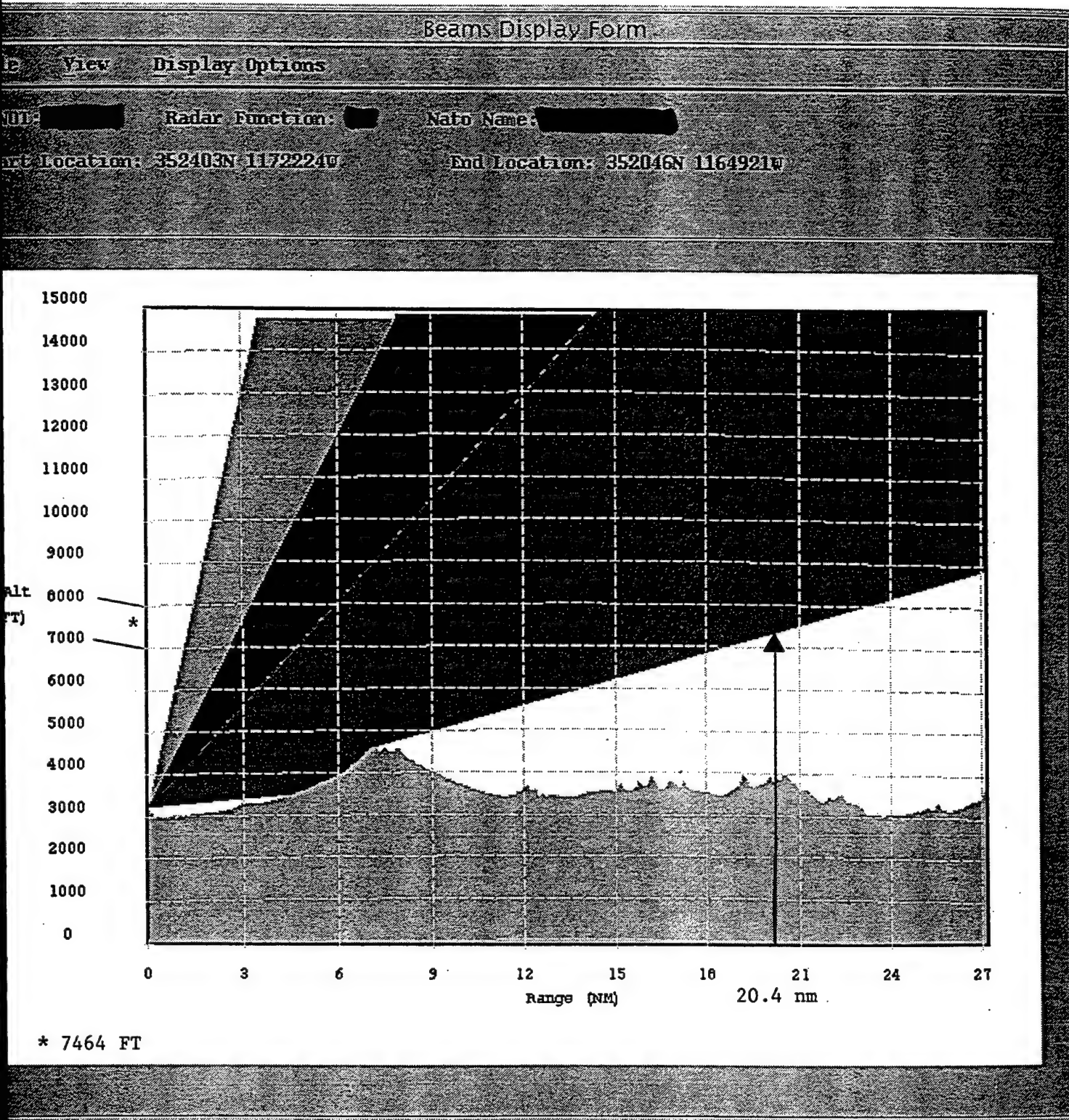
FIG. U-1

21.6 nm @ 85° True

FIG. U-2

Beams Display Form

View   Display Options

NOT: Radar Function: Nato Name:

art Location: 352403N 1172224W   End Location: 352606N 1164923W

* 7411
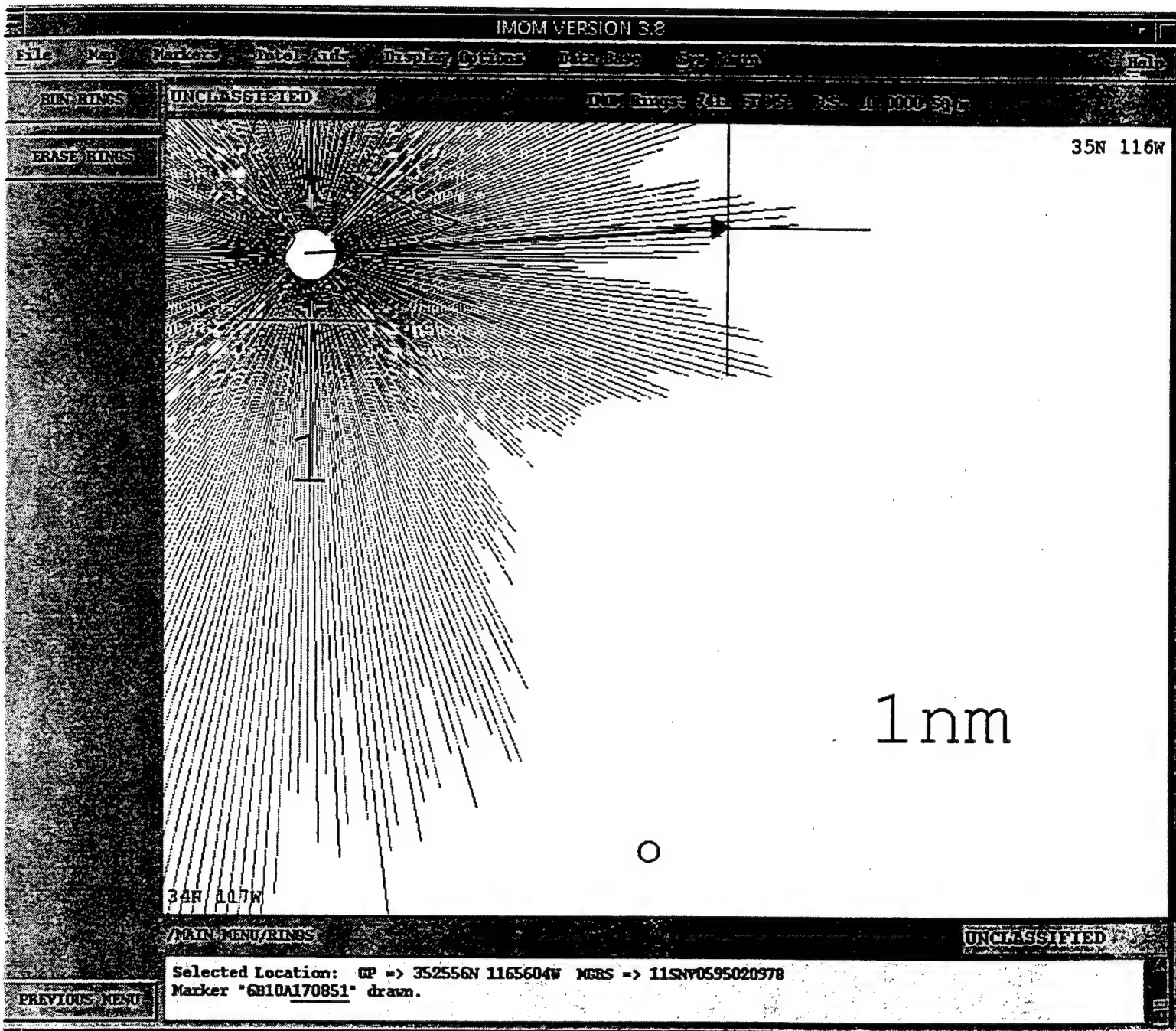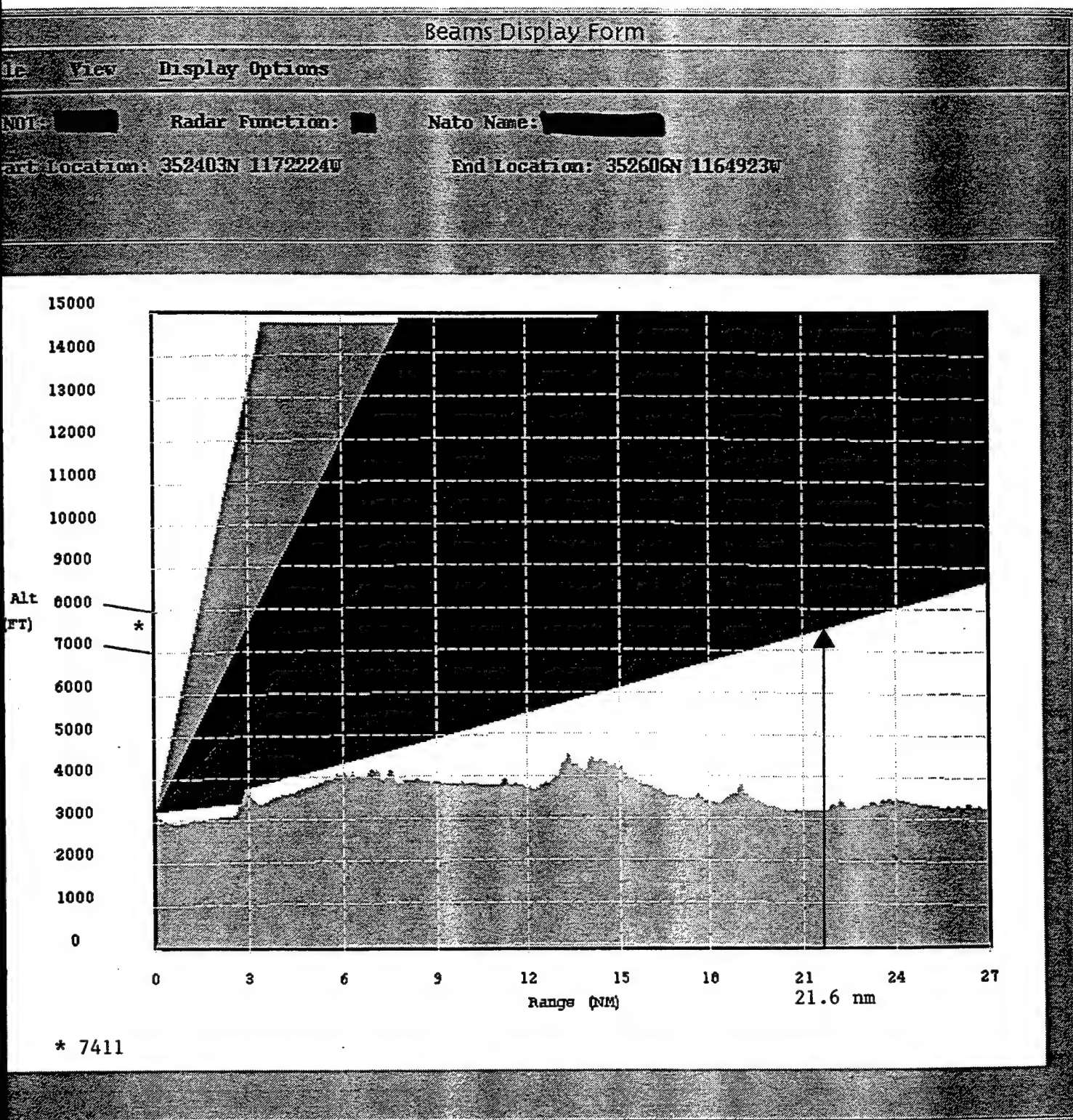
FIG. V-1

7.3 nm @ 91.3° True
(.2nm)

FIG. V-2

Beams Display Form

View   Display Options

NDT: Radar Function: Nato Name:

Start Location: 352403N 1172224W   End Location: 352346N 1170933W

Alt (FT) axis (vertical): 15000, 14000, 13000, 12000, 11000, 10000, 9000, 8000, 7000, 6000, 5000, 4000, 3000, 2000, 1000, 0

Range (NM) axis (horizontal): 0, 1, 2, 3, 4, 5, 6, 7, 8, 9, 10

Range (NM)   7.3 nm

* 5482 FT

6B11A171156

95

FIG. W-1

35N 117W

5.7 nm @ 92° True
(.2nm)

FIG. W-2

Beams Display Form

View   Display Options

NOr: ▮▮▮▮▮   Radar Function: ▮   Nato Name: ▮▮▮▮▮▮▮

Start Location: 352403N 1172224W   End Location: 352332N 1171325W

* 4052 FT

FIG. X-1

3.6 nm @ 93.9° True

FIG. X-2
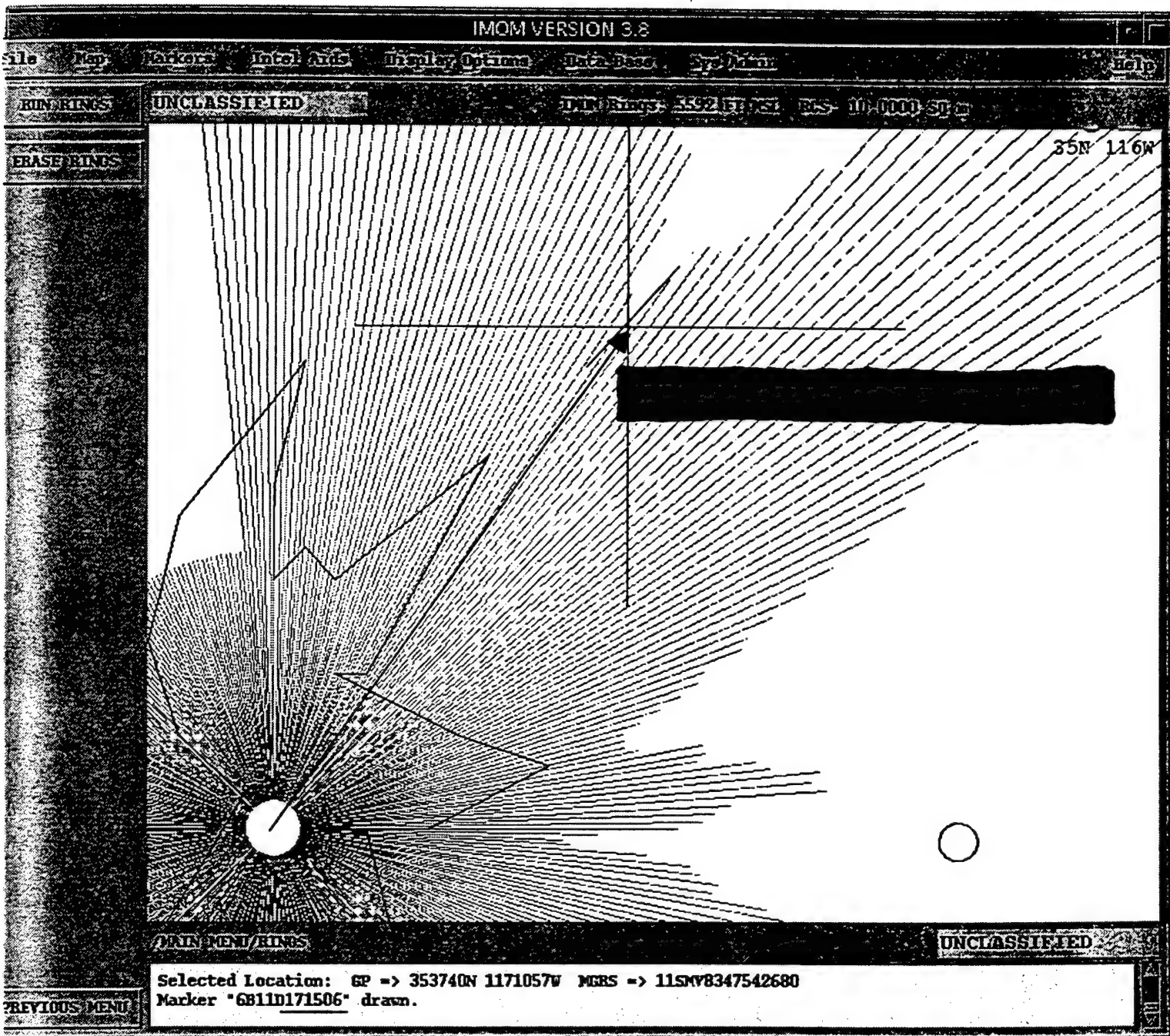
Beams Display Form

File   View   Display Options

NDT: ████   Radar Function: ██   Nato Name: ████████

Start Location: 352403N 1172224W   End Location: 352342N 1171558W

* 3726

6B11A171226

99

FIG. Y-1

16.5 nm @ 34.5° True

FIG. Y-2

Beams Display Form

File   View   Display Options

NDT: ▮▮▮   Radar Function: ▮   Nato Name: ▮▮▮▮▮▮▮

Start Location: 352403N 1172224W   End Location: 353935N 1170921W

* 5592 FT

6B11D171506

FIG. Z
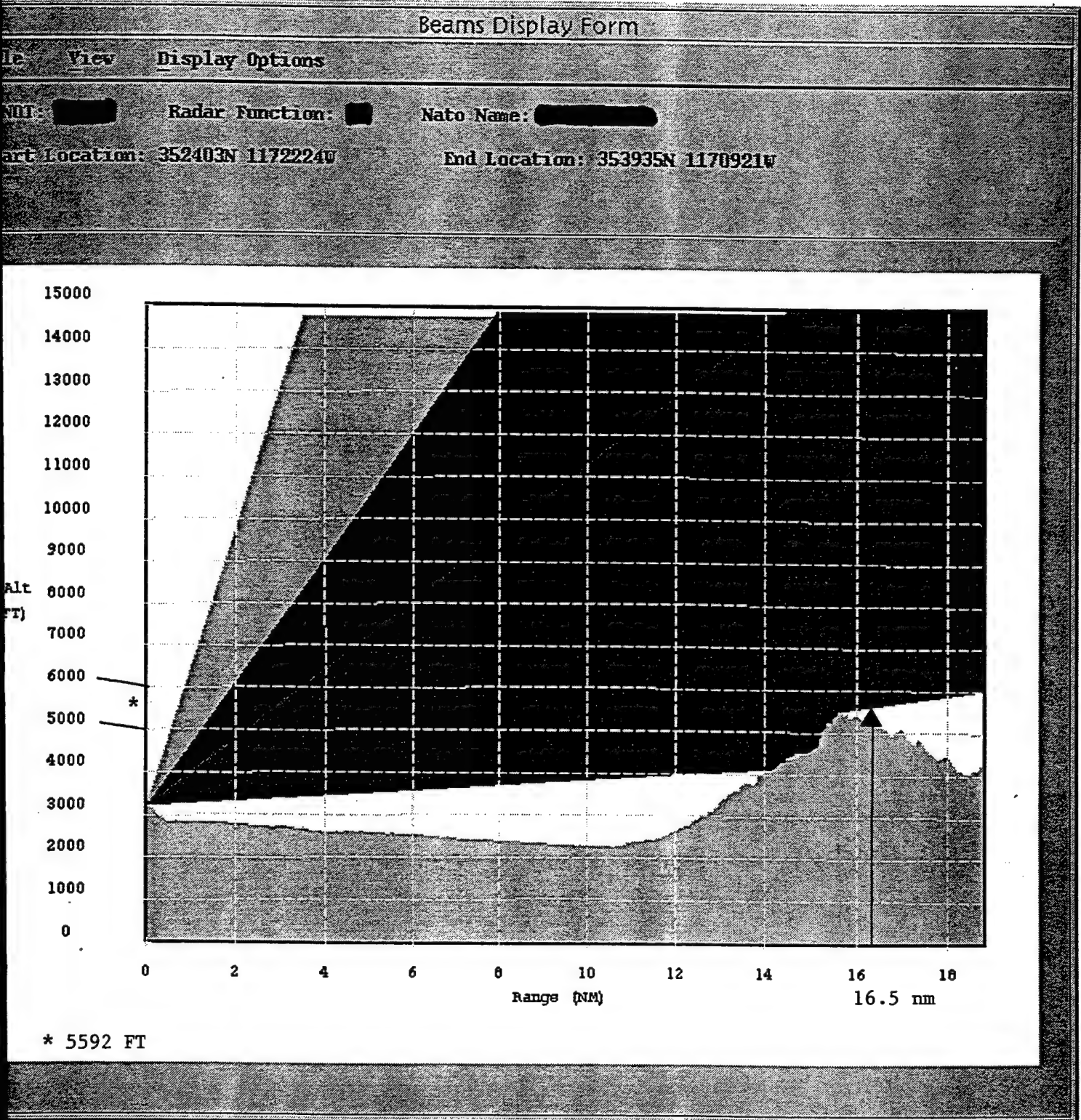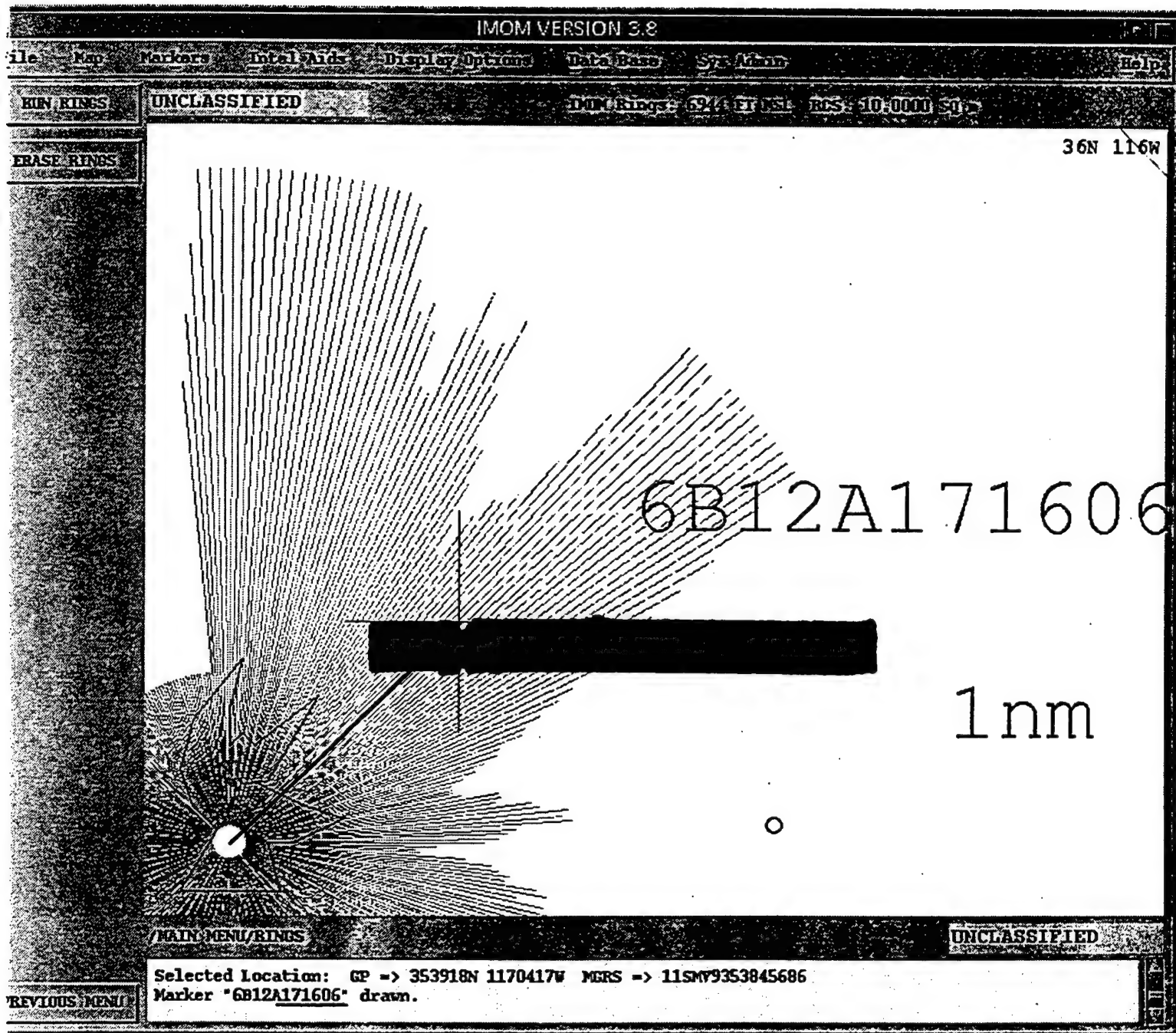
21.3 nm @ 44.1° True

20.6 nm @ 48.2° True
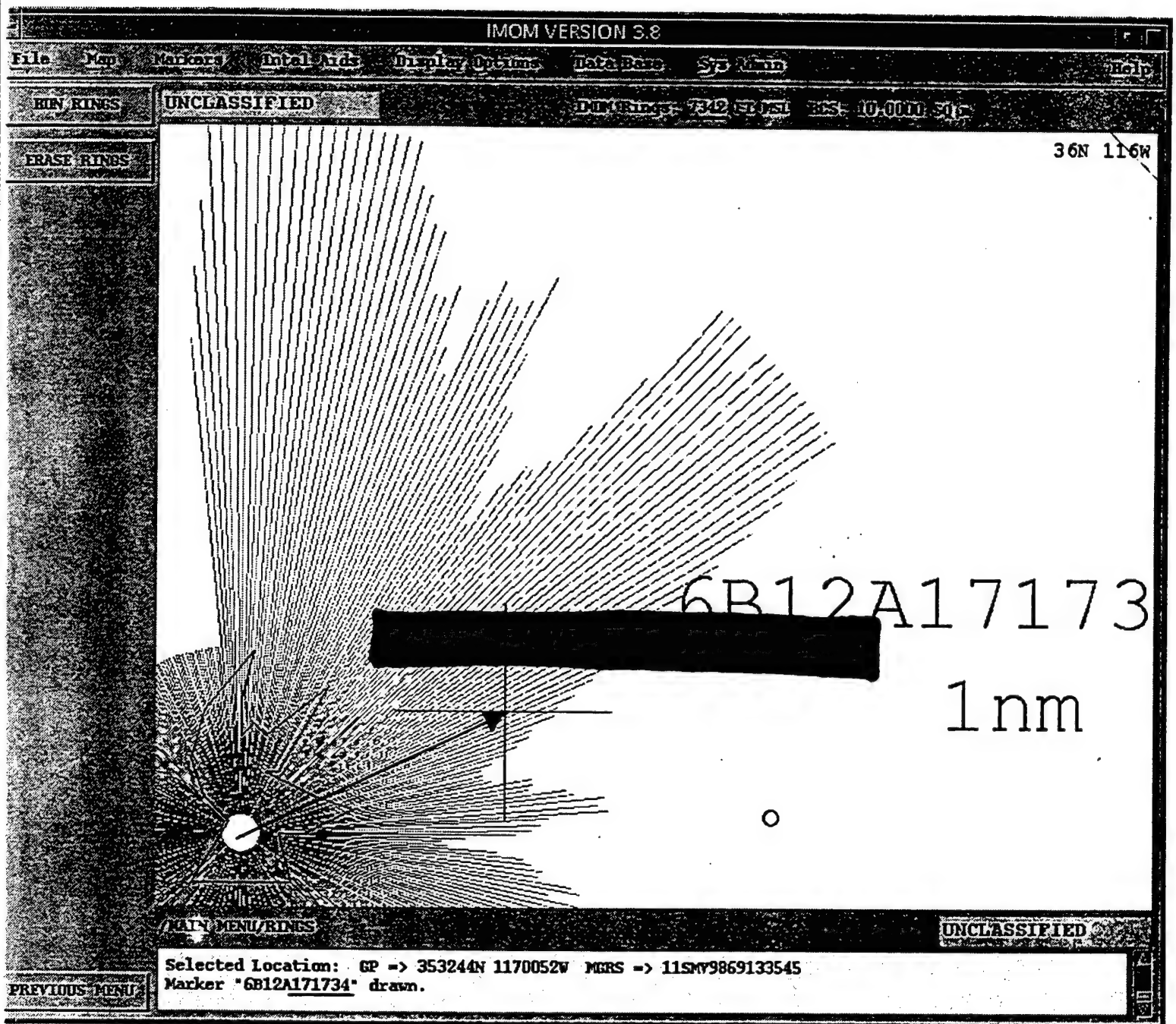
19.7 nm @ 63.4° True
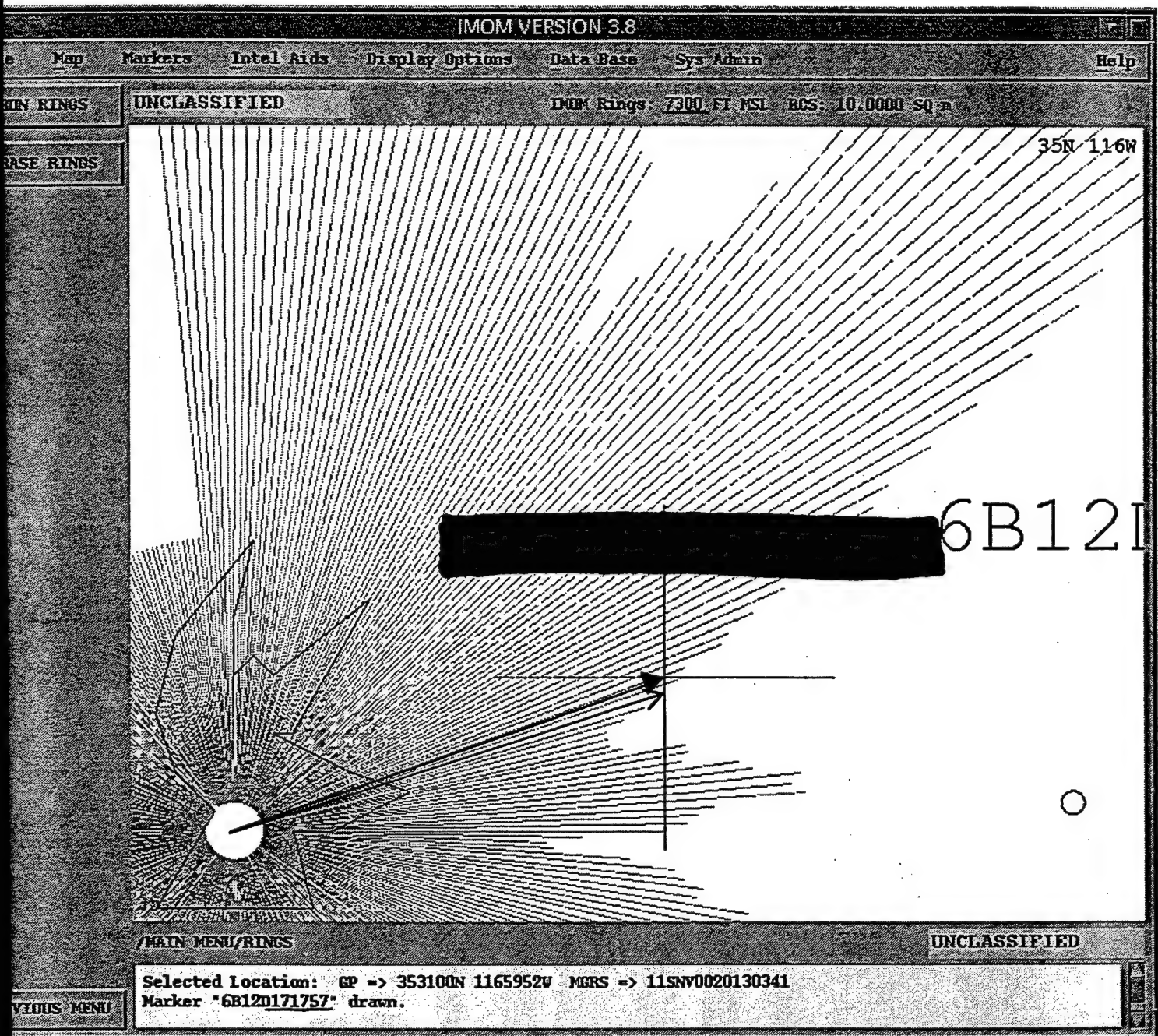
FIG. CC-1

19.7 nm @ 69.1° True
(.5 nm)

FIG. CC-2

Beams Display Form

File   View   Display Options

ELNOT: [redacted]   Radar Function: [redacted]   Nato Name: [redacted]

Start Location: 352403N 1172224W   End Location: 353259N 1165237W

* 7300 FT
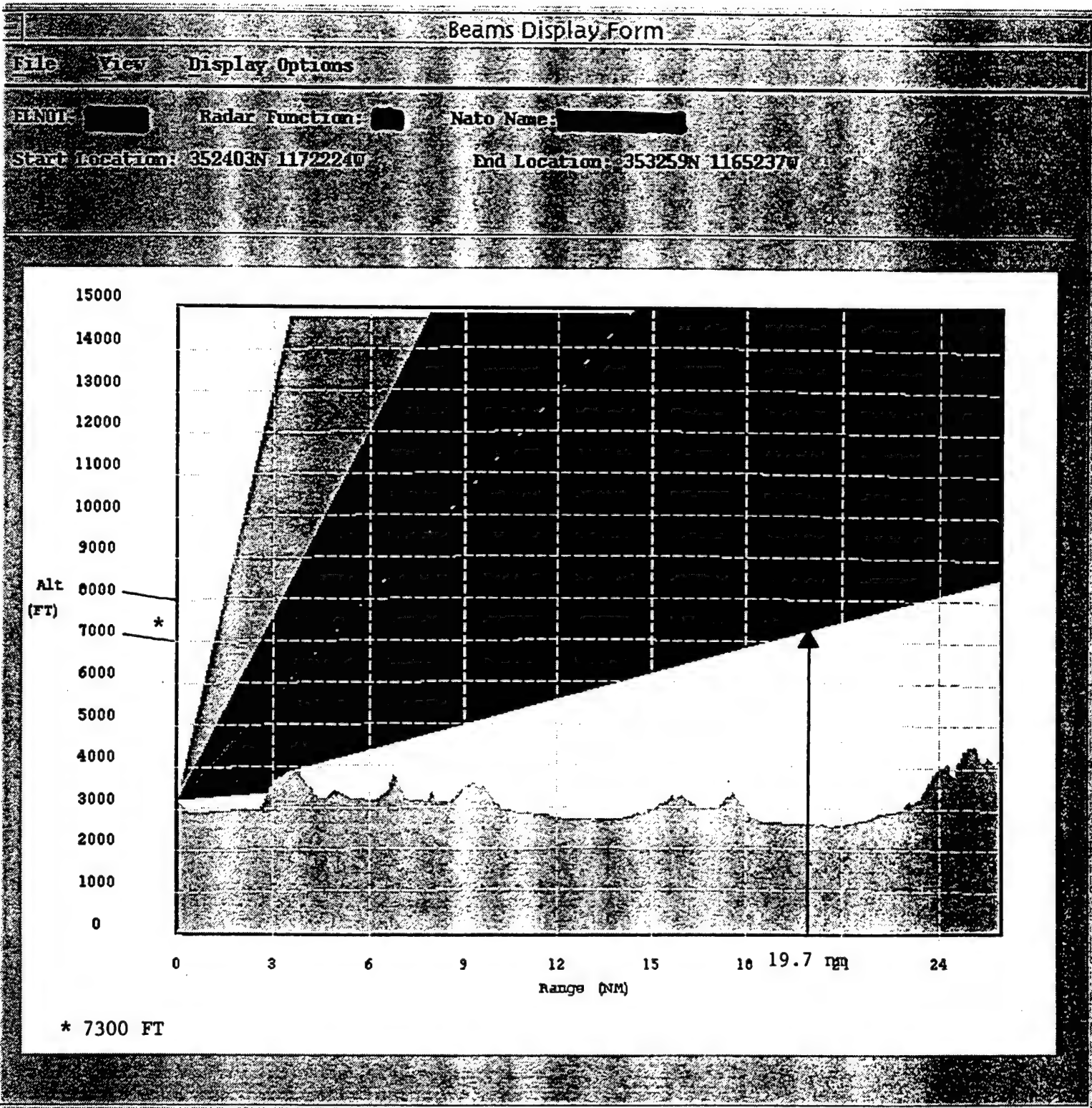
6B12D171757
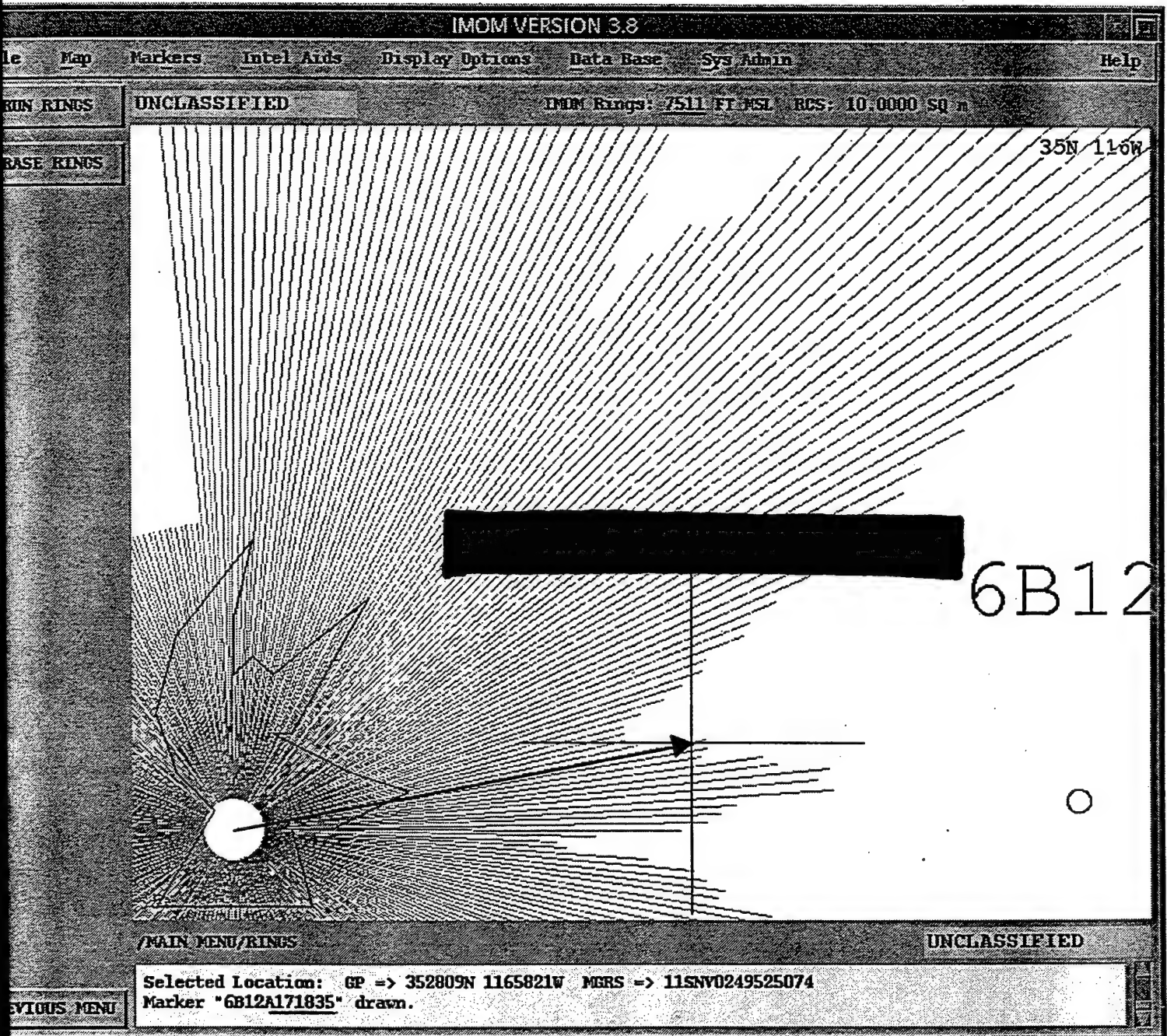
FIG. DD-1

20.1 nm @ 78.0° True

FIG. DD-2

Beams Display Form

File   View   Display Options

ELNOT: Radar Function: Nato Name:

Start Location: 352403N 1172224W   End Location: 352936N 1165039W

Alt (FT)

* 7511 FT

Range (NM)

20.1 nm
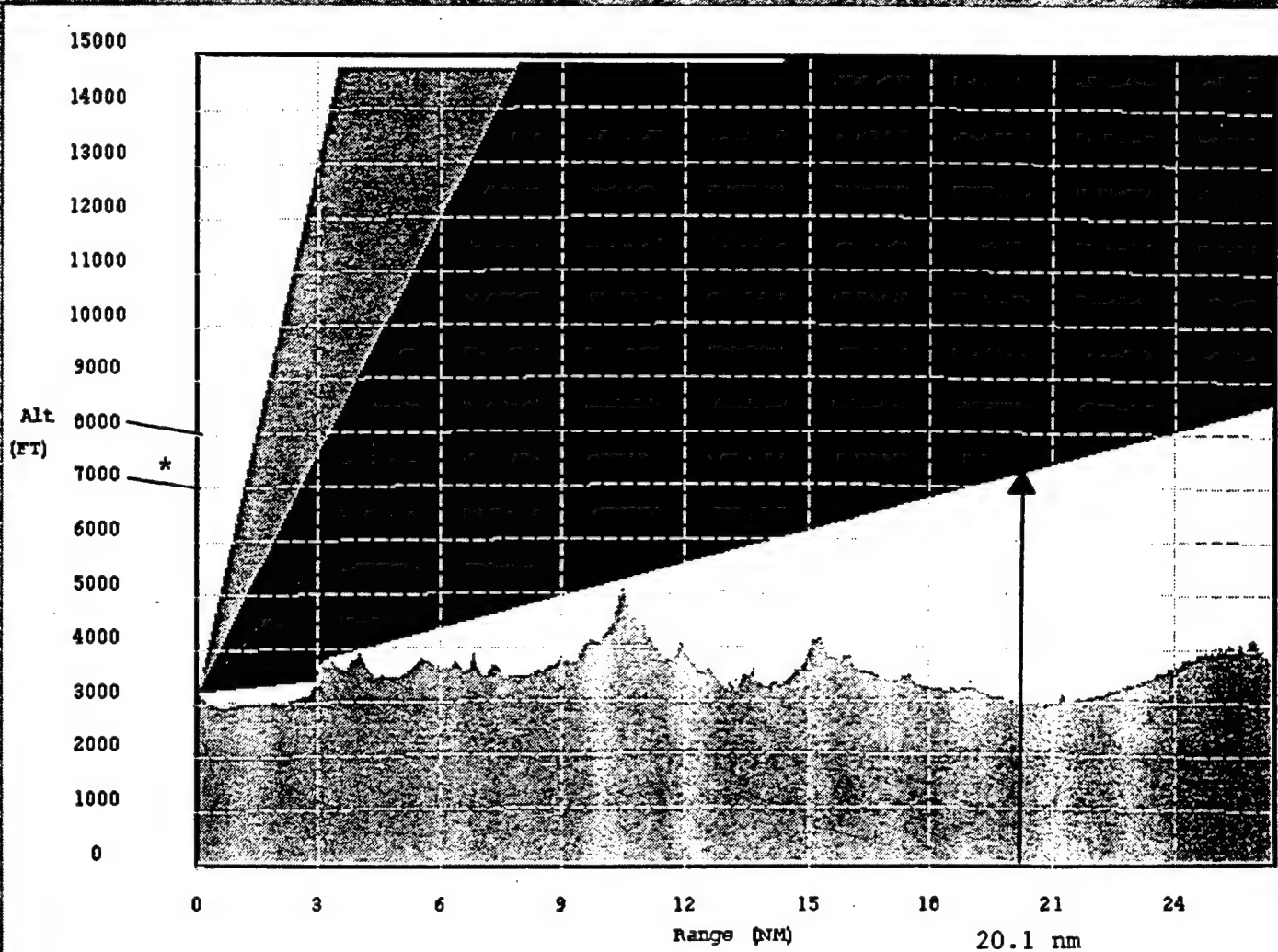
6B12A171835

FIG. EE-1

21.1 nm @ 87.8° True
(86.1° True .5nm)

FIG. EE-2

Beams Display Form

File   View   Display Options

ELNOT: ▮▮▮   Radar Function: ▮   Nato Name: ▮▮▮▮

Start Location: 352403N 1172224W   End Location: 352540N 1165312W

* 7430 FT

Range (NM)

21.1 nm

6B12D171719

110
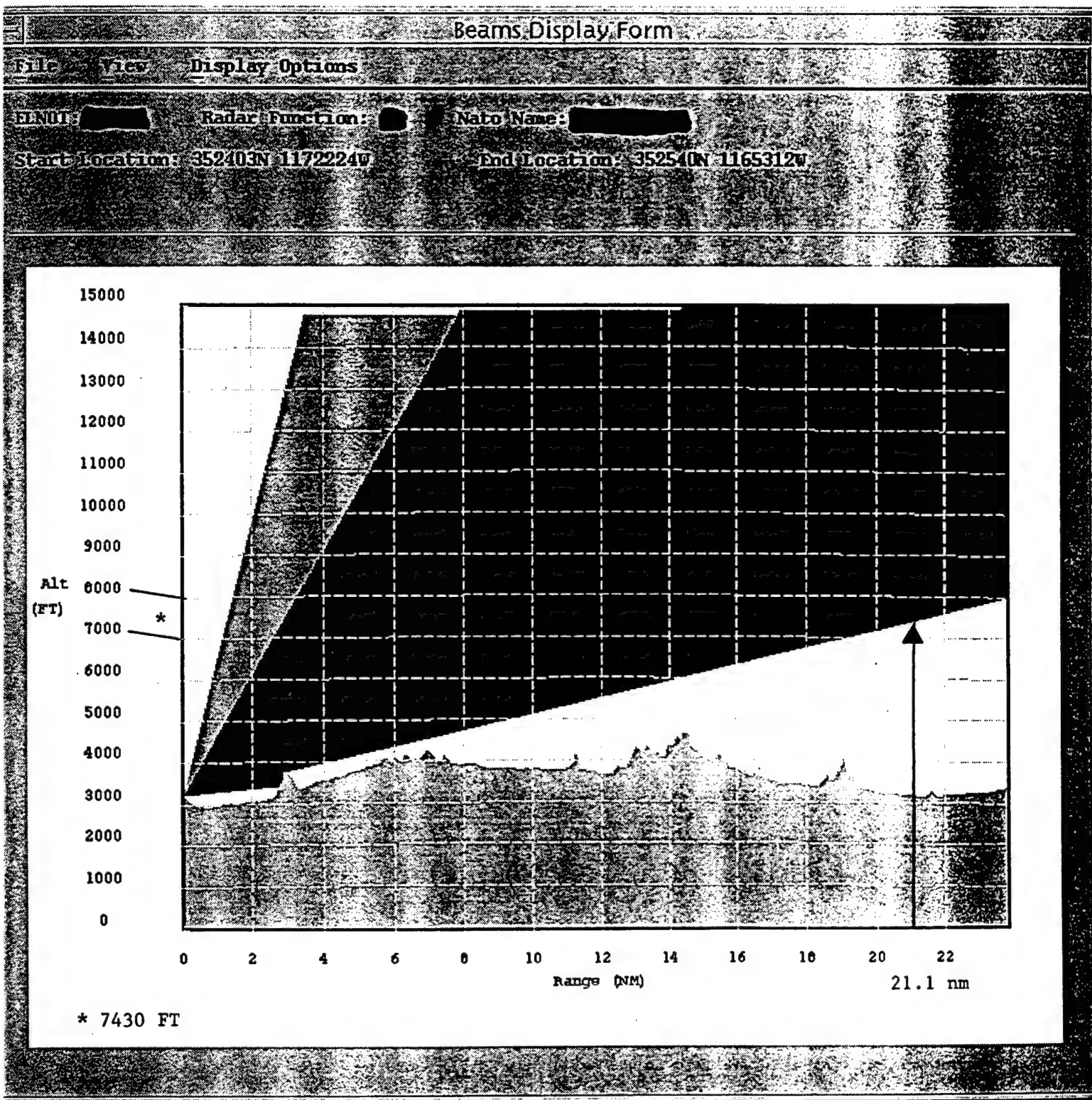
FIG. FF-1

18.1 nm @ 89.3° True

111

FIG. FF-2
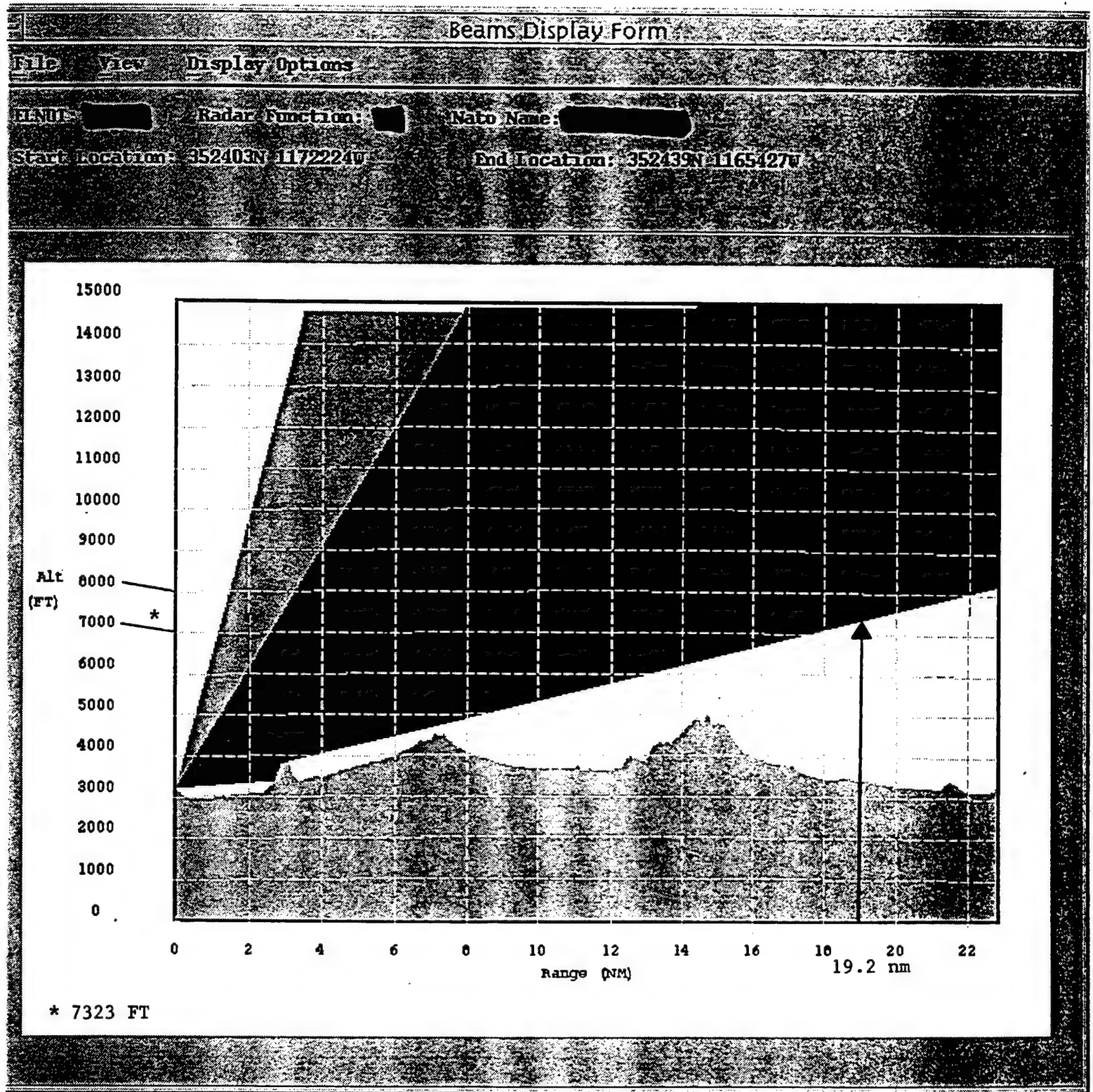

* 7358 FT
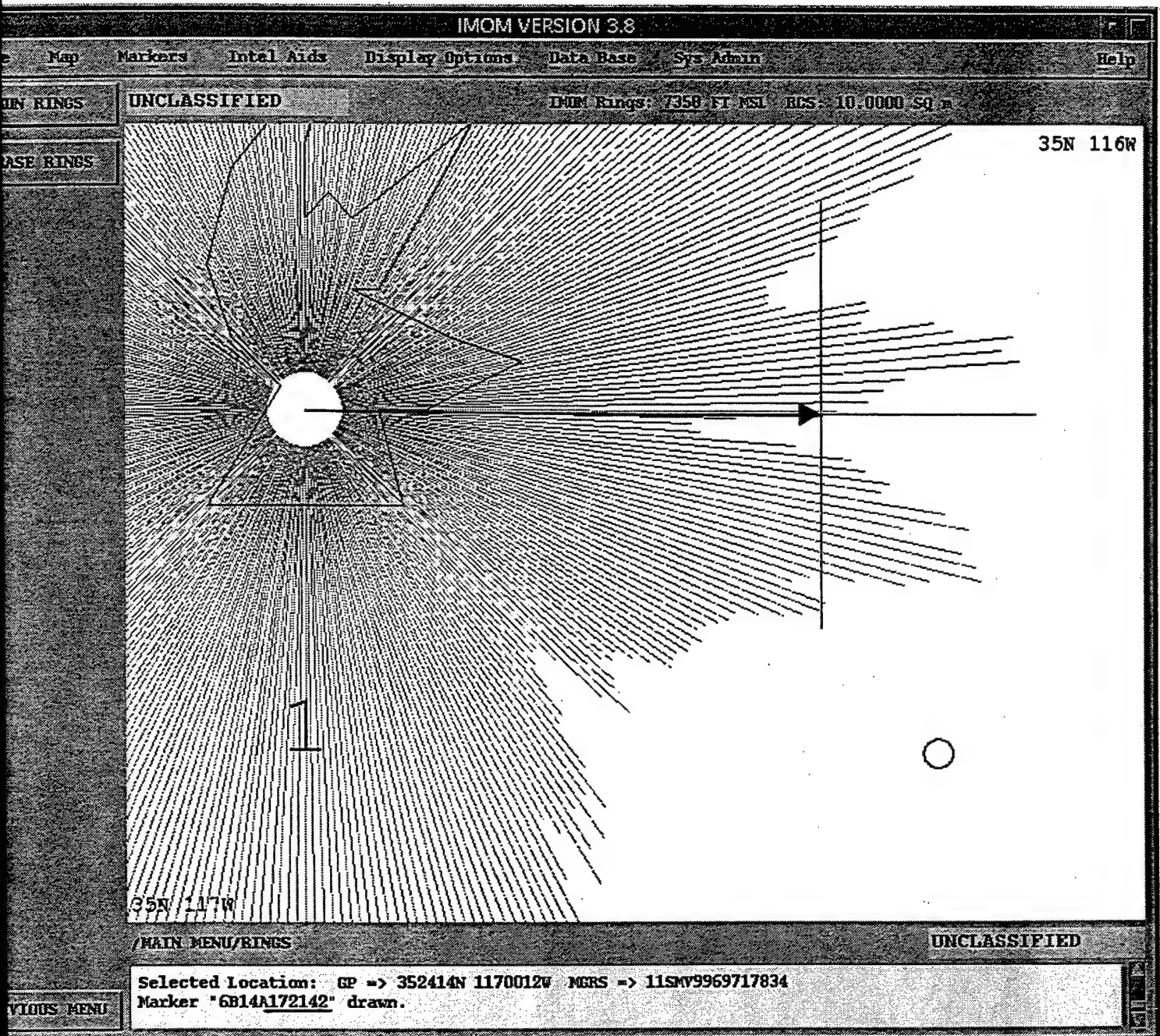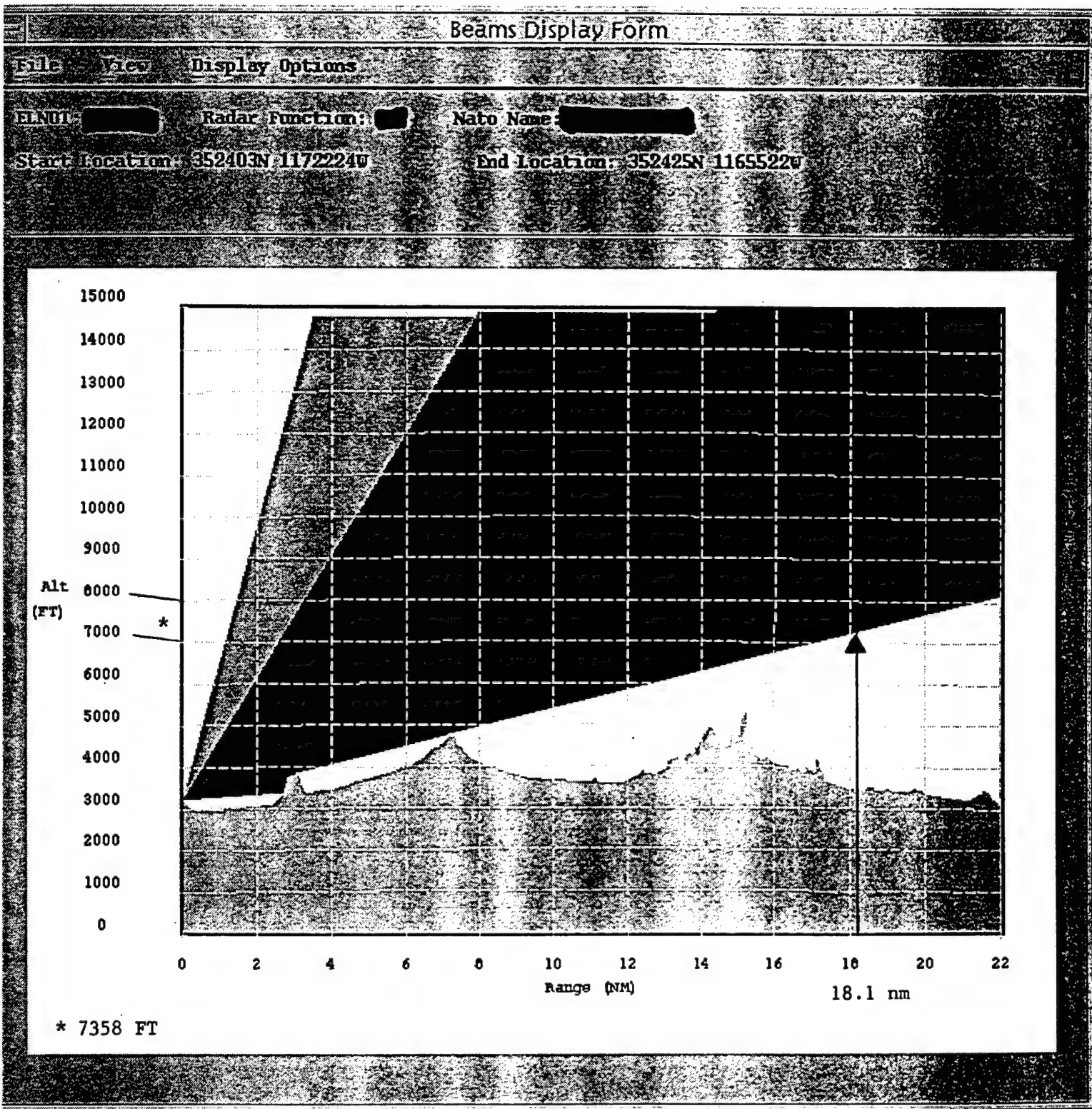
FIG. GG
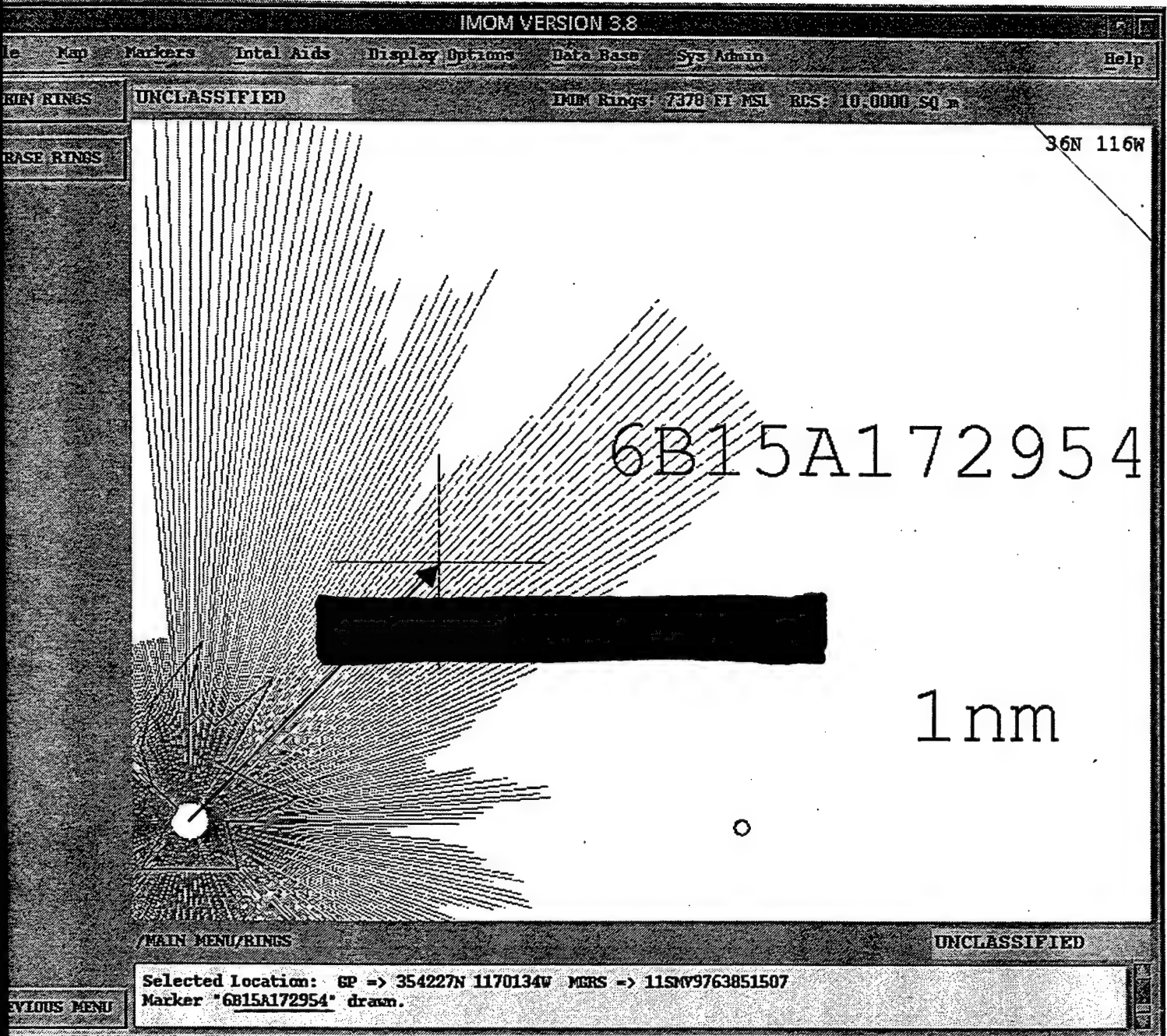
25.0 nm @ 43.0° True
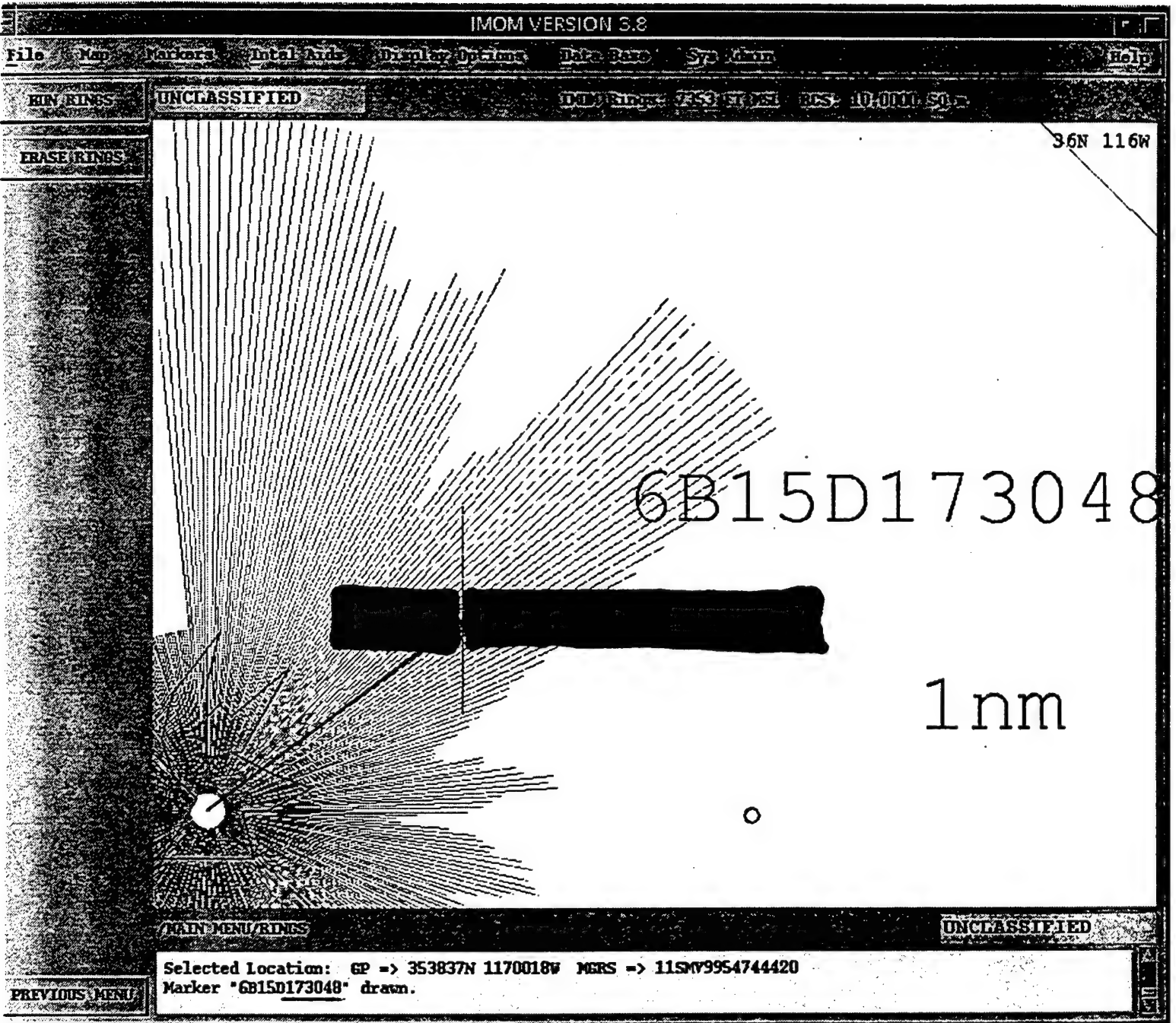
FIG. II-1

19.2 nm @ 88.8° True

FIG. II-2

Beams Display Form

File   View   Display Options

HNDI: Radar Function: Nato Name:

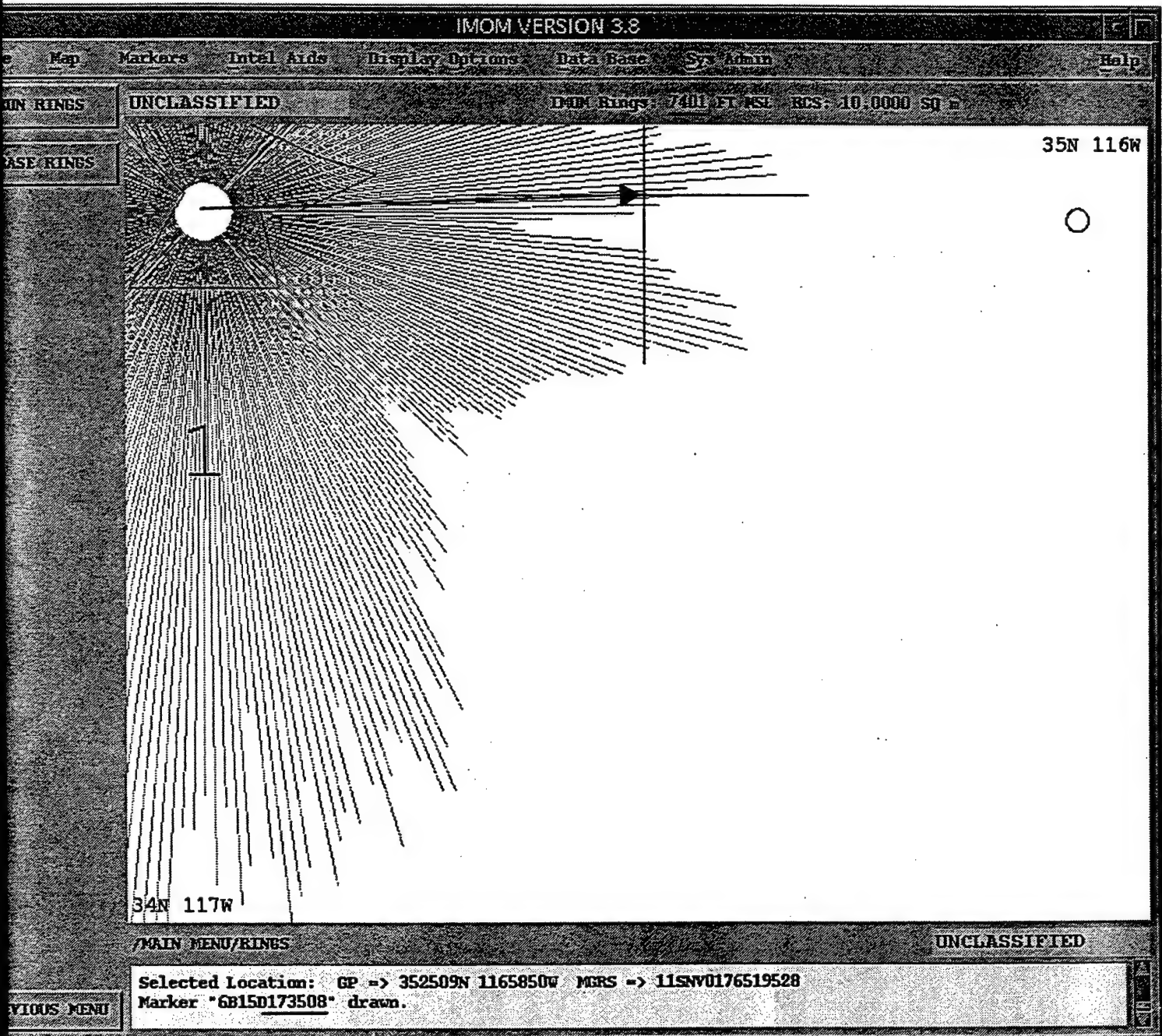Start Location: 352403N 1172224W   End Location: 352439N 1165427W

* 7323 FT
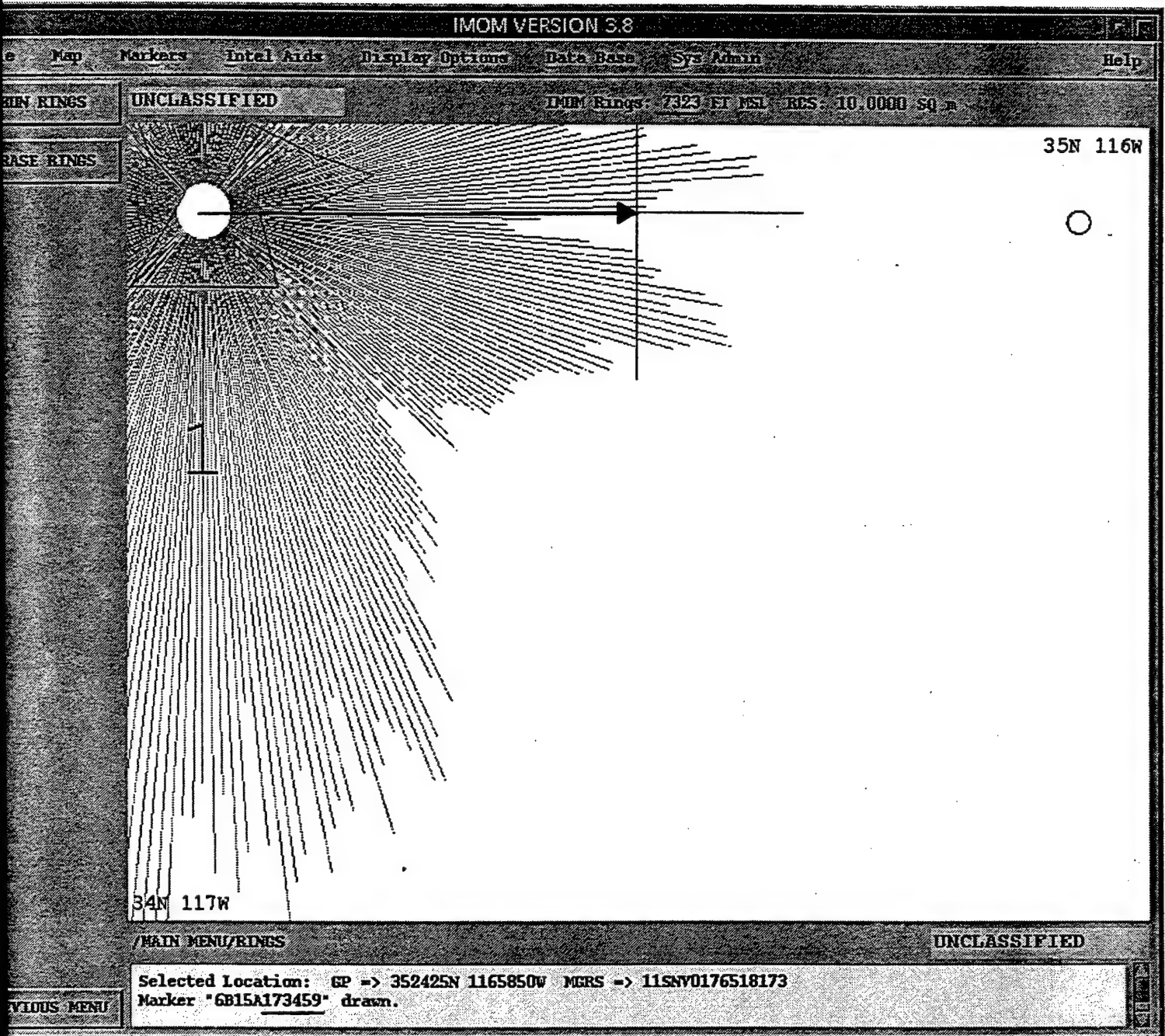
6B15A173459

FIG. KK-1

7.4 nm @ 91.6° True
(.3 nm)

118

FIG. KK-2

* 5525 FT
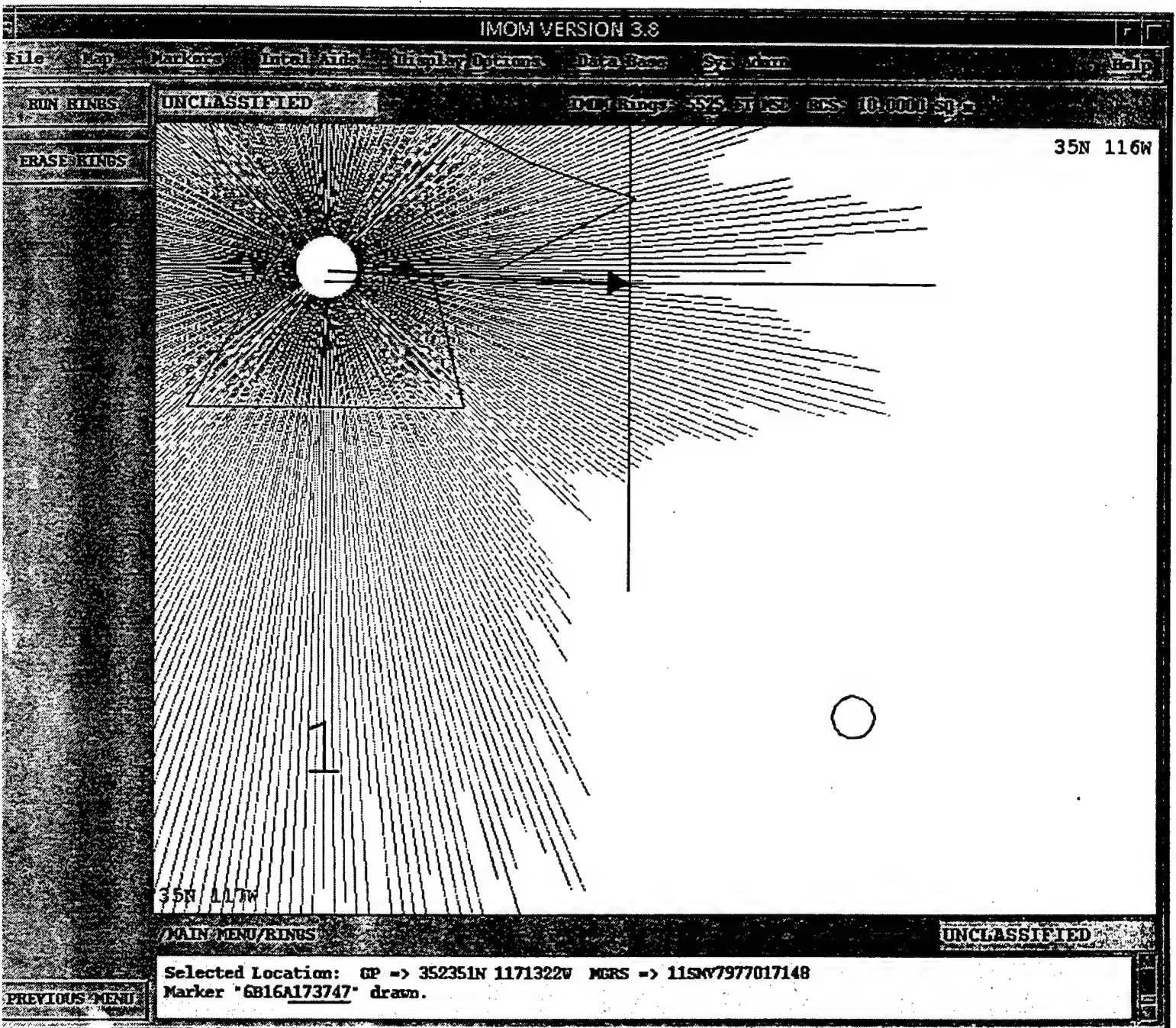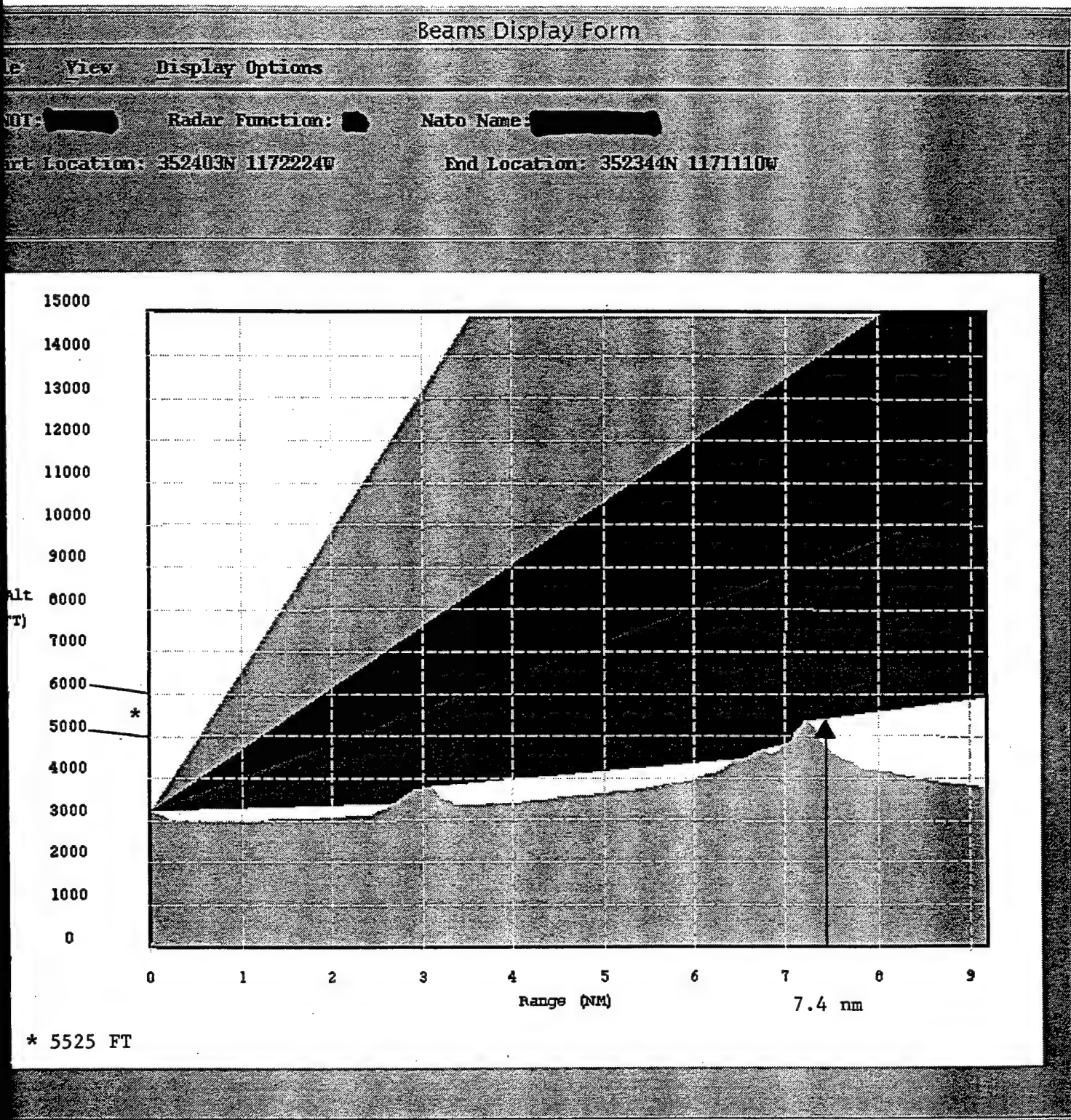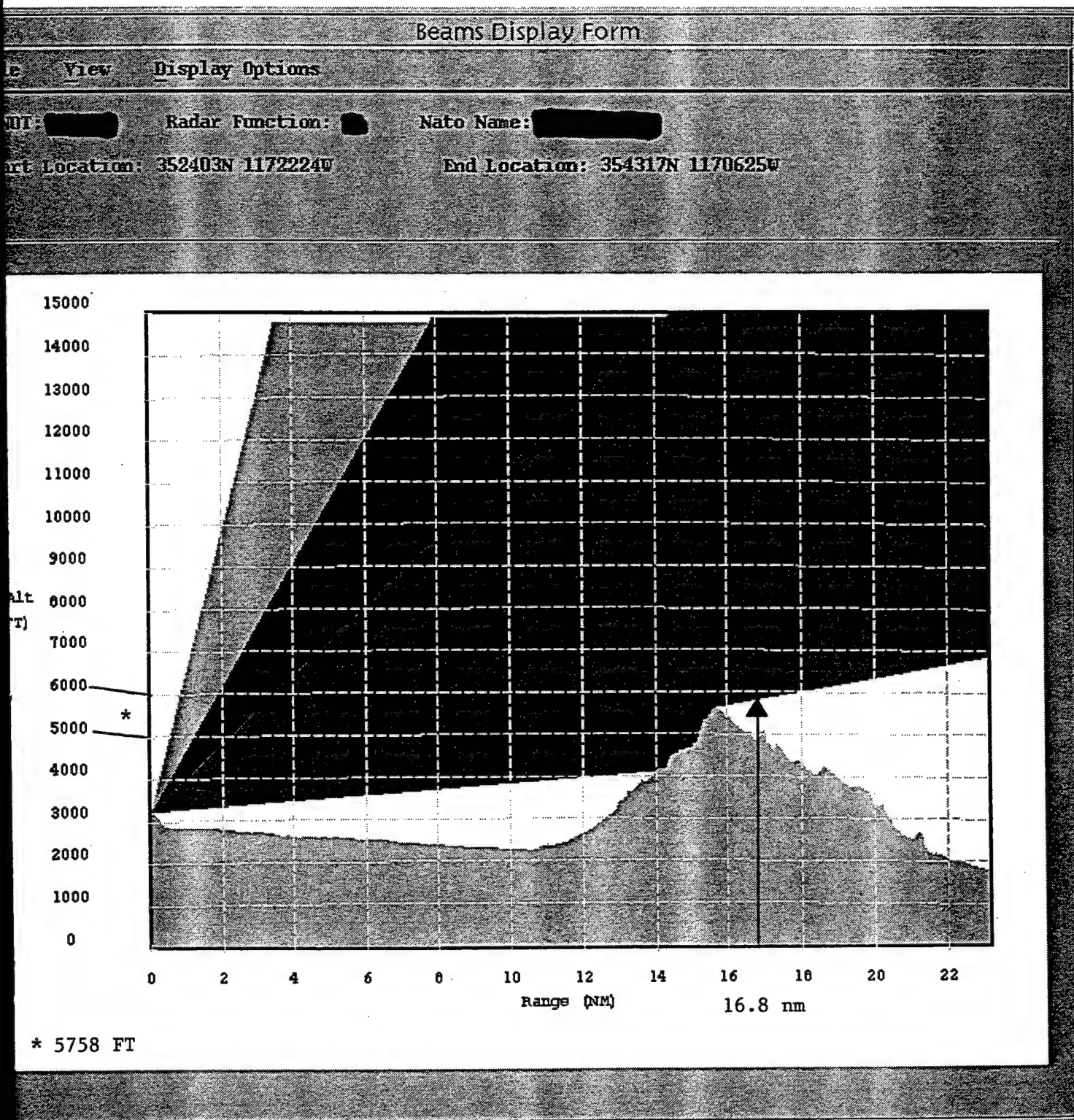
6B16A173747

FIG. LL-1
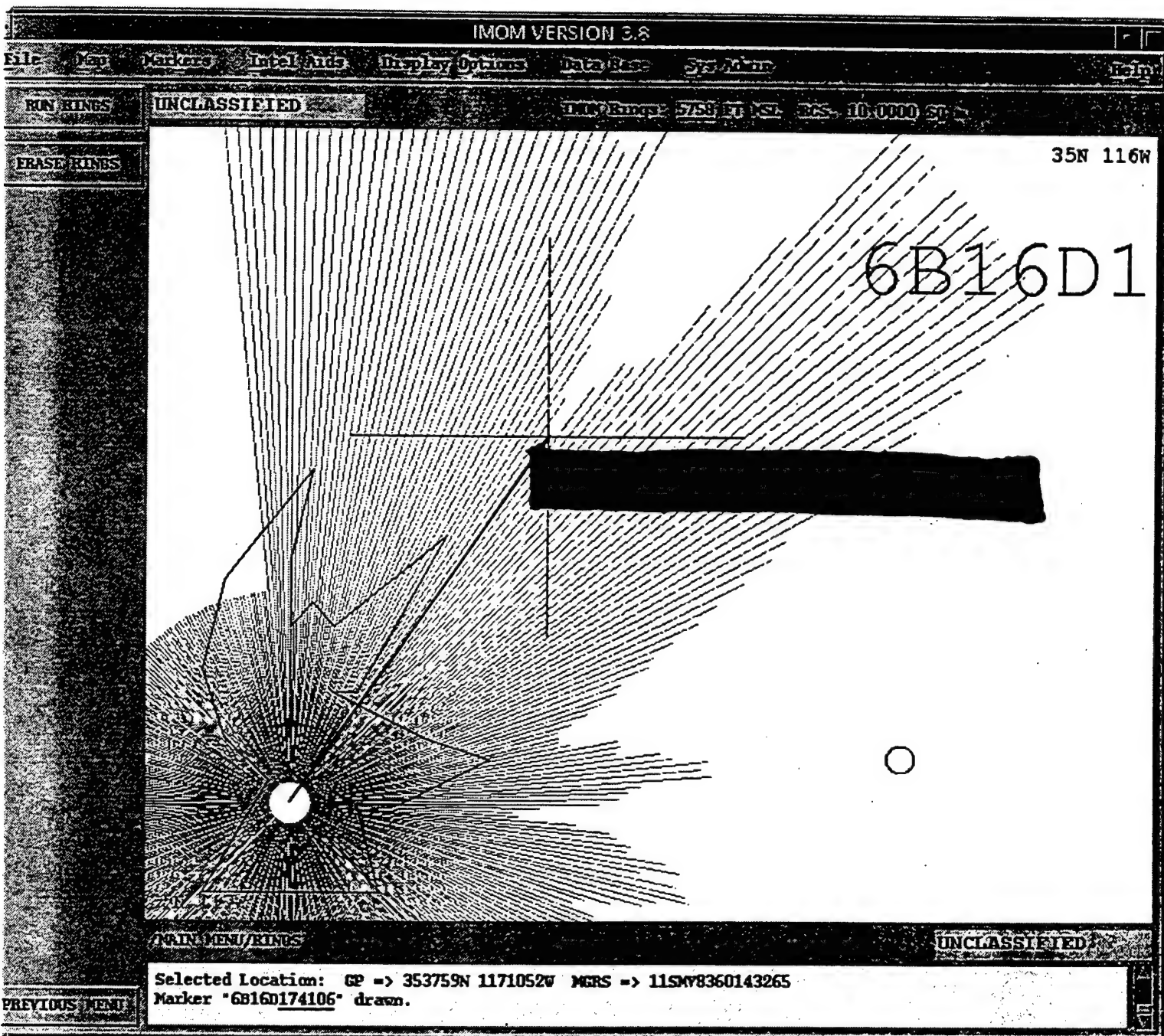
16.8 nm @ 34.0° True

FIG. LL-2
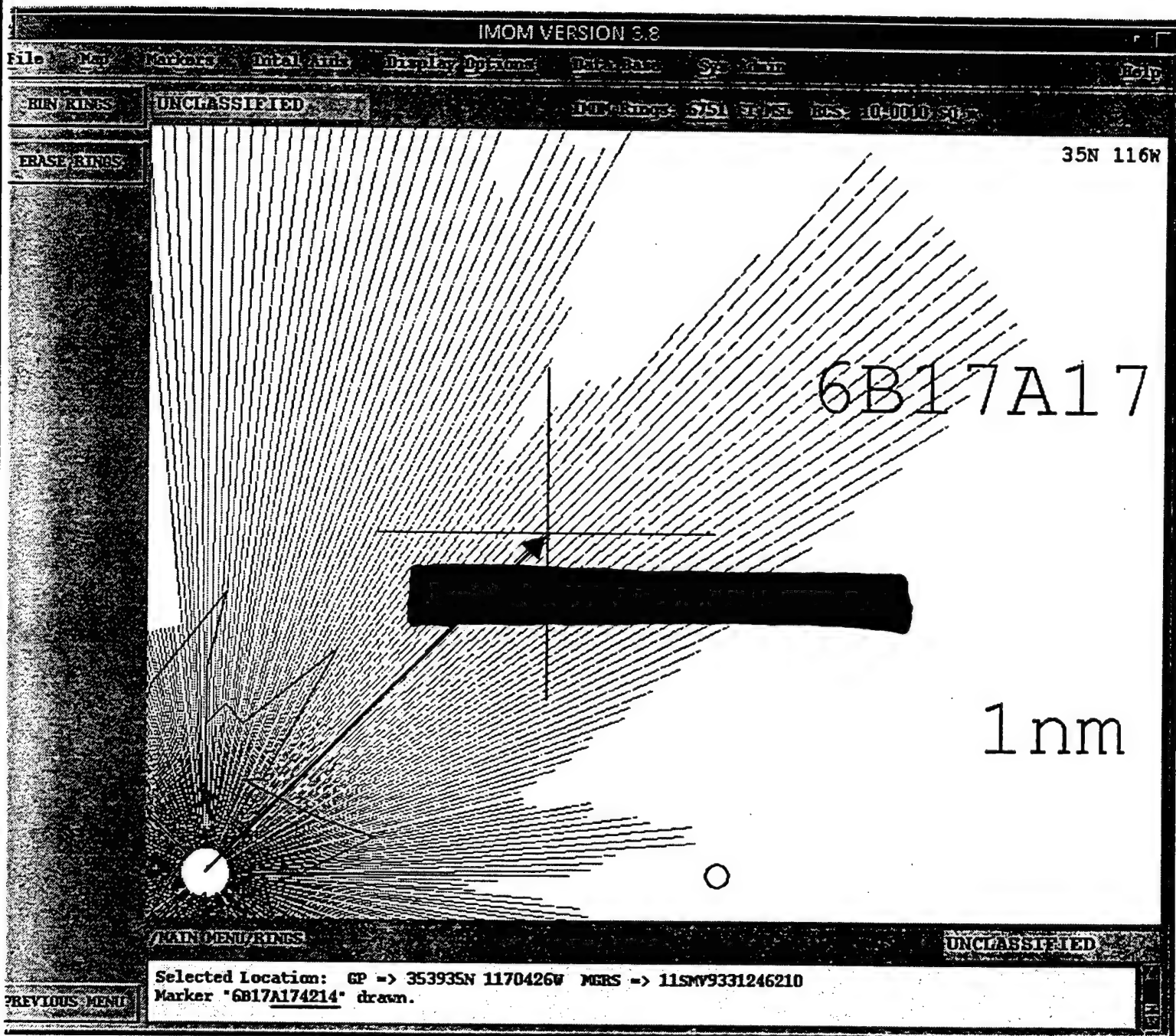
21.4 nm @ 43.6° True
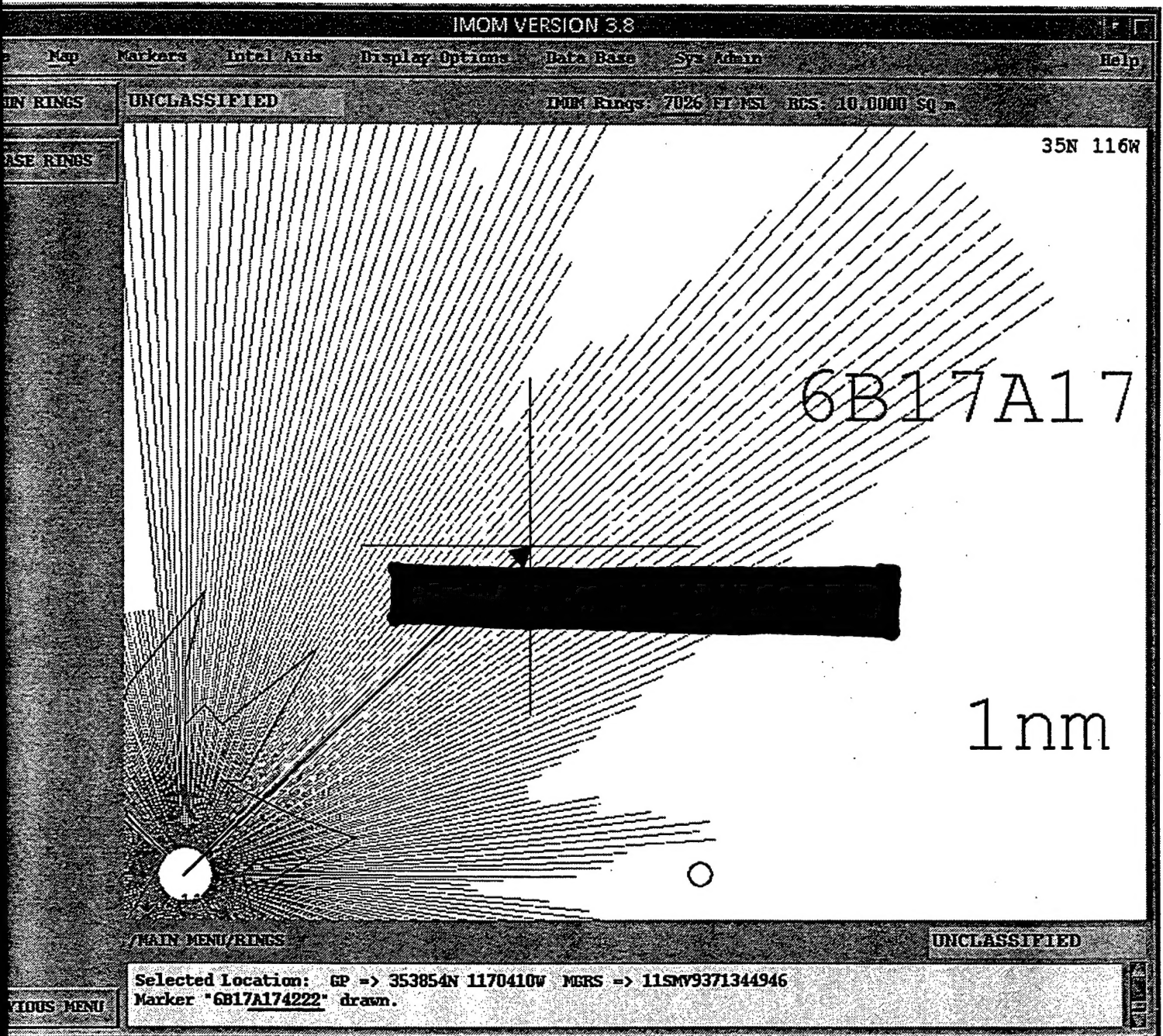
21.0 nm @ 45.1° True

INITIAL DISTRIBUTION LIST

		No. Copies
1.	Defense Technical Information Center 8725 John J. Kingman Rd, STE 0944 Ft. Belvoir, VA 22060-6218	2
2.	Dudley Knox Library, Code 52 Naval Postgraduate School 411 Dyer Road Monterey, CA 93943-5101	2
3.	Research Office, Code 09 Naval Postgraduate School 589 Dyer Road Monterey, CA 93943-5138	1
4.	Chairman, Code EC Department of Electrical and Computer Engineering Naval Postgraduate School 833 Dyer Road Monterey, CA 93943-5121	1
5.	Professor Fred Levien, Code EC/Lv Department of Electrical and Computer Engineering Naval Postgraduate School 833 Dyer Road Monterey, CA 93943-5121	2
6.	Mr. Paul Buczynski, Code EC Department of Electrical and Computer Engineering Naval Postgraduate School 833 Dyer Road Monterey, CA 93943-5121	2
7.	LCDR Todd Kiefer 98/99 Regular Course General Delivery Leavenworth, KS 66048	1

8. AIRTEVRON NINE   2
   Attn: Scott Leahy
   1 Administration Circle
   China Lake, CA 93555

9. National Imagery & Mapping Agency   1
   Attn: Cheryl Blake, ESTS, D-85
   4600 Sangamore Road
   Bethesda, MD 20816-5003

10. Sterling Software   1
    Attn: David Kolassa
    Beeches Technical Campus
    Route 26N
    Rome, NY 13440

11. NAVSTKAIRWARCEN   2
    Attn: CAPT Mayberry
    NAS Fallon
    Fallon, NV 89496-5000

12. JHUAPL   1
    Attn: Dan Henderson
    11100 Johns Hopkins Road
    Laurel, MD 20723

13. COMVAQWINGPAC   1
    Attn: CAPT Ohmstede
    3730 N. Charles Porter Avenue
    Laurel, MD 20723

14. ELATKWEPSCOL   1
    Attn: LCDR Herrera
    NAS Whidbey Island
    Oak Harbor, WA 98278-4200

15. Commander (Code 425110E)   1
    NAVAIRWARCENWPNDIV
    Attn: S. Burkholder
    Building 3008
    Point Mugu, CA 93042-5001

16. Commander (Code 41130D)   2
    NAVAIRWARCENWPNDIV
    Attn: R. Anderson
    China Lake, CA 93555

17. AFOTEC DET 2/c2   1
    Attn: LtCol Oniel
    303 West C Avenue, Suite 102
    Eglin AFB, FL 32542

18. 18 FTS/DOM   1
    Attn: LtCol Ferrira
    606 Cruze Avenue
    Hulbert Field, FL 32544-5736

19. ESC/AC   1
    Attn: Jeff Johnson
    50 Griffis Street
    Hanscom AFB, MA 10731-1619

20. AFIWC/SA   1
    102 Hall Blvd., Suite 343
    San Antonio, TX 78243-7020